Thermo Electron Corporation, 85 First Avenue, Waltham, Massachusetts 02154

Report No. TE4067-61-68

FINAL REPORT

HEAT PIPE THERMIONIC CONVERTER DEVELOPMENT

P. Brosens

Contract No. 951465

December 1967

Prepared for

The Jet Propulsion Laboratory
Pasadena, California

This work was performed for the Jet Propulsion Laboratory, California Institute of Technology, sponsored by the National Aeronautics and Space Administration under Contract NAS7-100.

NOTICE

This report was prepared as an account of Government-sponsored work. Neither the United States, nor the National Aeronautics and Space Administration (NASA), nor any person acting on behalf of NASA:

a. Makes warranty or representation, expressed or implied, with respect to the accuracy, completeness, or usefulness of the information contained in this report, or that the use of any information, apparatus, method, or process disclosed in this report may not infringe privately-owned rights; or

b. Assumes any liabilities with respect to the use of, or for damages resulting from the use of any information, apparatus, method, or process disclosed in this report.

As used above, "person acting on behalf of NASA" includes any employee or contractor of NASA, or employee of such contractor, to the extent that such employees or contractor of NASA, or employee of such contractor prepares, disseminates, or provides access to, any information pursuant to his employment with such contractor.

Requests for copies of this report should be referred to:

National Aeronautics and Space Administration
Office of Scientific and Technical Information
Washington 25, D. C.

Attention: AFSS-A

SUMMARY

This document constitutes the Final Report of the work performed under contract between the Thermo Electron Corporation and the Jet Propulsion Laboratory of the California Institute of Technology. The effort was conducted from 23 June 1966 to 6 November 1967. The Jet Propulsion Laboratory designation of this contract is No. 951465, and it was sponsored by the National Aeronautics and Space Administration under Contract NAS 7-100.

The objective of this program was to incorporate a heat-pipe heat-rejection structure in the design of the advanced SET converter developed concurrently by Thermo Electron Corporation for the Jet Propulsion Laboratory under JPL Contract No. 951263.

To accomplish this objective, the original statement of work required the design, fabrication and test of a heat-pipe model designated T/E-1. After interpretation of the test results, a second model, designated T/E-2, was to be designed, fabricated and tested. The work would then continue with the iterative design, construction and test of a complete heat-pipe converter model designated EM-1, and after test of EM-1, it would conclude with the design, fabrication and test of a final heat-pipe converter designated HP-1.

Severe difficulties encountered during the fabrication of T/E-1 and T/E-2 indicated that the fabrication of only two heat-pipe models might not be sufficient to lead to the development of a heat pipe which could be incorporated into a converter structure. Concurrently, work under JPL Contract 951263 on the development of advanced SET converters had nearly halted because of an important collector overheating problem, and it was judged that further progress would not be possible

without the incorporation of a heat-pipe collector-radiator into the structure of the advanced converter.

Consequently, JPL redirected the work under Contract 951465 to (a) ensure the successful development of a collector-radiator heat pipe, and (b) develop a heat pipe of the exact size required by the advanced SET converter. Under the redirected effort, the test of T/E-2 had to be followed with the design, fabrication and test of a third heat-pipe model, designated T/E-3. After test of T/E-3 a fourth and final model, designated T/E-4, with a heat-pipe of larger size, had to be designed, fabricated and tested. The test of all four models had to include a heat-transfer test, a thermal cycling test, and a 100-hour run at maximum heat load.

Model T/E-1 failed shortly after completion of the heat-transfer test due to an embrittling reaction that had occurred during assembly between the niobium heat pipe wall and its radiative coating.

Model T/E-2 also failed shortly after completion of the heat-transfer test. Its failure was due to a faulty capillary assembly, which resulted in collector overheating with the consequent failure of the heat pipe at the point where it is joined to the collector.

Model T/E-3 was actually fabricated with an emitter structure and operated as a converter. Its test yielded valuable data on converter radiator heat load for accurate heat pipe sizing. This model completed successfully the thermal cycling test and a 400-hour run at maximum load.

Model T/E-4 did not include an emitter structure. It had a larger radiator area than the three previous models, and it could accommodate

an output current of 71.5 amperes at the optimum collector temperature. This is 30% greater than the previous corresponding value of 55 amperes. This model also completed successfully the thermal cycling test and the 100-hour run at maximum load. Because the model did not include the emitter structure, it was possible to drive it with a considerably larger input than model T/E-3. In one instance the input power became so large that the heat pipe achieved burn-out conditions, and the internal capillary structure was damaged. The heat pipe became sensitive to sudden application of heavy thermal loads, and after 150 hours of operation at a heat input corresponding to a converter output current of 120 amperes, the device failed.

In conclusion, a collector-radiator structure suitable for incorporation in the JPL advanced SET converter has been successfully developed. The structure has exhibited no structural or functional weaknesses when used in a converter configuration. It offers the important advantages of improving converter heat transfer and of greatly reducing the weight of the T-200 converter. It will be used in converters T-208, -209 and -210, to be fabricated under JPL Contract 951263, and further refinements in heat pipe technology may be expected to result from this additional effort.

TABLE OF CONTENTS

TABLE OF CONTENTS (continued)

1. INTRODUCTION

The initial objective of this program was to develop a converter of the design used in Contract No. 951263, but incorporating a heat pipe concept to transfer heat between the collector and the radiator. The work involved the design, fabrication and test of two heat pipe models designated T/E-1 and T/E-2, and was to be followed by the design, fabrication and test of two heat-pipe thermionic converters designated EM-1 and HP-1. The four devices were to be fabricated and tested in sequence to allow a thorough evaluation of each design before proceeding with the next iteration. Since the development of a suitable heat pipe structure was the most important aspect of the work under this contract, the first two devices included only the heat pipe, and it was only in the last two that an attempt was to be made to fabricate a complete converter structure incorporating a heat-pipe collector-radiator.

The difficulties that were encountered in the fabrication of models T/E-1 and T/E-2 prompted JPL to redirect the effort so that the resources provided under the program could be more fully allocated to advance heat-pipe technology. Under the redirected effort, the development of models T/E-1 and T/E-2 was followed by the sequential design, fabrication and test of two more models, designated T/E-3 and T/E-4, to take the place of EM-1 and HP-1. Model T/E-4 was to involve substantial size changes in order to permit immediate incorporation in the structure of converter T-208, being developed under the concurrent JPL Contract 951263, and thereby solve a severe collector overheating problem that had been encountered in the course of that work.

2. DEVELOPMENT OF MODEL T/E-1

2.1 Design

To ensure compliance with the requirement that the heat pipe models be compatible with the converter structure being developed under the concurrent JPL contract 951263, the heat-pipe models were designed to enable the possible inclusion of an emitter structure, a cesium reservoir system, output leads and a mounting support.

The design of the model T/E-1 heat pipe including the components for converter fabrication is presented in Figure 1. This model can use the same emitter structure and ceramic seal as the T-200 converter. The heat-pipe structure is a single tube which extends from the collector at the front to the cesium reservoir at the rear. This tube is made of niobium in order to ensure compatibility with the heat-pipe liquid metal and to minimize expansion-matching problems with the ceramic seal. As shown in the figure, a concentric tubular element, part No. 10, serves as the inner seal flange, and is brazed to the heat pipe also. This part was used mainly to serve as a transition piece between the inside diameter of 0.660" of the standard T-200 ceramic seal to the outside diameter of the available heat-pipe tube, which was 5/8" in outside diameter. Later, tubing of 0.680" outside diameter was procured, and it became possible to eliminate the transition piece in model T/E-4.

The collector end of the heat pipe is a niobium slab with a hole at its center in order to connect to the cesium reservoir tubulation. This slab is made of niobium in order to facilitate matching the expansion of the heat pipe and welding to it. The heat-pipe space

7427

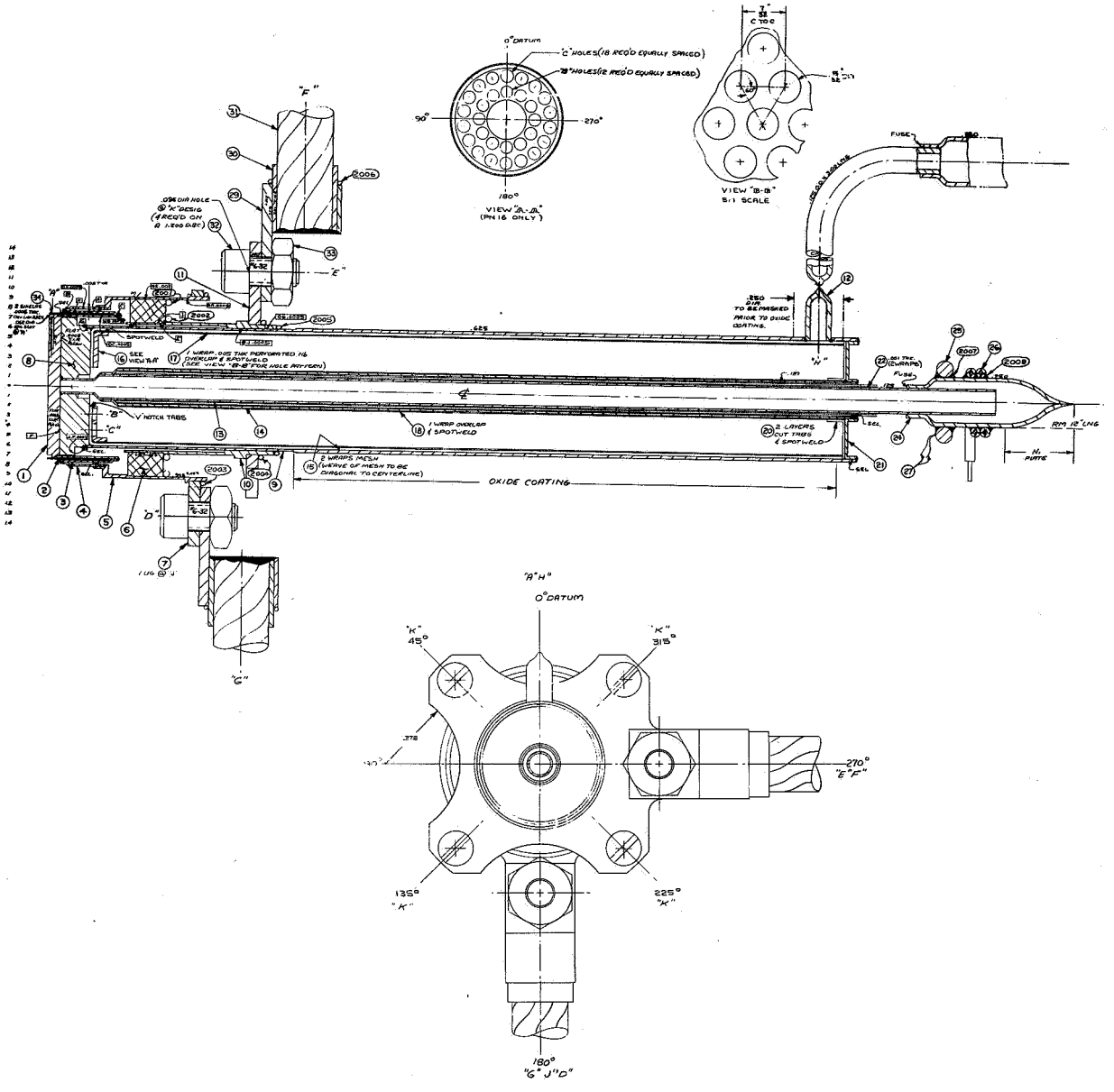

Figure 1

extends between two concentric tubes, parts Nos. 9 and 14. The inner tube, part 14, is provided in order to allow the free passage of the cesium reservoir tubulation, and to lengthen as much as possible the thermal path between the collector and the cesium reservoir without having to locate the cesium reservoir far from the end of the radiator heat pipe.

The most important design details are, of course, those that concern the heat pipe itself. The inside wall of the radiator heat pipe is coated with two wraps of 400-mesh stainless steel screen that extends from one end to the other and bends around the collector insert piece, part No. 16, to provide good thermal contact with the rear face of the collector slab. As shown in view A-A of Figure 1, part No. 16 has a large number of perforations so that any heat pipe fluid boiled off at the collector end can easily be transferred from the capillary mesh to the heat pipe conduit. The heat pipe fluid is sodium. To maintain the capillary mesh screen in good contact with the inside walls of the heat pipe, a single wrap of 5-mil-thick niobium sheet, part No. 17, perforated as shown in view B-B, is inserted to fit snugly against the mesh screen. View B-B of Figure 1 shows the center-to-center distance of the part No. 17 perforations to be 7/32". The distance was changed to 3/16" during the fabrication of T/E-1 because of the availability of the corresponding perforations dies at the perforated sheet supplier.

To circumvent the problem of condensation of sodium on the inside tube, part No. 14, a wrap of capillary mesh, part No. 18, is placed around the inner tube of the heat pipe. This wrap serves to direct any condensing sodium back to the rear of the heat pipe, where

it is further directed by radially extending portions of capillary screen to the outer wall capillary of the heat pipe. The tube, part No. 12, extending radially from the bottom of the heat pipe, is used to evacuate the heat pipe and fill it with sodium. To avoid problems of compatibility of liquid metal with the filled tube, part No. 12 is made of niobium, and is sealed by melting the material locally by inert-gas arc welding.

2.2 Heat Transfer Calculations

The important dimensions of the model T/E-1 design were as follows:

Useful Radiator Length:	2.93 in. = 7.45 cm
Radiator Diameter:	0.625 in. = 1.59 cm
Nominal Radiator Area:	37.2 sq cm

The corresponding converter design point conditions assumed for heat transfer calculations were:

Interelectrode Spacing:	Nominal value: 0.003 in.
Emitter Diameter:	0.710 in. = 1.81 cm
Emitter Area:	2.55 sq cm
Emitter Temperature:	2000°K
Collector Temperature:	1000°K
Reservoir Temperature:	610°K
Output Voltage:	0.8 V
Output Current Density:	20 A/sq cm
Output Power Density:	16 watts/sq cm
Output Current:	51.0 amperes
Output Power:	40.8 watts

The heat transfer was computed using these design conditions and the expressions of Block, Hatsopoulos and Wilson in their paper on "The Definition of Conversion Efficiency of Thermionic Energy Converters," presented at the Thermionic Conversion Specialist Conference at San Diego in 1965. The expressions are:

$$q_{\epsilon} = J\phi_E$$

$$q_r = 0.14\sigma\,(T_e^4 - T_c^4)$$

where the factor of 0.14 corresponds to an effective emissivity at the emitter surface of 0.26 and 0.30 at the collector,

$$q_g = \frac{\lambda_m (T_e - T_c)}{d + 1.15 \times 10^{-5} \frac{T_e + T_c}{p}}$$

$$q_s = J\sqrt{\rho_s K_s (T_e - T_c)(2-\eta_i)/2\eta_i}$$

where q_{ϵ} is the electron cooling, watts/cm^2

J is the output current density, A/cm^2

ϕ_E is the effective emitter work function, volts

q_r is the interelectrode thermal radiation, watts/cm^2

σ is the Stefan-Boltzmann constant, 5.6697×10^{-12} watt/cm^{2}deg^4

T_e is the emitter temperature, deg K

T_c is the collector temperature, deg K

q_g is the cesium heat conduction, watts/cm^2

λ_m is the thermal conductivity of the vapor at the mean gas temperature, watts/cm deg

d is the interelectrode spacing, cm

p is the vapor pressure, torr

q_s is the optimized-lead heat loss, watts/cm^2

ρ_s is the electrical resistivity of the lead material at its mean operating temperature, ohm-cm

K_s is the thermal conductivity of the lead material at its mean operating temperature, watts/cm deg

η_i is the ideal converter efficiency

The effective emitter work function ϕ_ε at 2000°K, 20 A/sq cm, is 2.94 volts. The electron cooling for the assumed nominal output was then 58.8 watts/sq cm. This is a conservative value because the general experience with the T-200 converter is that the effective emitter work function for electron cooling calculations is 2.72 volts rather than 2.94. The interelectrode radiation was 11.9 watts/sq cm. The thermal conductivity of cesium vapor at a mean temperature of 1500°K is 6.15×10^{-5} watts/cm - °K, and the cesium vapor pressure at 610°K is 4.65 torr. The cesium conduction calculated at a spacing of 0.0075 cm was then 4.1 watts/sq cm. Figure 2 gives the value of the cesium conduction loss at other reservoir temperatures and for an emitter-collector temperature difference of 900°K; to apply it to the case of a temperature difference of 1000°K, the values given must be multiplied by 1.111. The

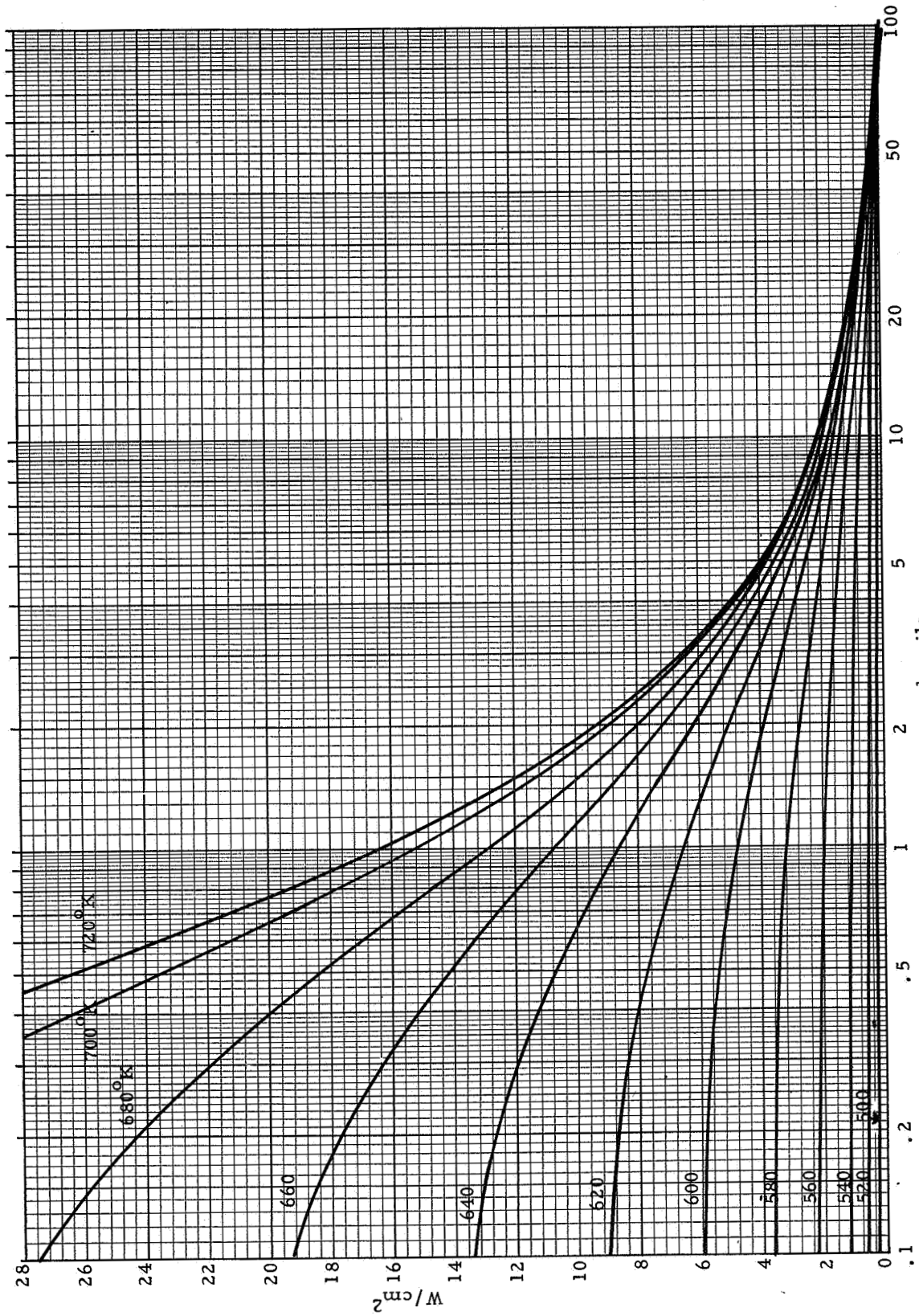
W/cm²
d, mils
720°K
700°K
680°K
660
640
620
600
580
560
540
520
500
28
26
24
22
20
18
16
14
12
10
8
6
4
2
0
.1
.2
.5
1
2
5
10
20
50
100

Figure 2

thermal conductivity of rhenium at 1493°K was assumed to be 0.259 watt/cm - °K* (Final Report, Task IV, JPL 950671). The electrical resistivity of rhenium at the same temperature is given by Kohl as 84 microhm-cm. Assuming an ideal converter efficiency of 0.19, the optimized-lead loss found was 6.4 watts/sq cm. The actual lead loss due to conduction for the design configuration was computed as follows:

Average lead diameter: 0.760 in. = 1.93 cm

Developed length of lead: 0.800 in. = 2.03 cm

Thickness of lead wall: 0.008 in. = 0.0204 cm

Cross-sectional area of lead: 0.124 sq cm

Heat transfer = $K_s A(T_e - T_c)/\ell$ = 15.8 watts total

Heat transfer per unit emitter area = 6.2 watts/sq cm

The comparison of the calculated heat conduction for the actual lead with that of the optimized lead showed that the actual lead deviated only slightly from the ideal one. The total calculated heat transfer for the converter was then

(58.8 + 11.9 + 4.1 + 6.2) = 81.0 watts/sq cm, or 207.0 watts.

*This value is excessively low, and the calculations were later corrected to use more reliable values for the thermal conductivity of rhenium. The heat transfer per unit emitter area was then found to equal 12.0 watts/sq cm instead of the value of 6.2 calculated originally as explained above.

The electrical losses in the collector lead were calculated as follows:

Lead dimensional data:

Effective length:	0.75 in. = 1.91 cm
Average diameter:	0.61 in. = 1.55 cm
Thickness:	0.010 in. = 0.025 cm
Cross-sectional area:	0.0191 sq. in. = 0.122 sq. cm

Resistivity of niobium at 700°C: 43×10^{-6} ohm-cm

Lead resistance = $43 \times 10^{-6} \times 1.91/0.122 = 0.673 \times 10^{-3}$ ohm

Voltage drop at rated current of 51.0 amperes: 34 millivolts

The above voltage drop was calculated assuming that all of the current flows in the heat-pipe wall. Actually, it was estimated that a large amount flows through the sodium-filled capillary. The electrical resistivity of sodium at 700°C is approximately 30.5×10^{-6} ohm-cm. It was therefore expected that the actual voltage drop in the collector lead would not exceed 20 millivolts.

2.3 Heat Pipe Design

After the converter heat transfer had been calculated, it was then possible to calculate the heat-pipe operating parameters.

The heat transfer to the converter radiator was taken as 207.0 watts less the electrical power output and the heat conducted by the electrical leads. Allowing 10 watts for each lead, the radiator heat transfer was then 207.0 - 40.8 - 20 = 146.2 watts.

With the nominal radiator area of 37.2 sq cm, the radiant emittance of the radiator had to equal 3.92 watts/sq cm. A total

emissivity of 0.85 was assumed for the radiator surface, and the radiator temperature required to achieve the desired radiant emittance was found to be 951°K, which allowed for miscellaneous losses and a design margin from the desired collector temperature of 1000°K.

The nominal heat pipe dimensions were:

Length of vapor conduit:	3.84 in. = 9.75 cm
Cross section of vapor conduit:	0.595 in. diam - 0.200 in. diam = 1.60 sq cm
Capillary mesh wire diam:	0.001 in. = 0.0025 cm

At the heat-transfer rate of 146 watts, the flow rate of sodium calculated was

$$\dot{M} = 146/3900 = 3.74 \times 10^{-2} \text{ g/sec}$$

where 3,900 is the heat of vaporization of sodium as given by the corresponding figure, at 700°C, in the property graphs for sodium that are presented in Figures 3 to 8.

The vapor velocity corresponding to this flow rate was

$$3.74 \times 10^{-2}/(4.6 \times 10^{-5})(1.60) = 506 \text{ cm/sec}$$

where 4.6×10^{-5} gm/cc is the density of sodium vapor at a saturation temperature of 700°C. The velocity of 506 cm/sec was only 17 feet per second and was well within typical design range.

The pressure drop in the vapor conduit was calculated from:

$$\Delta p_g = 8 \nu_g \dot{M} L/A$$

wjere ν_g is the kinematic viscosity of the vapor, $\dot{M}$ is the flow rate, L is the length of the vapor conduit, and A is its cross-sectional area.

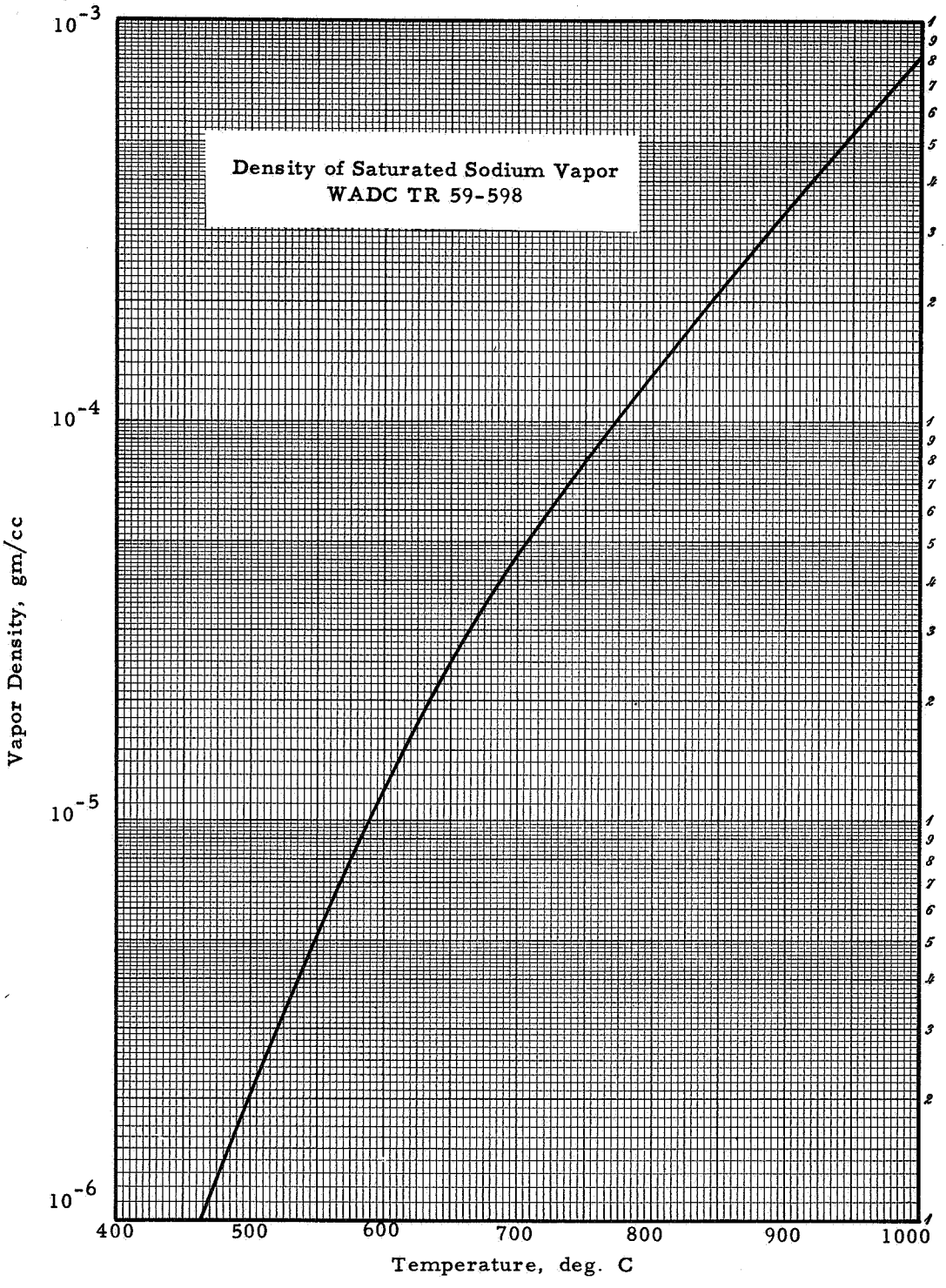
Density of Saturated Sodium Vapor
WADC TR 59-598
Vapor Density, gm/cc
10^-3
10^-4
10^-5
10^-6
400
500
600
700
800
900
1000
Temperature, deg. C

Figure 3

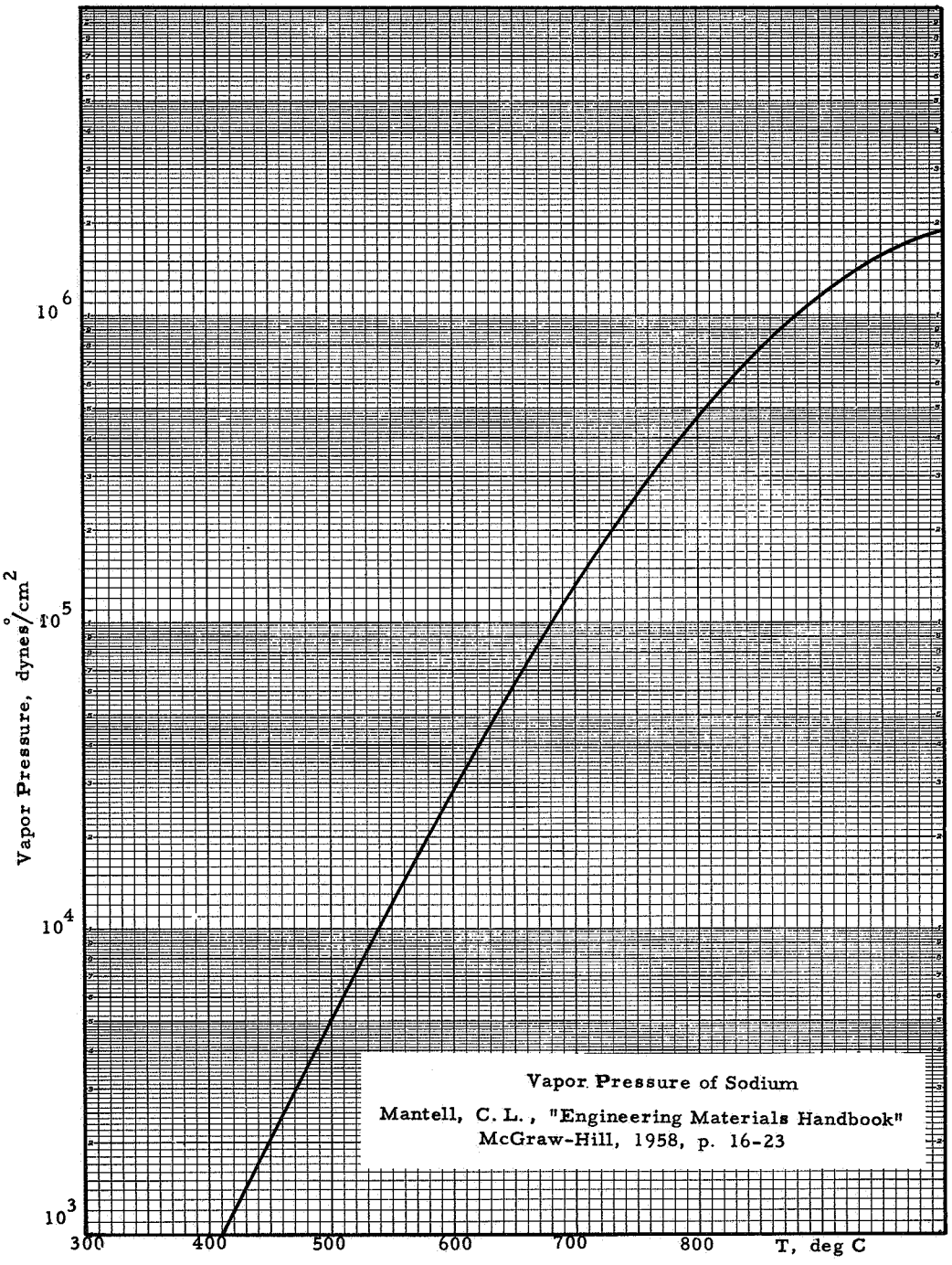
Vapor Pressure, dynes/cm^2
10^6
10^5
10^4
10^3
300
400
500
600
700
800
T, deg C
Vapor Pressure of Sodium
Mantell, C. L., "Engineering Materials Handbook"
McGraw-Hill, 1958, p. 16-23

Figure 4

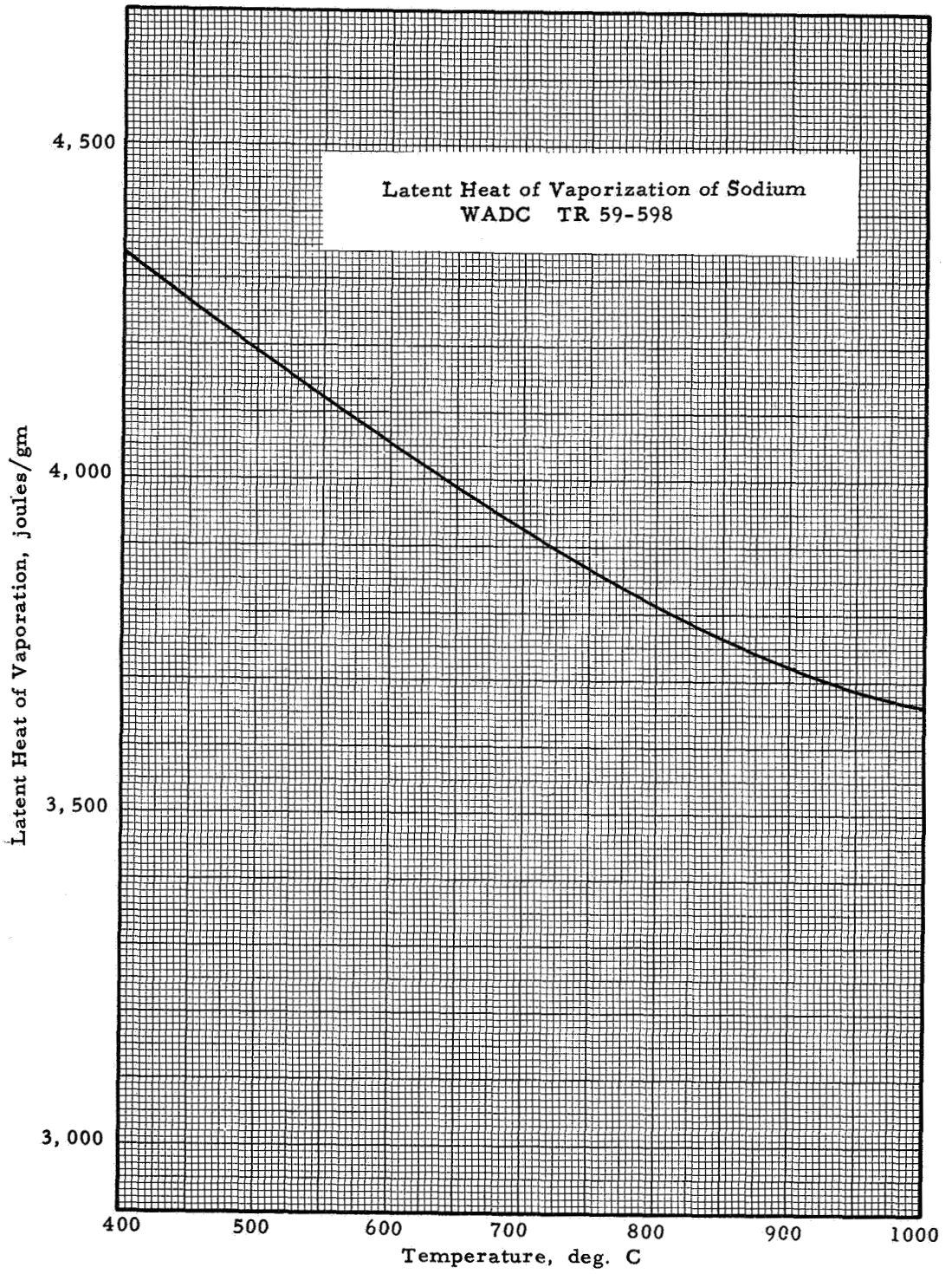
Latent Heat of Vaporization of Sodium
WADC TR 59-598
Latent Heat of Vaporation, joules/gm
4, 500
4, 000
3, 500
3, 000
400
500
600
700
800
900
1000
Temperature, deg. C

Figure 5

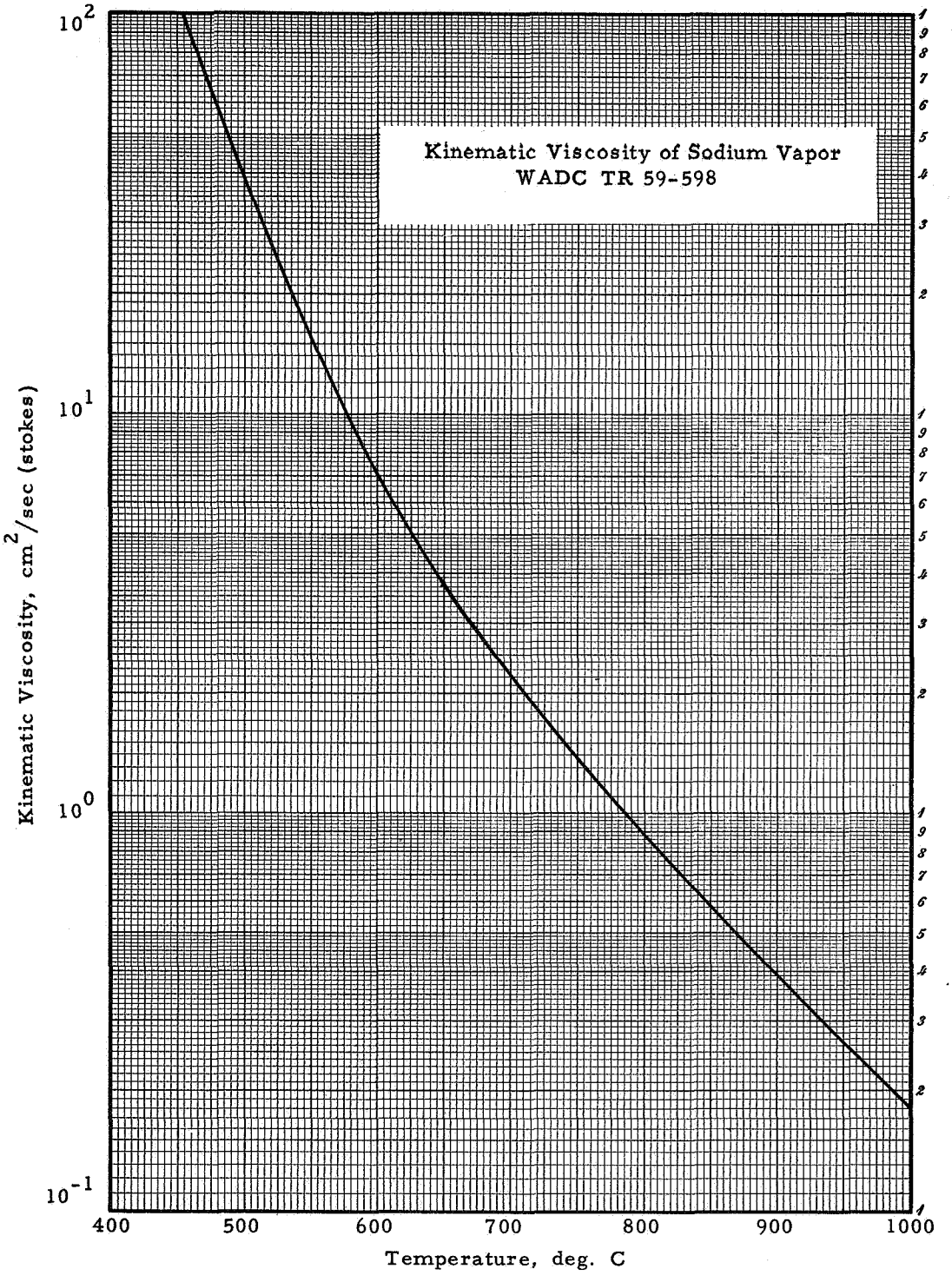
Kinematic Viscosity of Sodium Vapor
WADC TR 59-598
Kinematic Viscosity, cm²/sec (stokes)
10²
10¹
10⁰
10⁻¹
400
500
600
700
800
900
1000
Temperature, deg. C

Figure 6

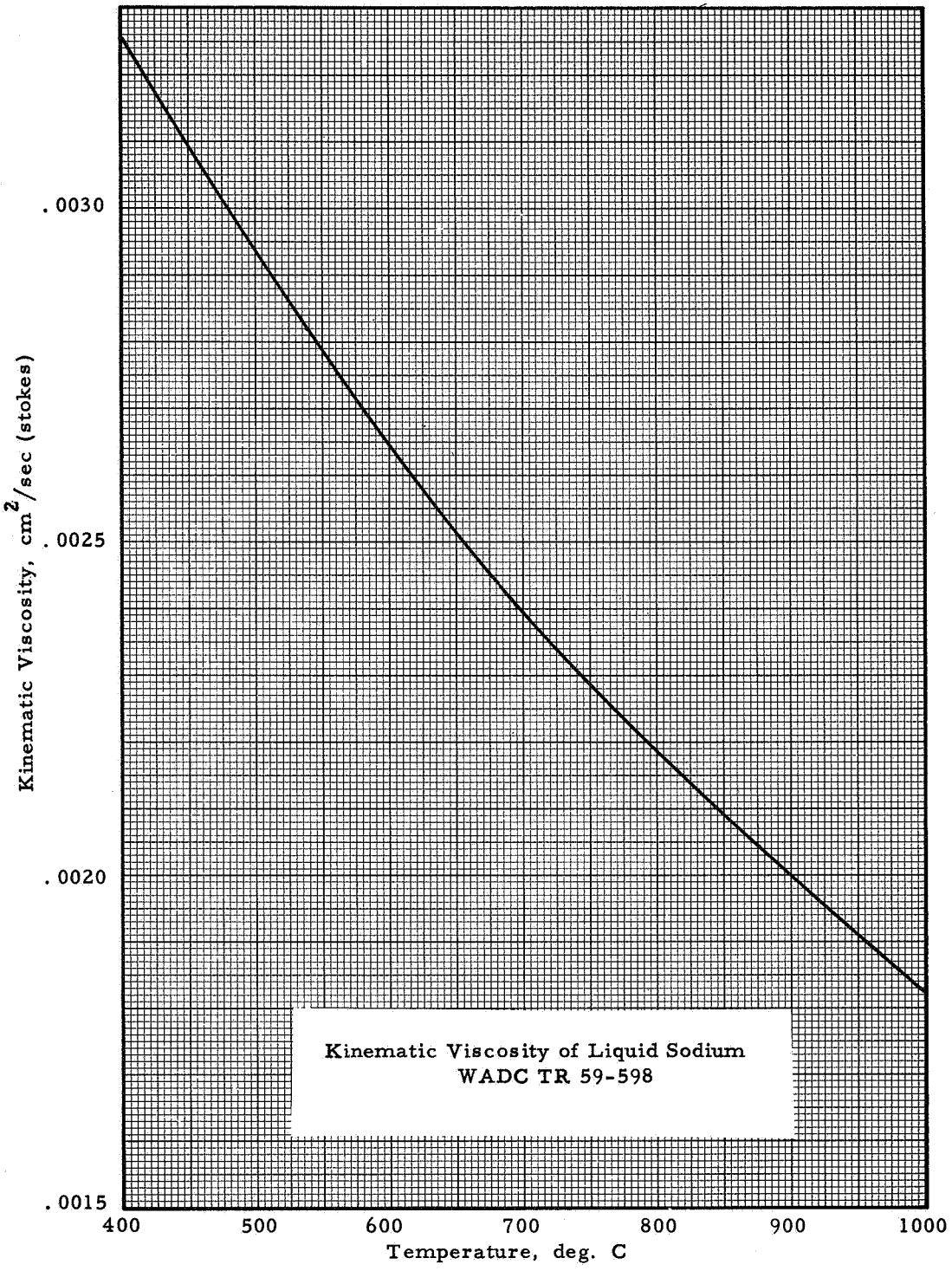
Kinematic Viscosity, cm²/sec (stokes)
.0030
.0025
.0020
.0015
400
500
600
700
800
900
1000
Temperature, deg. C
Kinematic Viscosity of Liquid Sodium
WADC TR 59-598

Figure 7

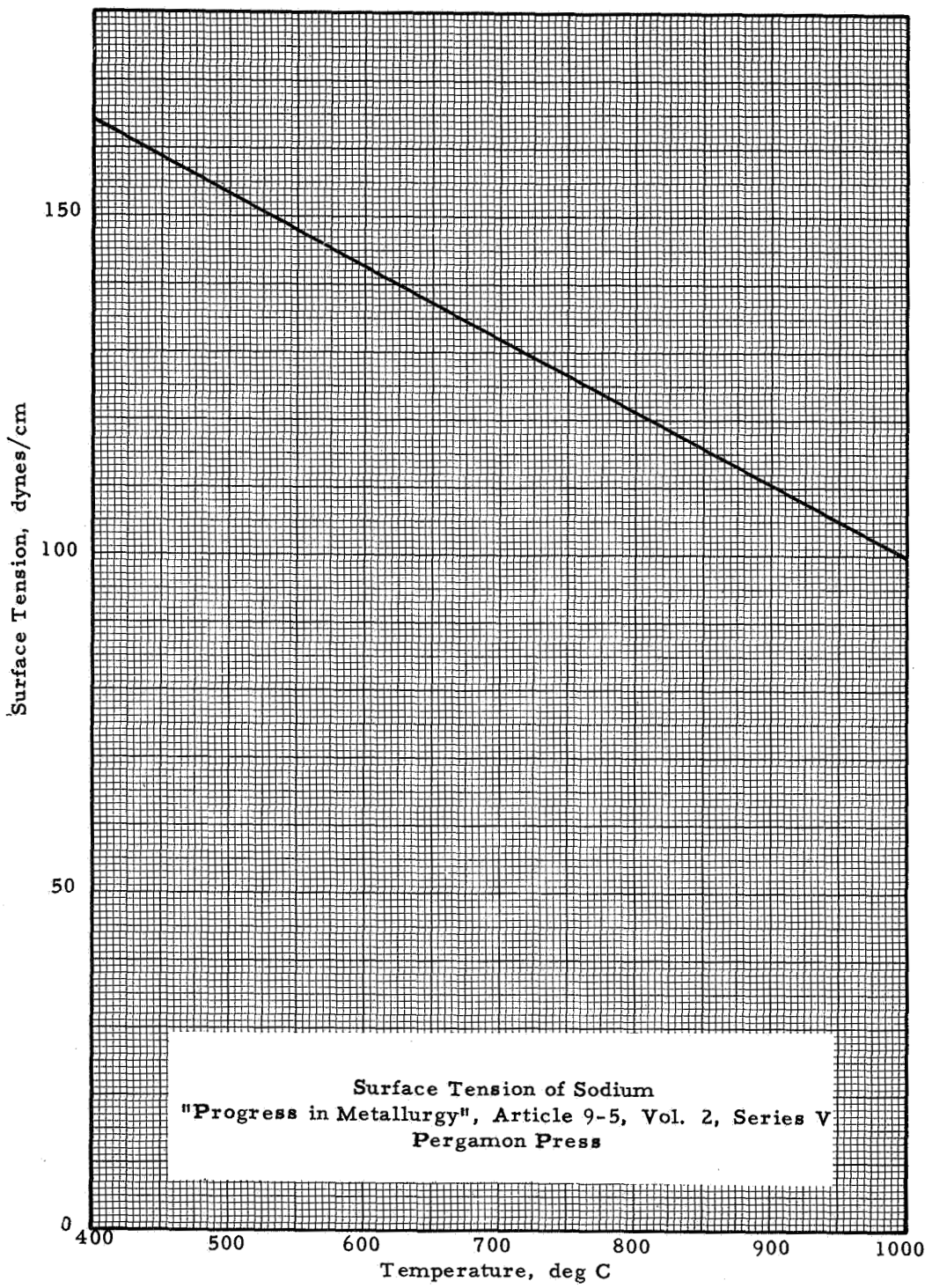
Surface Tension, dynes/cm
150
100
50
0
400
500
600
700
800
900
1000
Temperature, deg C
Surface Tension of Sodium
"Progress in Metallurgy", Article 9-5, Vol. 2, Series V
Pergamon Press

Figure 8

$$\Delta p_g = 8 \times 2.2 \times 3.75 \times 10^{-2} \times 9.75/1.60$$
$$= 3.8 \text{ dynes/sq cm}$$

The pressure drop due to gravity forces was:

$$\Delta p_h = \rho gh$$
$$= 0.776 \times 981 \times 9.75$$
$$= 7,400 \text{ dynes/sq cm}$$

The maximum pressure drop in the capillary mesh was:

$$\Delta p_f = 0.098 \nu_f \dot{M} L/N d^4$$

where ν_f is the kinematic viscosity of the liquid, $\dot{M}$ is the flow rate, L is the length of the capillary wick, N is the effective number of capillaries, and d their effective diameter.

$$\Delta p_f = 0.098 \times 0.0024 \times 3.74 \times 10^{-2} \times 9.75/N (0.0025)^4$$
$$= 2.30 \times 10^6/N$$

where N was the number of capillaries.

The available capillary force to overcome these pressure drops was assumed to be*:

$$\Delta p_{max} = 0.196 \sigma/d$$
$$= 0.196 \times 132/0.0025$$
$$= 1.03 \times 10^4 \text{ dynes/sq cm}$$

*This is an excessively low value. Recent experience by workers such as J. Kemme at Los Alamos Scientific Laboratory indicates that the capillary forces are greater, and the factor of 0.196 should be approximately 4.0.

The minimum permissible number of capillaries was therefore given by the pressure drop inequality:

$$\Delta p_f \leq \Delta p_{max} - \Delta p_g - \Delta p_h$$

$$N \geq 2.30 \times 10^6/(1.03 \times 10^4 - 3.8 - 7,400)$$

$$N \geq 800 \text{ capillaries}$$

This meant that for a 400-mesh size capillary mesh, a perimeter length of 2.0 inches was required. To allow a margin for operation at more intense heat fluxes, 2 wraps of mesh were selected, which provided a perimeter length of 3.7 in. They were supported by a perforated niobium sheet with 46% open area.

2.4 Converter Weight

The estimated weight of each converter part was as follows:

Part No.	Volume cc	Density grams/cc	Weight grams
1	0.390	21.02	8.20
2	0.094	21.02	1.97
3	0.091	21.02	1.91
4	0.072	21.02	1.53
5	0.399	8.57	3.42
6	0.880	3.97	3.49
7	0.179	8.57	1.53
8	0.912	8.57	7.82
9	1.620	8.57	13.84
10	0.411	8.57	3.52
11	0.468	8.57	4.01
12	0.039	8.57	0.33
13	0.281	16.6	4.66
14	0.348	8.57	2.98
15	0.127	8.89	1.14
16	0.061	8.57	0.53
17	0.274	8.57	2.35
18	0.021	8.89	0.19
19	0.0006	8.89	0.01
20	0.004	8.89	0.04
21	0.068	8.57	0.59
22	0.029	16.6	0.48
23	0.031	16.6	0.51

Part No.	Volume cc	Density grams/cc	Weight grams
24	0.166	8.96	1.49
25	0.088	8.89	0.78
26	6 cm	0.065 gram/cm	0.39
Sodium charge			2.00
Braze			1.00

The total converter weight calculated was 70.71 grams or 0.156 lb, not including the electrical leads and the mounting hardware. The specific power which corresponded to this weight, assuming an output power of 40.8 W, was 262 W per lb. The corresponding specific weight was less than 4 lbs/kW.

2.5 Ability to Resist Shock and Vibration

As a measure of the ability of the design to resist shock and vibration, the g-level that the ceramic seal is able to withstand was calculated, and a similar calculation was also made for the converter support screws.

A shear strength of 3000 psi was assumed for the ceramic at the seal, and the failure load for the seal was calculated approximately as the product of this stress and the inner cylindrical area of the seal of 0.374 sq in. This failure load was 1120 lb. To produce such a load with the mass of parts Nos. 1, 2, 3, 4, 5, 6, 7 and a lead weighing approximately 15 grams, i.e., a total of 37.05 grams, or 0.082 lb, the required g-level was 13,700 g's, which showed that the seal structure is very strong.

A tensile strength of 50,000 psi for the converter support screws, and a minor diameter of 0.0667 in. were assumed. The total cross-sectional area for 4 screws was 0.0140 sq in., and the failure load was then 700 lb. To produce this failure load with a converter structure weighing 0.156 lb, a required g-level of 4,500 g's was calculated. Thus the converter mounting also proved to be exceptionally rugged.

Other converter components were judged to be designed with the same magnitude of failure load-to-mass ratios, and therefore were expected to exhibit similar resistance to shock and vibration.

3. FABRICATION OF MODEL T/E-1

3.1 Preliminary Fabrication Efforts

The preliminary fabrication efforts concentrated on the aspects of heat pipe construction and sodium handling. As shown in Figure 1, the heat pipe fill tube, part No. 12, is connected to the heat pipe by means of a weld. This weld must be performed manually because of the particular geometry of the weld, and preferably should be done from the inside of the heat-pipe tube. A prototype assembly was welded, and no difficulties were encountered.

Similarly, the sealing-off of the fill tube, part No. 12, by localized electron-bombardment melting, was explored. A piece of the niobium evacuation tube to be used, 1/8" o.d. x 0.020" wall, was set up under simulated conditions of electron-bombardment pinch-off, and it was found that the operation required 500 watts of electrical power, and the amount of gas released was undetectable in a 400-liter/second vacuum system operating at 2×10^{-6} torr. Both ends of the pinch-off, shown in Figure 9, were leak-checked and found to be leak-tight. Following this test, a fixture was designed to permit the same operation to be carried out with a completed heat pipe. This fixture is shown in Figure 10.

Also, the compatibility of sodium metal with encapsulating glass was tested in stainless steel test tubes, as shown in Figure 11, at possible distillation temperatures of 400°C and 500°C. It was found that the glass reacts slightly at 500°C and that at this temperature it also softens considerably, as shown in Figure 12. From previous experience with cesium capsules, it appeared that distillation temperatures of up to 500°C could be acceptable. The sodium vapor pressure is 1 torr at 430°C.

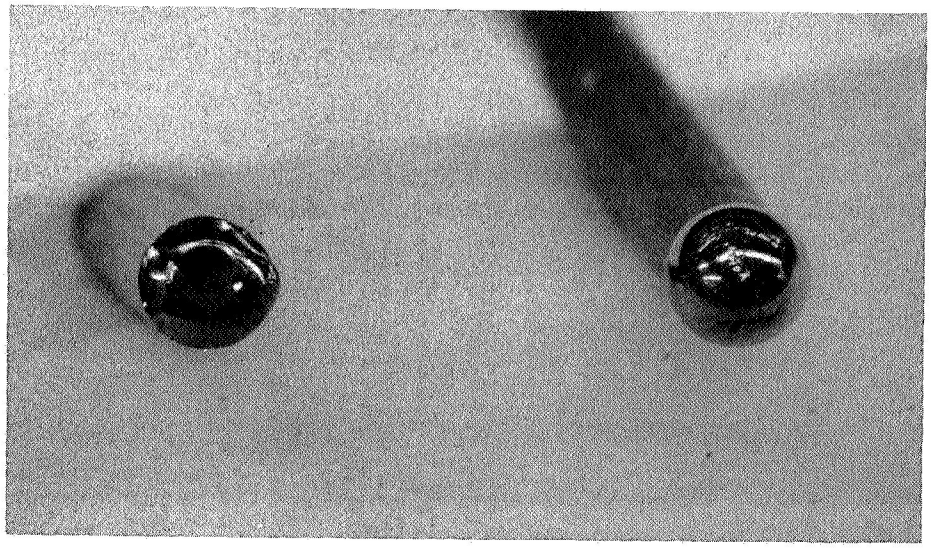

Figure 9

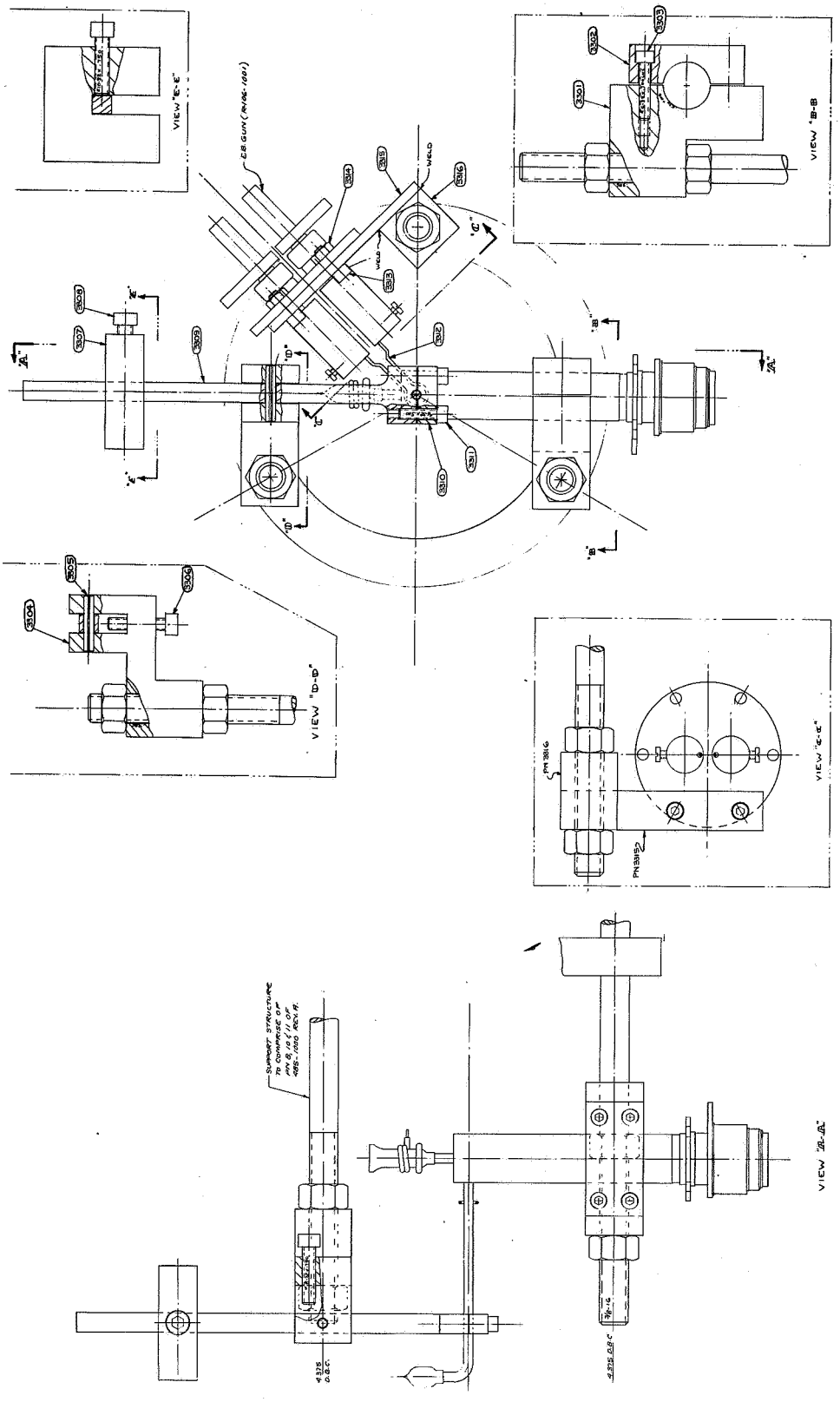
VIEW "E-E"
E.B. GUN (REF. 1001)
WELD
VIEW "B-B"
VIEW "D-D"
VIEW "C-C"
VIEW "A-A"
SUPPORT STRUCTURE TO COMPRISE OF PART OF ASSY. 495-1010 REV. H.

Figure 10

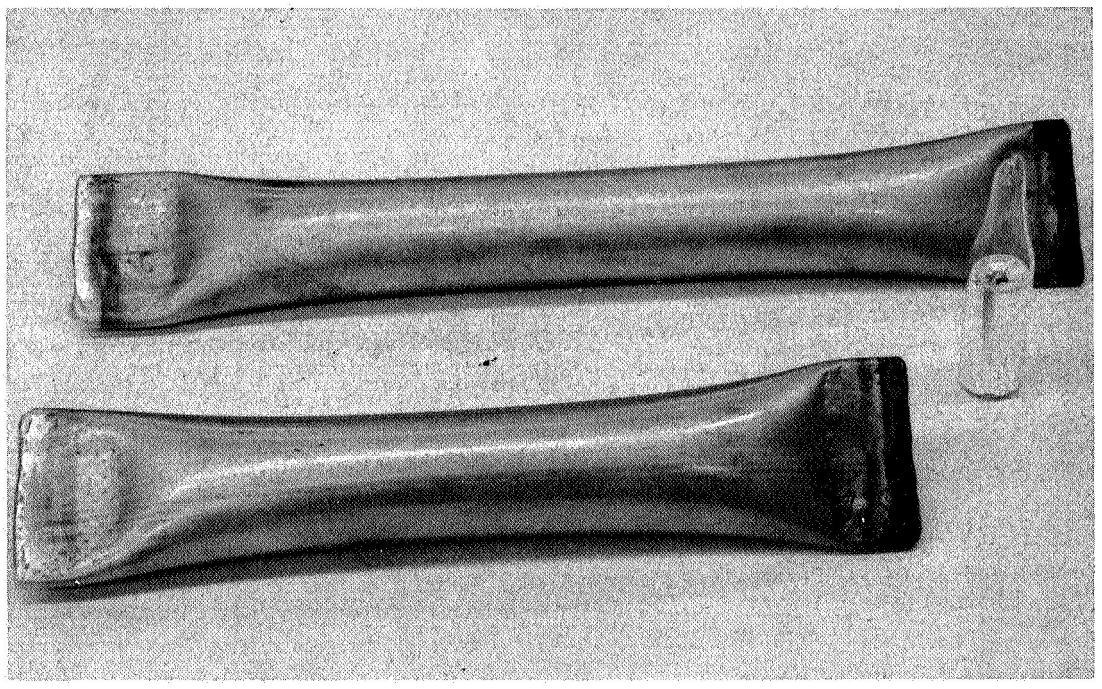

Figure 11

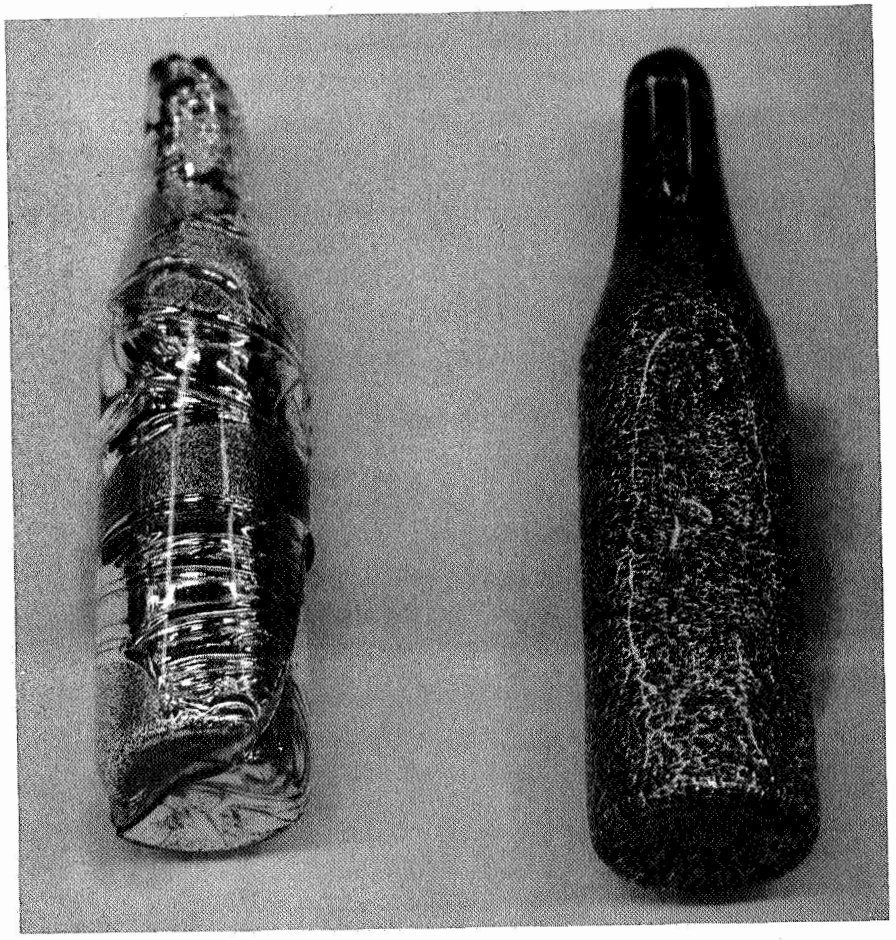

Figure 12

3.2 Fabrication Attempts

Several attempts had to be made before the fabrication of model T/E-1 was completed. These are designated T/E-1-A to T/E-1-D, and they are discussed in detail in the next sections of this report. A similar situation arose in the fabrication of model T/E-2.

3.3 Fabrication of T/E-1-A

The fabrication of T/E-1-A was started with the weld of the cesium reservoir tube assembly, parts Nos. 13 and 14, to the collector, part No. 8 (see Figure 1). Because it was found extremely difficult to reduce the diameter of the tantalum cesium tube at the end that is inserted in the collector, the design was changed to omit the diameter reduction of the tube and to enlarge the corresponding collector hole. The weld of the tube to the collector required a relatively large amount of heat, and although it could be successfully made, it resulted in a large amount of erratic melting on the collector face near the center hole. Also, the collector face was considerably oxidized, and the oxidation was suspected at that time to be due to outgassing of the electrode support in the welding chamber.

Next, the radiator tube subassembly, parts Nos. 9 and 12, coated by New England Hard Facing with Norton's Rockide C coating, was welded to the edge of the collector. For this operation the three parts of the seal assembly, Nos. 6, 10 and 11, were inserted around the radiator rube before the tube was fitted to the collector. The weld required a very large amount of heat, which made the collector face concave by several thousandths of an inch. Further evidence of oxidation was noted. In spite of the close proximity of the seal ceramic,

part No. 6, to the collector weld, it was found that the ceramic had withstood the exposure to the weld heat without cracking. After this step was completed the assembly was accidentally dropped, and the tube 13 broke at the collector end. The fracture was found to be completely brittle, which was a fact consistent with the evidence of oxidation near the welding areas. Since it was a simple matter to re-machine the collector to insert and weld a new cesium tube, and no other radiator tubes were immediately available to start a new assembly, a repair of the failed assembly was attempted. Before the new cesium reservoir tube was welded, however, the assembly was fired at 1400°C to clean the oxidized material. Figure 13 shows the assembly after the new cesium reservoir tube was welded. As can be seen, the 1400°C firing had caused some of the coating to disappear or flake off. Leak-checking of this assembly showed that the collector weld to the radiator tube was cracked and leaked.

At this point it was definitely suspected that the welding chamber must have had air leaks in spite of having passed recent examinations for leaks. A thorough leak-check revealed that the argon-pressure manometer had a large leak, which was further traced to a cracked soft-solder joint of its sensing bellows. The manometer was repaired, and sample niobium welds were run to check that no further oxidation would occur in the chamber during welding. The check was performed by purging the chamber, performing a weld, and then after letting the chamber stand one hour without further attention, performing a second weld. Both welds were clean and ductile, while previously the second weld had completely oxidized and embrittled the sample.

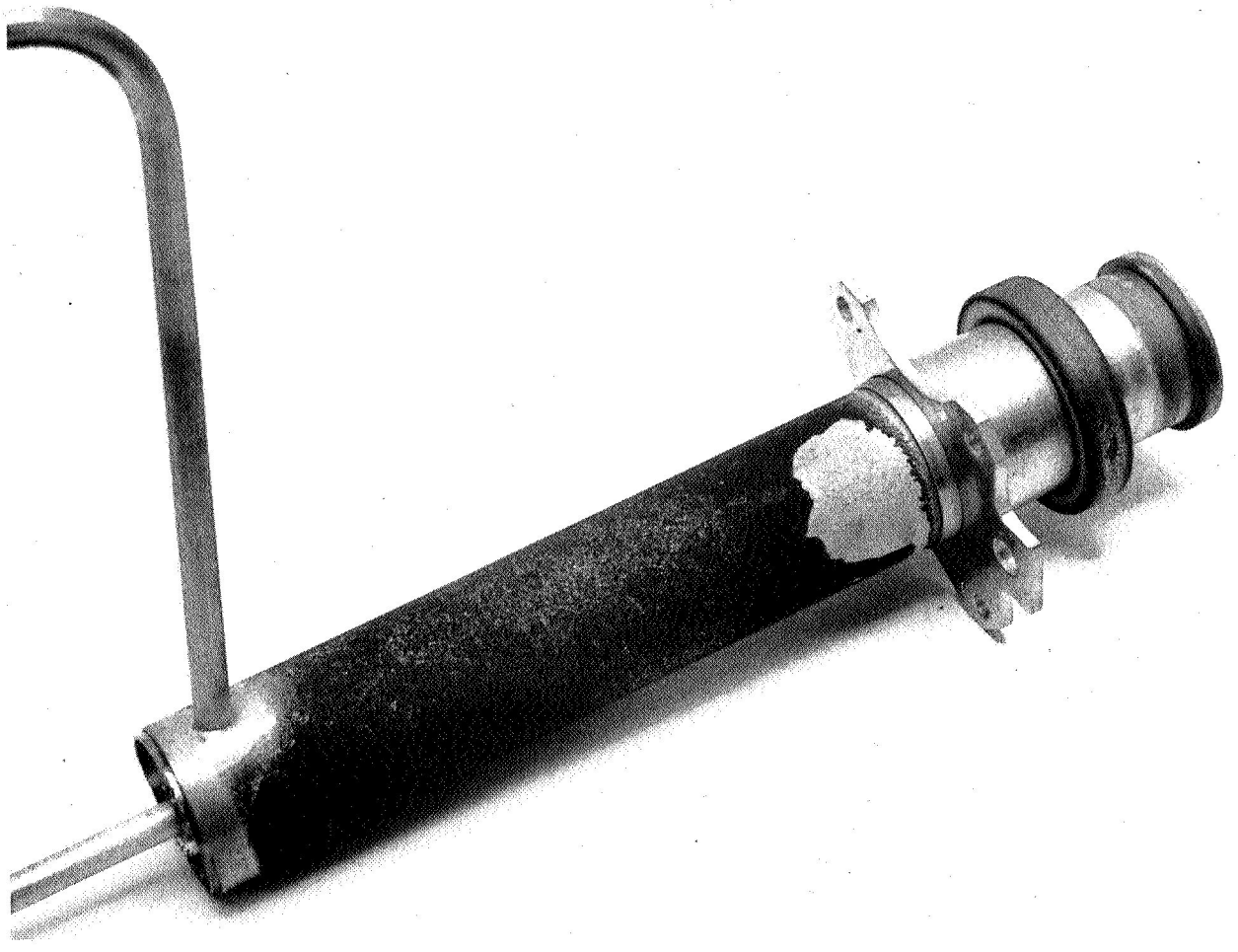

Figure 13

Because the structure of T/E-1-A had become embrittled at the area of the weld of the collector to the radiator tube it could not be repaired, and consequently the fabrication of T/E-1-A was abandoned.

3.4 Embrittlement of Coated Radiator Tubes

As the next attempt to fabricate the heat pipe model T/E-1 was about to start, a new batch of radiator tubes was received, coated with chromium oxide by the Linde Co. Because the surface of these tubes appeared contaminated, the tubes were cleaned with abrasive cloth and fired at 1400°C. When attempts were made to weld the sodium fill tube, part No. 12, the resulting joint was found to be extremely brittle. Further examination, as shown in Figure 14, indicated that the entire coated surface was brittle, but the uncoated portion of the tube was not. To check whether the embrittlement was common to the coatings of both Linde Co. and New England Hard Facing, the previously welded assembly of T/E-1-A was tested too. As Figure 15 shows, it also was brittle in the area of the coating.

Consequently, a meeting with a representative of the Linde Co. was held to discuss the details of the coating procedure and determine the cause of embrittlement. The representative took note of the facts, and two days later he submitted a tube of the original batch which had been returned to him in order to point out the problem of contamination during coating. This tube was not embrittled. It then became immediately obvious that the embrittlement must have resulted from the vacuum-firing at 1400°C that had been used to clean the impurities noticed after coating. This tube sample was then heated for 15-minute intervals to 925°C, 1010°C, 1200°C and 1425°C, and it was found that

Figure 14

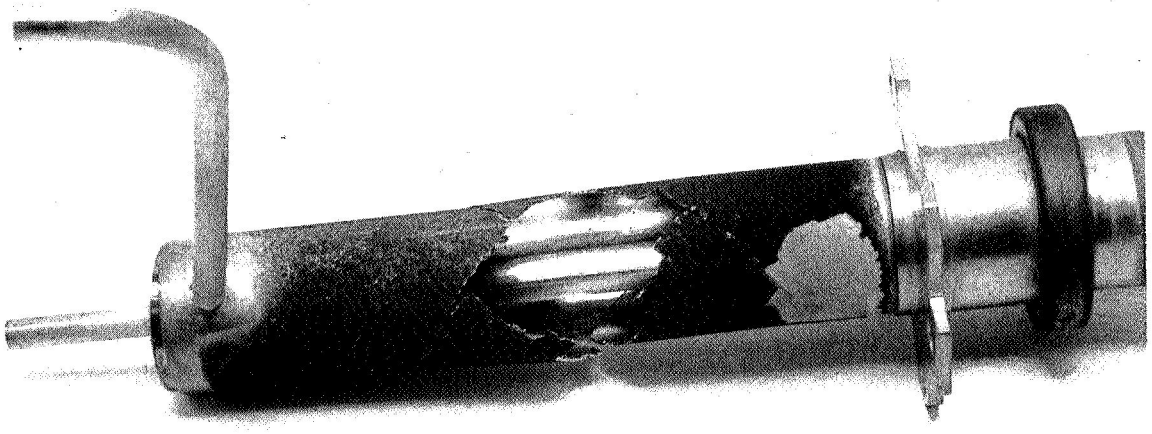

Figure 15

after the first three firings it was ductile, but after the fourth it was totally embrittled over the coating area. Therefore, the chromium oxide coating material reacts with niobium at some temperature in the range from 1200°C to 1425°C to form a brittle compound.

In order to avoid the need to fire the heat pipe radiator tubes at high temperature to remove residual impurities, an improved fixture was designed and fabricated to carefully shield the portions of the heat pipe that should not be coated during the coating process. This fixture is shown in Figure 16 with a heat-pipe radiator tube in position after coating. Figure 17 shows the coated tube as it appeared after removal. With the use of such fixtures it was possible to avoid the need for firing the tubes after they were coated, and the embrittlement problem was thus avoided also.

3.5 Fabrication of T/E-1-B

Since the longest-lead-time part for the fabrication of the heat pipe was the coated heat-pipe radiator, and since no un-embrittled ones were immediately available, it was decided, with the approval of the JPL Technical Representative, to omit the coating step in order to save time in the fabrication of T/E-1-B. Also, it was found that the cesium tube, part No. 13, could be joined to the collector face, part No. 8, by means of a palladium braze much easier than it could be arc-welded. Except for these changes, then, the new fabrication attempt was in accordance with the design of Figure 1.

The assembly sequence was as follows: First the heat-pipe inner tube, part No. 14, was welded to the cesium tubulation, part No. 13, at the point corresponding to the vicinity of the collector.

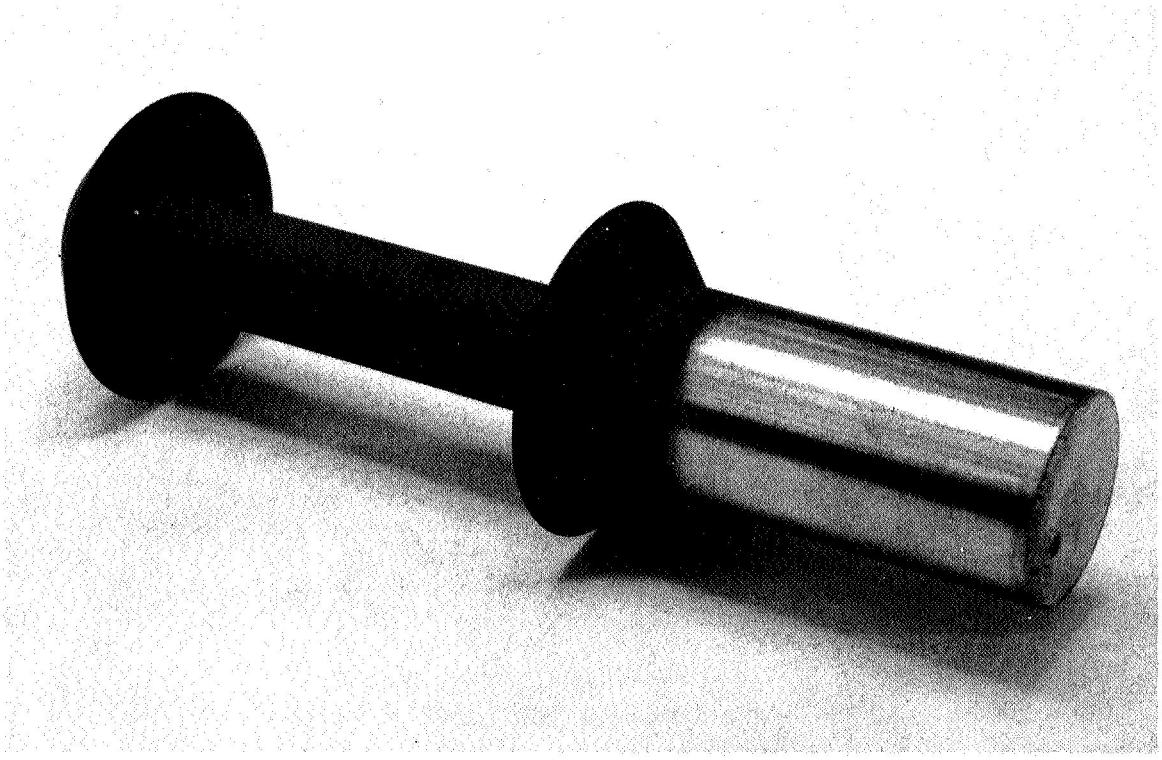

Figure 16

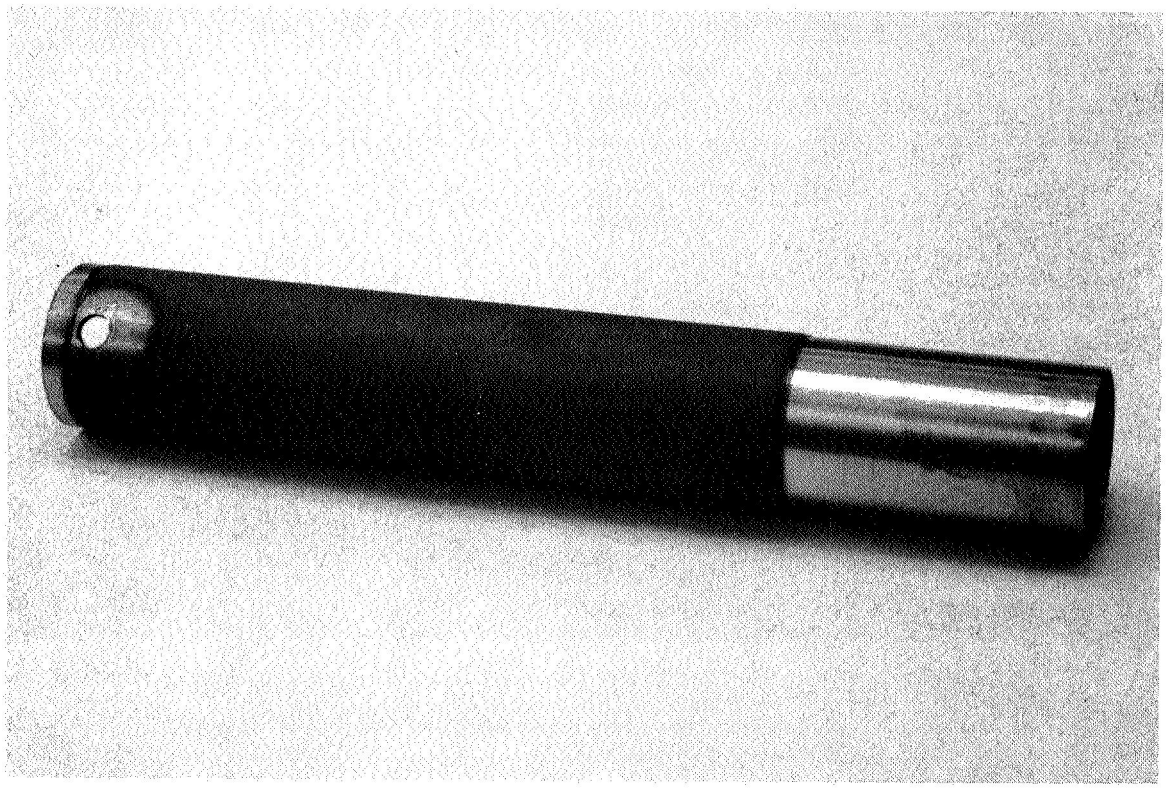

Figure 17

Next this assembly was palladium-brazed to the collector face, part No. 8. A sodium fill tube, part No. 12, was arc-welded to the outer heat pipe wall, part No. 9, and this assembly was then set up for welding to the collector face, part No. 8, after insertion of the seal sleeve and support plate, parts Nos. 10 and 11. Upon attempting to weld the collector face to the outer heat pipe tube, part No. 9, it was found that there was enough variation in position of the arc from the arc welder tip to cause an accidental blow-hole through the wall of the heat pipe close to the location of the weld bead. This accident was remedied by the insertion of a fragment of niobium and localized melting to seal the hole. After this was successfully completed the heat pipe assembly proceeded with the insertion of the capillary mesh screen of the outside wall of the heat pipe and its retaining elements, parts Nos. 16 and 17. One wrap of inner tube mesh was added, and the rear end seal plate, part No. 21, was positioned for final welding, after appropriate insertion of the end mesh elements, part No. 20.

During the welding of the end plate, it was noticed that the weld bead did not behave in the characteristic manner of niobium weld beads. While the final outer weld on part No. 21 was being performed, the welding arc suddenly flashed and pierced a hole through the entire thickness of part No. 21. It was immediately suspected that the capillary mesh, made of stainless steel, was near enough to the weld area to have melted and run into the weld bead, thereby contaminating it with materials that would both embrittle the bead and make the welding arc erratic. To verify this, the end of the heat pipe was opened, and it is shown in Figure 18. Although this may not be readily apparent in the photograph, melting of the capillary mesh was observed both

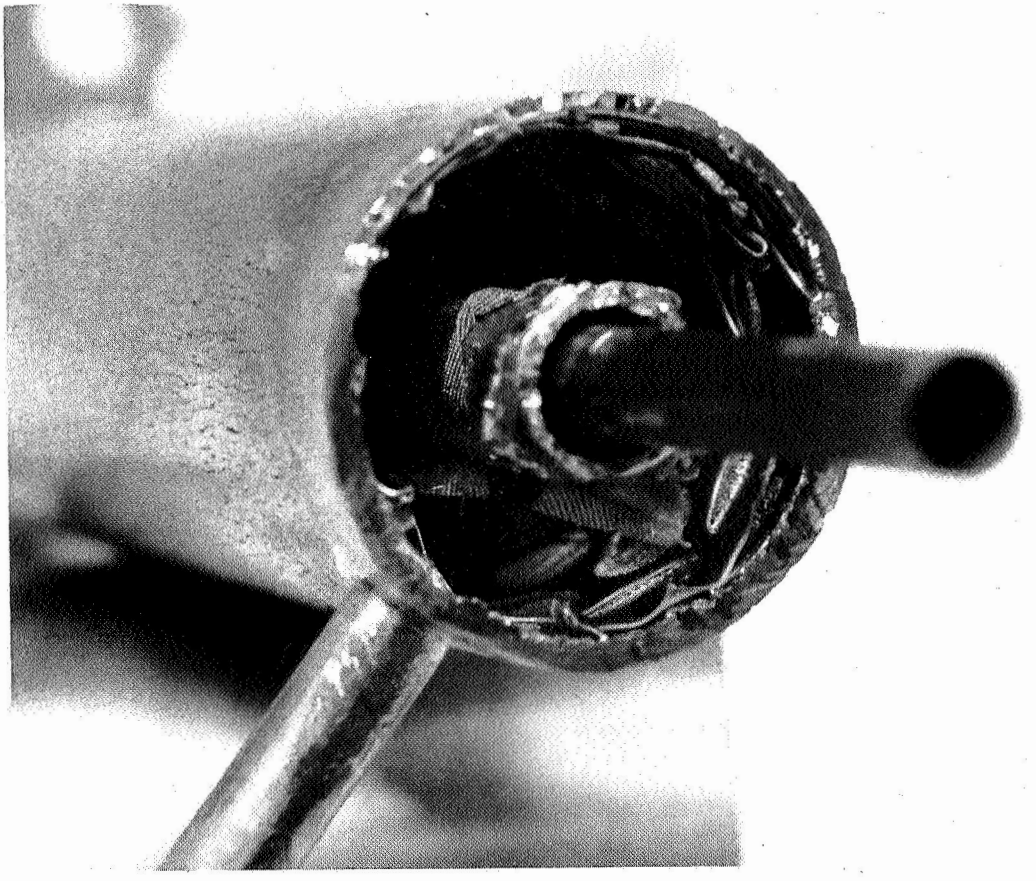

Figure 18

at the inside and outside tubes of the heat pipe. At that point it was decided that the structure could not be salvaged, and the assembly of T/E-1-B was abandoned.

3.6 Fabrication of T/E-1-C

The assembly of this third heat pipe model was carried out in exactly the same manner as that of the second model. The radiator coating step was omitted, and the same welding difficulties were encountered when an attempt was made to weld the outer heat pipe tube, part No. 9, to the collector face. The welding arc jumped twice on the heat pipe tube, causing blow holes which had to be filled with fragments of niobium locally. In view of this experience, it was decided that in future heat pipe prototypes this weld would be performed by electron-beam welding, to control the position of the welding bead with greater accuracy. In order to avoid the same type of capillary mesh melting which had occurred with T/E-1-B, the capillary mesh was cut short from the end of the tube so that the nearest point would be half an inch away from the welding bead locations. The perforated capillary mesh support, part No. 17, was still extended to the end of the heat pipe so as to provide a capillary path for the return of the sodium to the capillary mesh. It was then possible to weld the end cap, part No. 21, in place without any difficulty. Figure 19 shows the appearance of the welds of the end cap, and Figure 20 shows the completed heat pipe model, where the repair to the joint at the collector face is apparent.

3.7 Sodium Charge of T/E-1-C

The heat pipe T/E-1-C was connected to a copper manifold containing a sodium capsule, by fuse-brazing the connecting copper tube shown in Figure 1 to the niobium fill tube, part No. 12, with electron bombardment. The assembly was then connected to a Vac-Ion

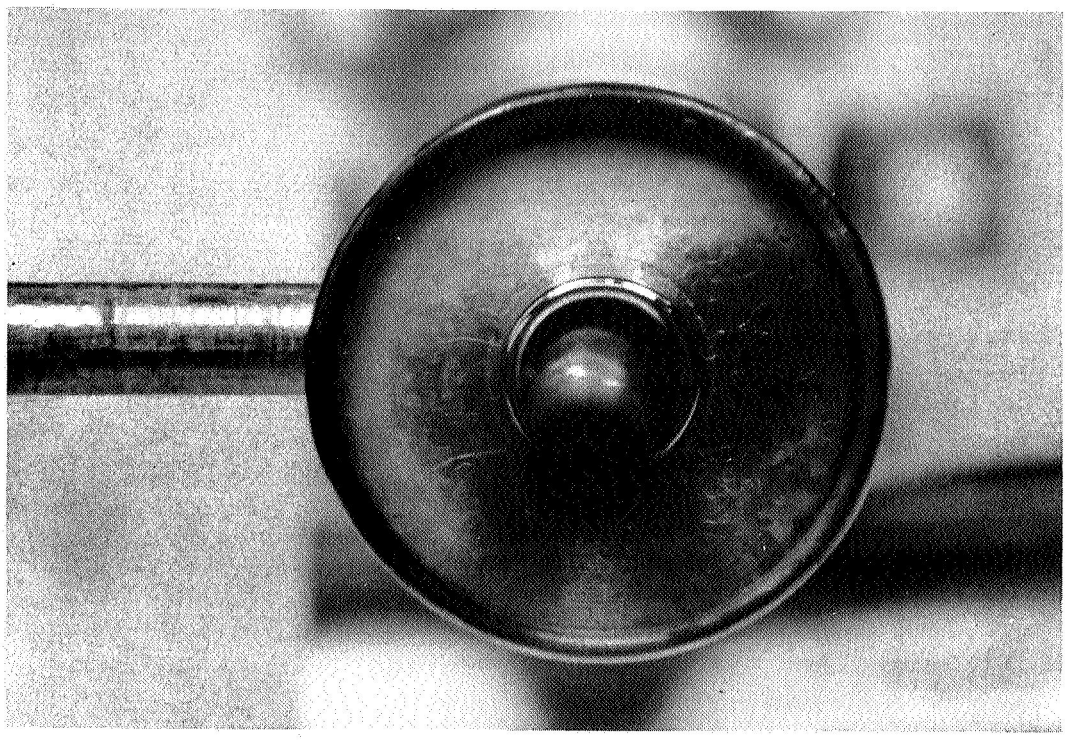

Figure 19

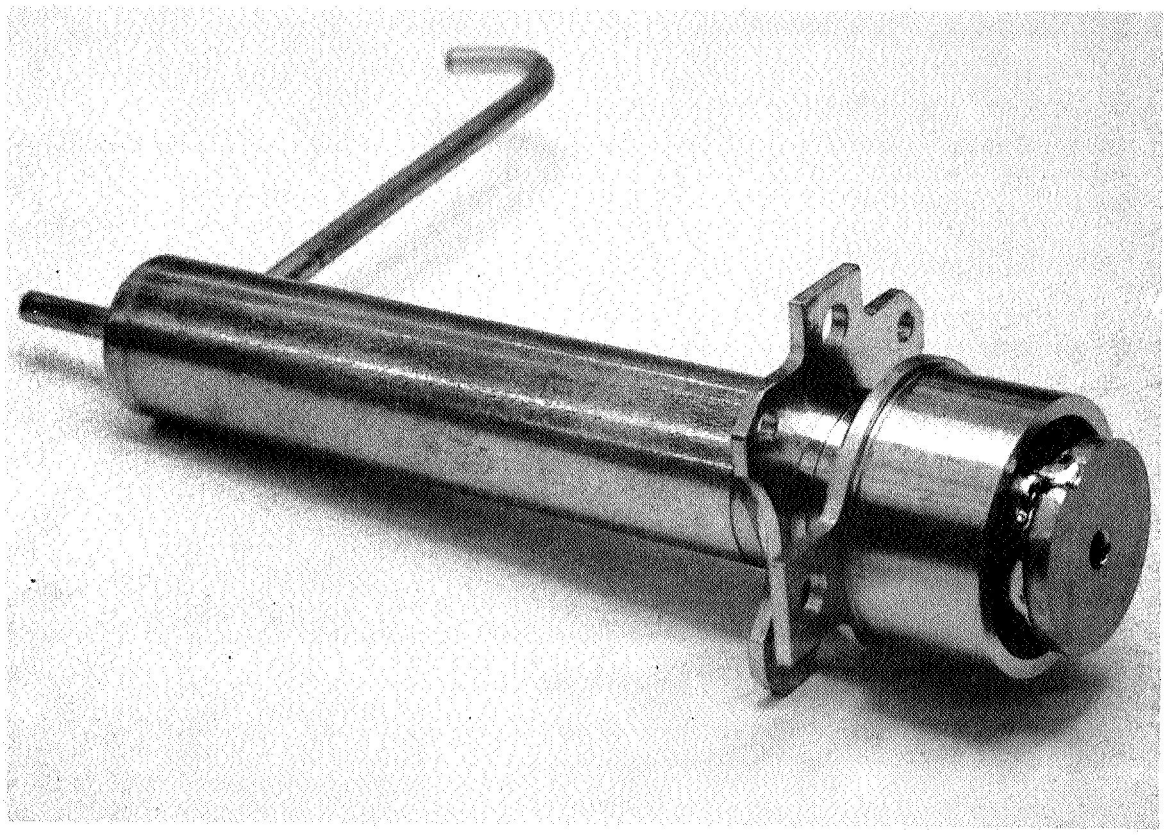

Figure 20

outgassing stand, heaters were mounted on the heat pipe, the connecting tube and the region of the sodium capsule. The heat pipe was heated under vacuum to 550°C, the connecting tube to 500°C, and the sodium capsule area to 300°C while the internal volume of the heat pipe was pumped with a Vac-Ion pump. After 9 days of continuous pumping the sodium capsule was broken, exhausted for one additional hour, and pinched off at a vacuum of 4×10^{-8} torr. Heat was then applied to the sodium capsule region with the intent of transferring the 2-gram sodium charge into the heat pipe by distillation. It was estimated that this would require 48 hours at 430°C. At the end of 24 hours, however, the bell jar of the vacuum system used for distillation was found to be coated with sodium. A leak in the sodium reservoir was located at a BT braze of copper pieces.

The sodium capsule manifold was then severed from the heat pipe, and the heat pipe was placed in vacuum at 700°C for 24 hours to remove the sodium distilled into it. A new manifold was attached, and the heat pipe was again outgassed to a vacuum of 4×10^{-8} torr. The outgassing time was 6 days. The same distillation procedure was again attempted, but in one hour the copper pinch-off of the manifold developed a sodium-vapor leak.

The distillation procedure was then reviewed, and it was decided to abandon it in favor of direct gravity transfer of molten sodium. The heat pipe with the leaky manifold was quickly inverted and placed back under vacuum in such a way that the sodium could be taken to the melting point and caused to flow into the heat pipe. Once this was done, the copper manifold was pinched off, and the heat pipe was set up for the final sealing operation, which involved pinching off the niobium fill tube, part No. 12, by electron bombardment.

The electron-bombardment pinch-off operation was carried out by placing a one-turn 0.030-in.-diam tantalum filament around the fill tube. This filament turn was 0.35 in. in diameter, and included a turn overlap of 0.20 in. so as to avoid the effect of local bombardment current, which is caused by lower filament temperature at the connection legs. When the fill tube was bombarded, the bombardment opposite the filament overlap area was found to be excessive; the fill tube melted locally at that point and developed a hole. Since a substantial amount of sodium vapor evaporated through this hole, the bombardment filament could no longer be maintained at a high potential difference with respect to the fill tube without violent arcing. The bell jar was heavily coated with sodium.

The vacuum system was opened to air in order to determine that this was what had happened. Since air leaked into the heat pipe in large amounts then, it was deciced to use the heat pipe structure to repeat the electron-bombardment pinch-off operation with a filament that did not have a turn overlap. This second pinch-off was successful, and is whon in Figure 21. The failed attempt is also evident in this figure. The complete structure of T/E-1-C is shown in Figure 22.

3.8 Fabrication of T/E-1-D

The heat pipe model T/E-1-D was fabricated according to the standard design of Figure 1 except that, as a result of the experience gained in the previous fabrication attempts, it incorporated the palladium braze of the cesium tube to the collector to avoid the distortion of the collector which occurs when welding is used, an electron-beam weld of the radiator tube to the collector to avoid the blow-holes caused by inert gas welding, and a shortened capillary mesh such as that used in T/E-1-C to avoid mesh melting during the weld of the end cap. The

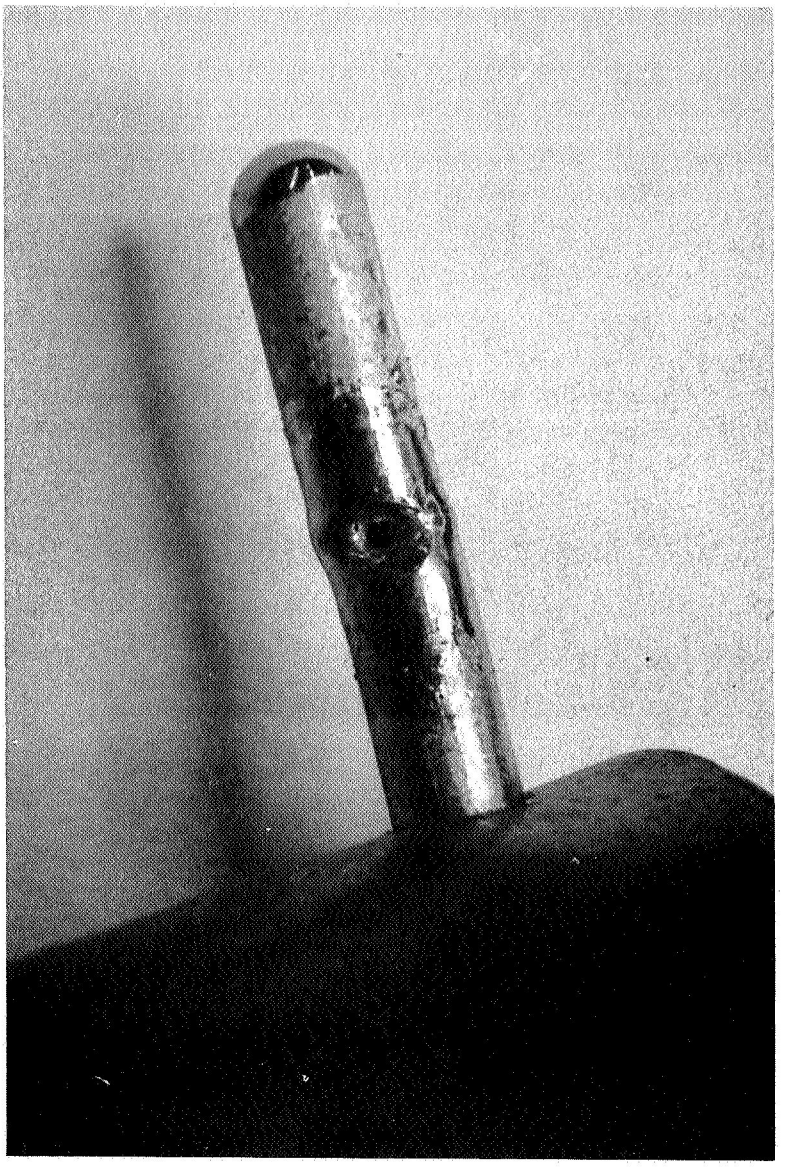

Figure 21

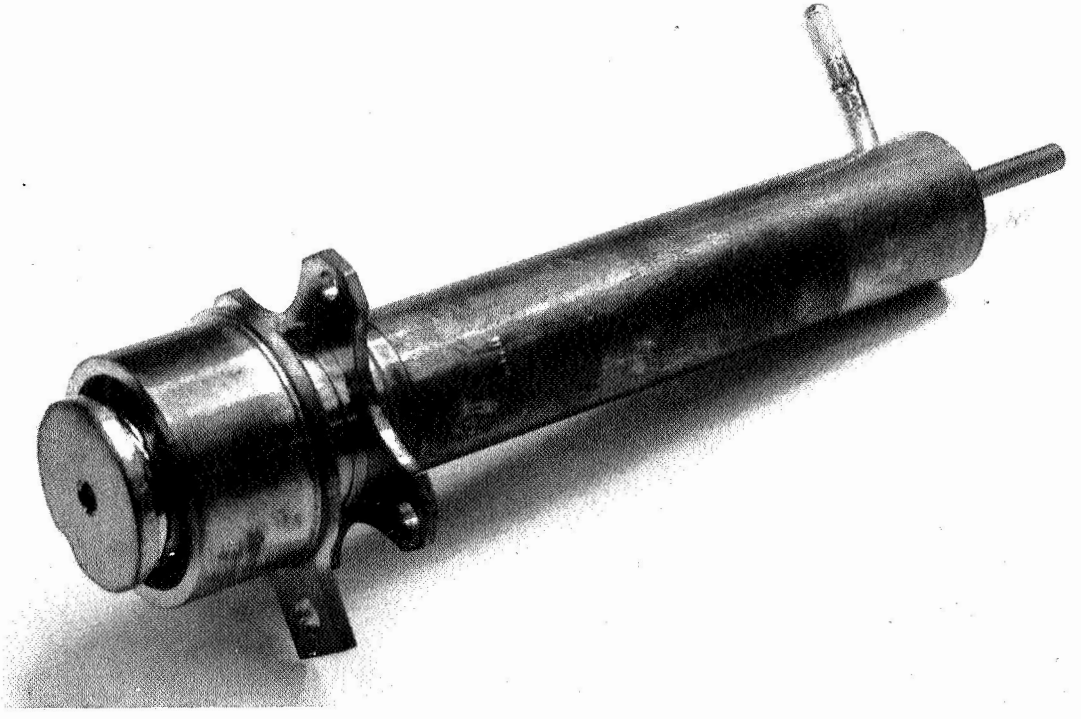

Figure 22

model also incorporated a coated radiator tube. In the first attempt, the electron-beam weld between the radiator tube and the collector leaked, and it was repaired by re-welding.

No further problems were encountered in the fabrication of this model except that it was discovered after assembly that the inner capillary mesh screen, part No. 18, which is wrapped around the inner heat pipe tube, had been omitted accidentally. Another minor difficulty which may be of interest was encountered when making the final heat pipe weld between the end cap, part No. 21, and the inner heat pipe tube, part No. 14. The difficulty is that the cesium reservoir tube, part No. 13, never lies perfectly concentric with the inner heat pipe tube, part No. 14, and as a result it tends to rest at some point around the circumference of tube 14 right next to the region where a weld must be made between the end of tube 14 and the end cap 21. There is then the danger that, during the welding operation, the cesium reservoir tube will be welded to the inner heat pipe tube in the region of the weld. This problem was avoided by a coiled 5-mil-diameter tungsten wire around tube 13, slipped between tubes 13 and 14 in order to ensure concentricity. The weld could then be performed with no further difficulty, but the wire which had been inserted could not be removed, and as a result parts 22 (two wraps of tantalum shielding around the cesium reservoir tube) could no longer be inserted in order to shield the cesium reservoir tube from the radiation from the inner heat-pipe tubulation.

Since no experimental evidence was yet available that these shields were necessary for proper operation of the cesium reservoir, they were omitted from the assembly of T/E-1-D. Subsequent tests have shown that these shields are unnecessary for proper operation of the cesium reservoir.

3.9 Sodium Charge of T/E-1-D

To charge the model T/E-1-D with sodium, a copper manifold containing the sodium capsule was connected to the heat pipe. The capsule was broken under vacuum, and the entire assembly was heated to approximately 150°C for half an hour. The position of the entire assembly was such that the molten 2-gram sodium charge would flow into the heat pipe. While the heat pipe was still connected to the exhaust pump, its temperature was raised to 425°C under vacuum, keeping the reservoir of sodium at 160°C. Pumping continued for a period of approximately 26 hours, at which time the copper manifold was pinched off from the heat pipe. The pinch-off of the niobium tube, part No. 12, was then accomplished by electron-beam melting of the tube.

After completion of the electron-beam pinch-off operation, the copper tubulation simulating the cesium reservoir was fuse-brazed to the cesium tube. The tubulation was then pinched off and given a thin coating of black paint in order to help achieve low reservoir temperatures.

4. TEST OF MODEL T/E-1

4.1 Test Set-Up

Figure 23 shows the fully instrumented model T/E-1-D. Six thermocouples were placed along the radiating portion of the heat pipe at equal spacings, and a seventh thermocouple was placed on the cesium reservoir.

The thermal connection between the thermocouples and the wall on which they were attached was effected by means of ceramic cement, and to minimize the mechanical load on this junction, an additional wire support was wound around the insulated thermocouple leads as shown in the figure.

After the instrumentation was mounted on the heat pipe, the heat pipe was placed in a vacuum chamber in an upright position with the collector facing upwards, and an electron-bombardment unit was installed to heat the collector face. The data obtained at various heat inputs is shown in Table 1.

4.2 Interpretation of T/E-1 Data

Data point No. 1 is the temperature distribution preceding test. Data point No. 2 shows the temperature distribution obtained with a nominal amount of filament heating and no electron-bombardment power applied to the heat pipe. Data points Nos. 3 to 8 give the temperature distributions obtained at various amounts of electron-bombardment power input, which are listed at the bottom line of Table 1. It can be seen that up to 311 watts of electron-bombardment power input, excluding filament heating, was applied, and heat pipe temperatures in excess of 800 °C were obtained. The thermocouple

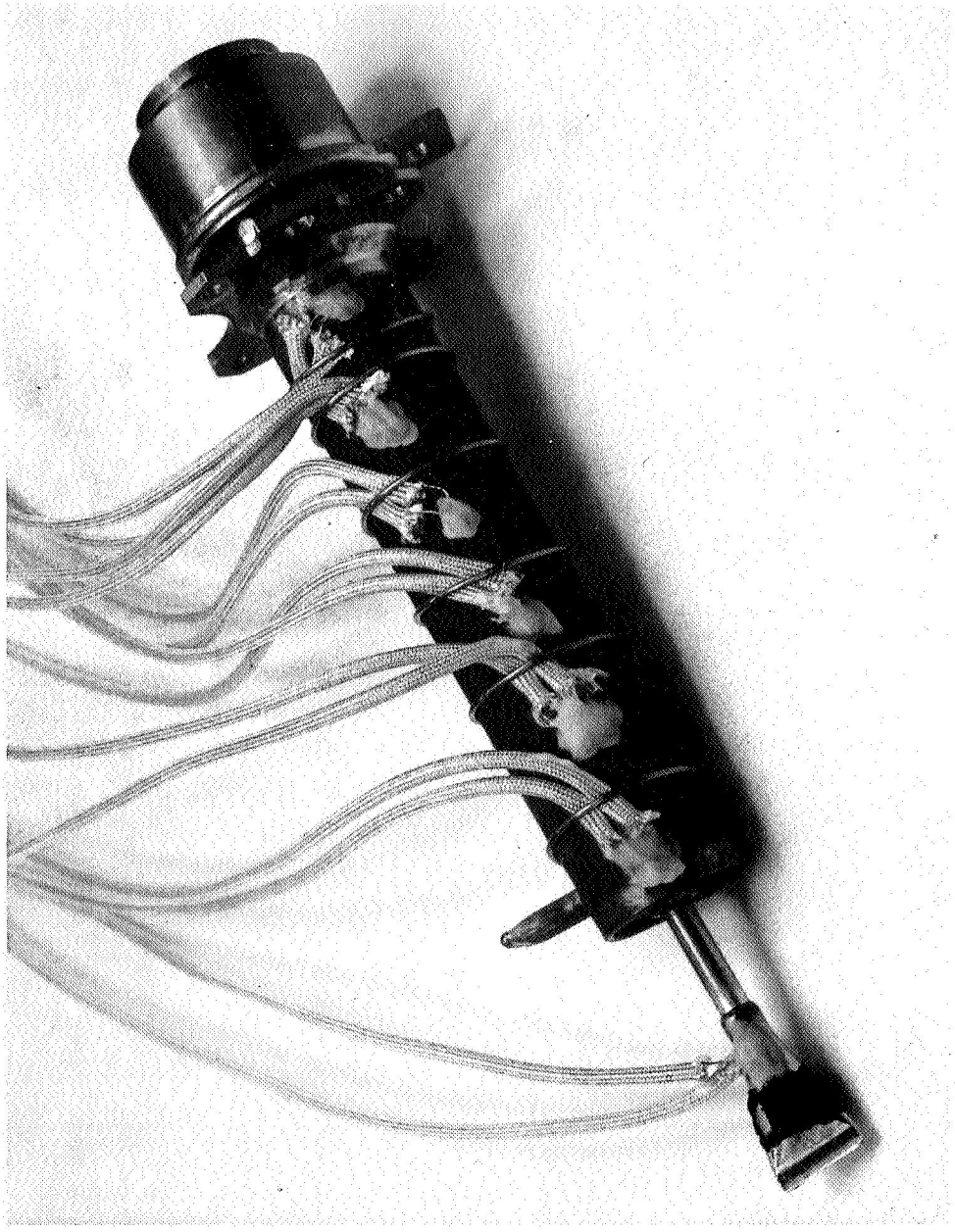

Figure 23

THERMO ELECTRON
ENGINEERING CORPORATION

TABLE 1

HEAT PIPE TEST DATA — DATE: 1-30-1967 — SHEET 1

MODEL: T/E-1D — OBSERVER: P. Brosens

	1	2	3	4	5	6	7	8	9	10	11	12
Time	10:20	13:07	13:45	15:15	15:48	16:07	16:22	16:37				
V_{eb}, volts	0	0	1027	1010	997	983	976	968				
I_{eb}, mA	0	0	43.6	76.1	121.4	191.5	251.7	321.4				
V_{Fil}, volts	0	4.4	4.4	4.6	4.8	5.1	5.2	5.4				
I_{Fil}, amps	0	20	20	20.8	21.7	22.6	23.0	23.6				
W_{Fil}, watts	0	88	88	95.6	104.1	115.2	119.5	127.5				
T.C.'s: Reservoir (14)	1.6	6.30	8.79	9.94	11.07	12.43	13.04	13.74				
°C °	40	154	217	245	272	305	320	337				
HP #1 (top) (8)	1.6	11.75	19.07	22.44	25.84	29.65	31.90	33.86				
°C	40	289	463	542	622	712	766	814				
HP #2 mV (9)	1.6	10.50	18.36	21.84	24.97	28.44	29.82	30.60				
°C	40	258	446	528	601	681	716	735				
HP #3 mV (10)	1.6	9.90	18.30	21.67	24.90	28.62	30.29	31.71				
°C	40	244	445	524	600	687	728	761				
HP #4 mV (11)	1.6	7.60	14.65	17.35	20.15	23.78	25.66	27.62				
°C	40	187	358	423	488	574	617	664				
HP #5 mV (12)	1.6	7.12	14.18	16.85	19.61	22.83	24.69	27.41				
°C	40	175	347	410	476	552	595	659				
HP #6 (bottom) (13)	1.6	9.00	18.36	21.76	24.98	28.65	30.87	32.47				
°C	40	222	446	526	602	688	741	780				
Average of #1 & #6, °C	40	255	454	534	612	700	753	797				
W_{eb}, watts	0	0	44.7	76.8	121.1	188.3	245.4	310.6				
Pyrometer Reading, °C	(very high background reflections)							970				

locations on the heat pipe were numbered 1 to 6, starting from the top of the heat pipe.

Thermocouples 2, 3, 4 and 5 had a tendency to read substantially lower than thermocouples 1 and 6, at the top and bottom of the heat pipe. This was assumed to be due to a shorting of the leads of the low-reading thermocouples by the clamping wires shown in Figure 23. Later tests on Model T/E-2-C have shown that even the readings of the highest-output thermocouples are low because of thermal contact resistance between the heat pipe wall and the ceramic cement used for thermocouple bonding. For this reason, the temperature data given in Table 1 is discussed in Section 6.3 with that of Model T/E-2-C.

One particular observation which was made during the test of Model T/E-1-D turned out to have pivotal importance in the interpretation of the data collected on both models. This is the pyrometer reading which was taken during the test condition # 8 in Table 1. It was taken next to the collector face in an attempt to determine the extent to which the collector temperature is the same as the heat pipe temperature, and, as is shown in Section 6.3, only a very small difference occurs.

After completion of the thermal test shown in Table 1, the heat pipe was maintained at the maximum operating heat input of 335.4 watts (including the contribution by radiation from the filament given further below in Table 3) overnight in order to accumulate an operating time of 100 hours at maximum power input, as specified in the Statement of Work. A thermal cycling test of 12 cycles would have followed the steady-state run of 100 hours. Sometime in the next 16 hours of running, however, the heat pipe developed a leak and lost the sodium charge.

4.3 Analysis of the Failure of Model T/E-1-D

When the test chamber was opened to air, it became evident that the location of the sodium leak was near the weld between the sodium fill tube, part No. 12, and the heat pipe radiator tube, part No. 9. Figure 24 shows this area of the heat pipe, and the location of the leak can be identified by the white deposit of sodium hydroxide at the transition between the uncoated and coated portions of the heat pipe. The hydroxide is the result of the reaction of the residual sodium at the leak with the water vapor in the atmosphere.

The leak itself seemed to be in the form of a crack in an area where it appeared that a very narrow zone of the chromium oxide coating of the heat pipe had reacted with the heat pipe wall, presumably as a result of excessive heat during welding. To verify the fact that this weakening of the wall had occurred before exposure to sodium, another structure, which had been welded to serve as a back-up for T/E-1-D, was inspected. Figure 25 shows that it revealed the same characteristic reaction region at exactly the same location. Since this structure had not yet been filled with sodium, it was concluded that the reaction was caused by weld heat. Consequently, a new assembly was welded using copper chill blocks, and as shown in Figure 26, it was possible to obtain a very clean weld with no traces of any coating reaction.

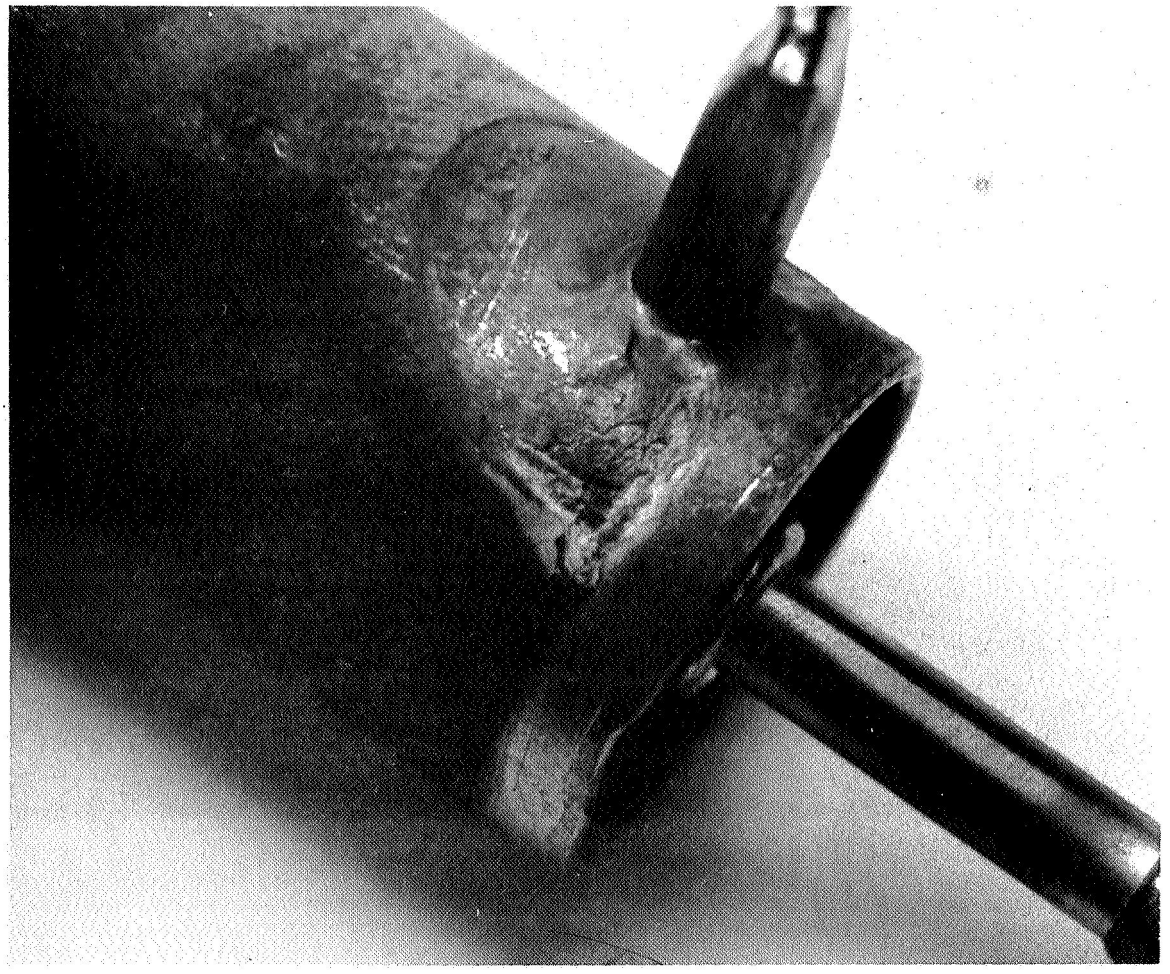

Figure 24

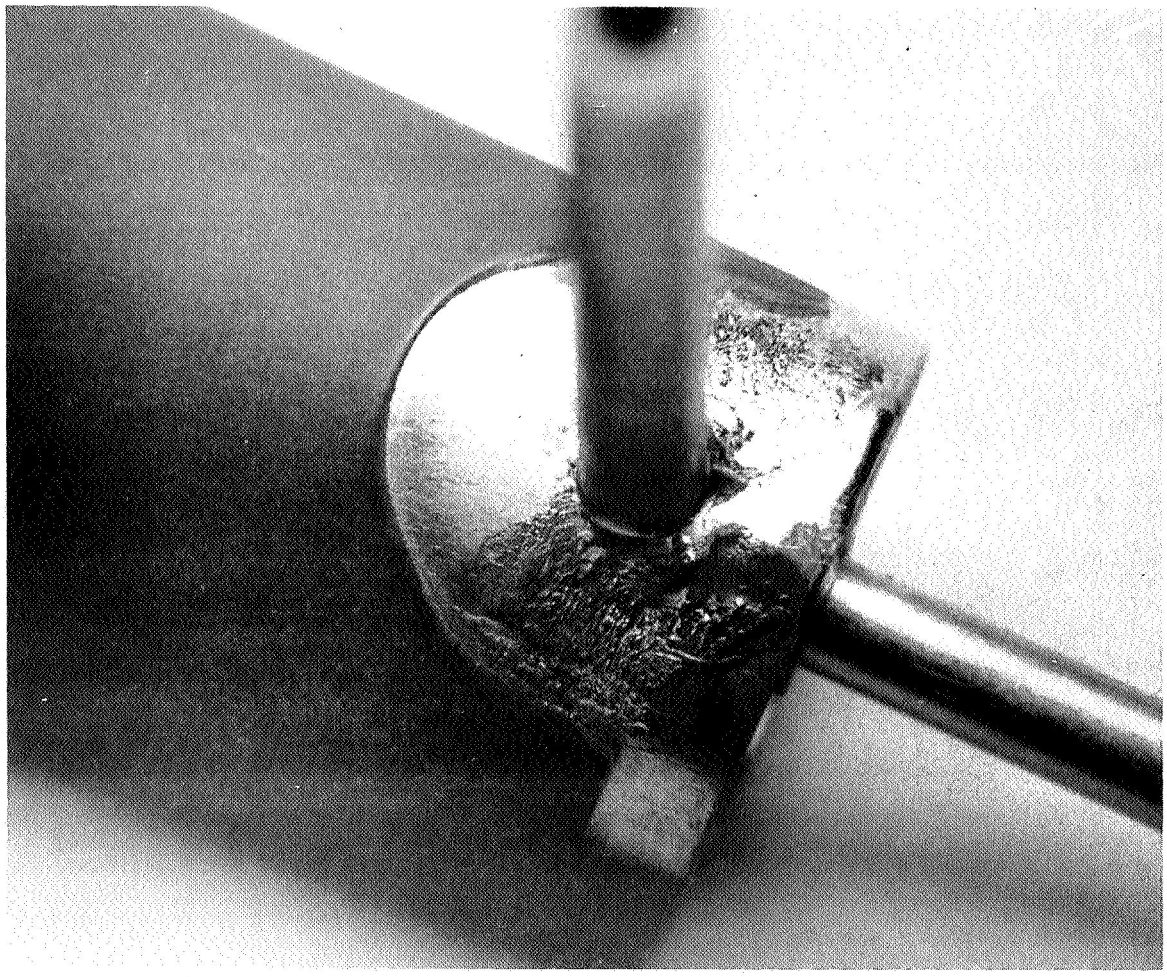

Figure 25

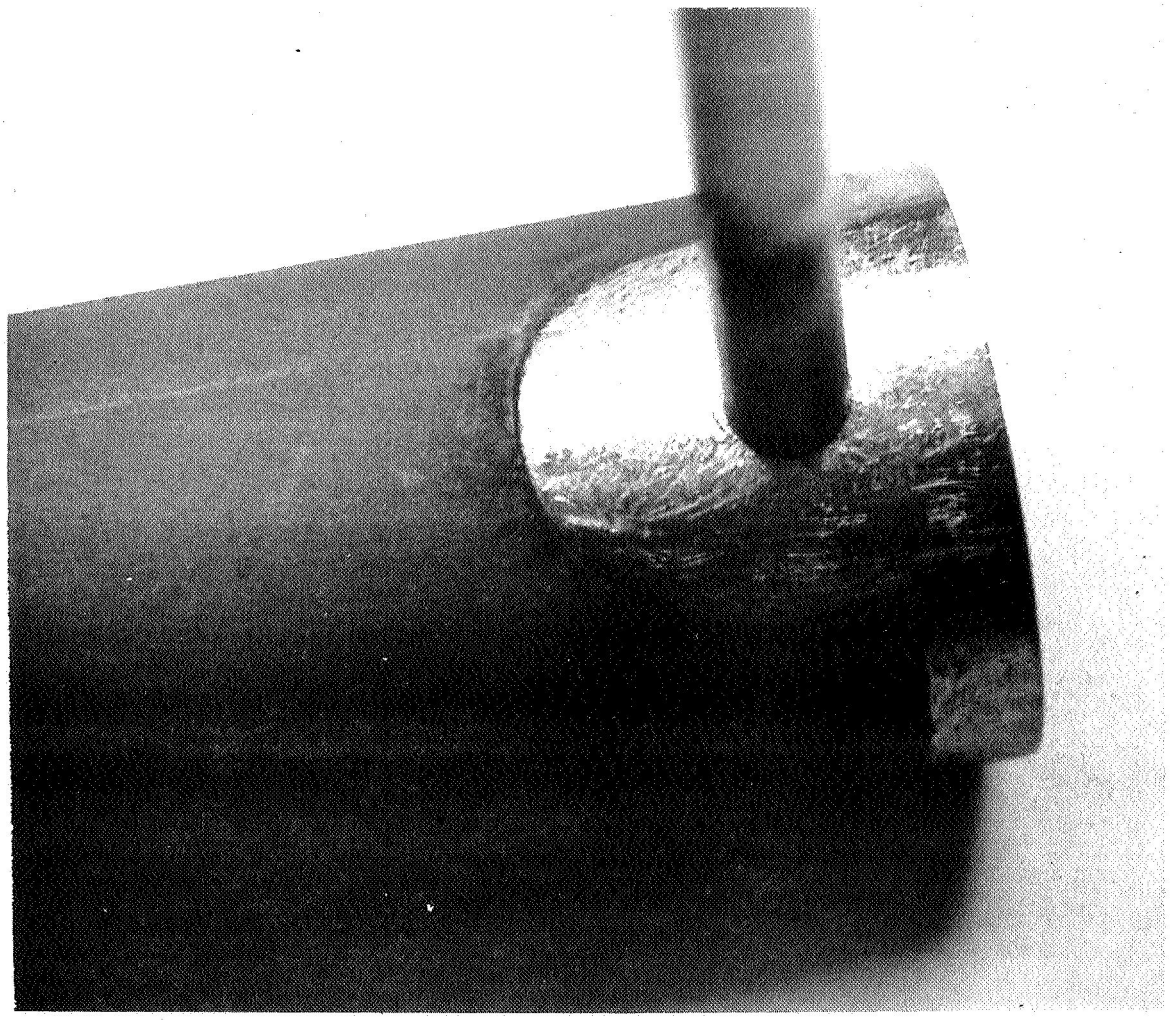

Figure 26

5. FABRICATION OF MODEL T/E-2

5.1 Fabrication of T/E-2-A

Model T/E-2-A differed only in that the cesium reservoir was made of a chromium oxide-coated nickel piece on which thermocouples could be mechanically fastened, and Figure 27 shows a photograph of the unit fully instrumented. The instrumentation also differed in that seven thermocouples were provided along the length of the heat pipe instead of six, and a thermocouple was attached to the collector face. The model was sodium-charged in the same manner as T/E-1-D except that the final niobium pinch-off was performed by electron bombardment rather than by electron-beam melting.

5.2 Testing of T/E-2-A

This model was set up for test, and the test data showed that no temperature uniformity could be achieved along the length of the heat pipe wall. This was an indication of either the presence of large amounts of gases or a lack of sodium within the heat pipe. The test was discontinued, and the heat pipe was opened by cutting its fill tube to examine whether any traces of sodium were visible. As none were seen, the model was placed in a vacuum furnace and heated at 900°C for two hours. A slight coating of sodium was produced over the surface of the vacuum bell jar in the first few minutes of heating. The amount so accumulated was so small that it was concluded that model T/E-2-A failed to operate because it lacked a sufficient charge of sodium to establish full wetting of the capillary conduit between the collector and the radiator surface. When full wetting is not obtained, the sodium can be expected to collect at the cool end of the heat pipe, and thus completely interrupt heat pipe operation.

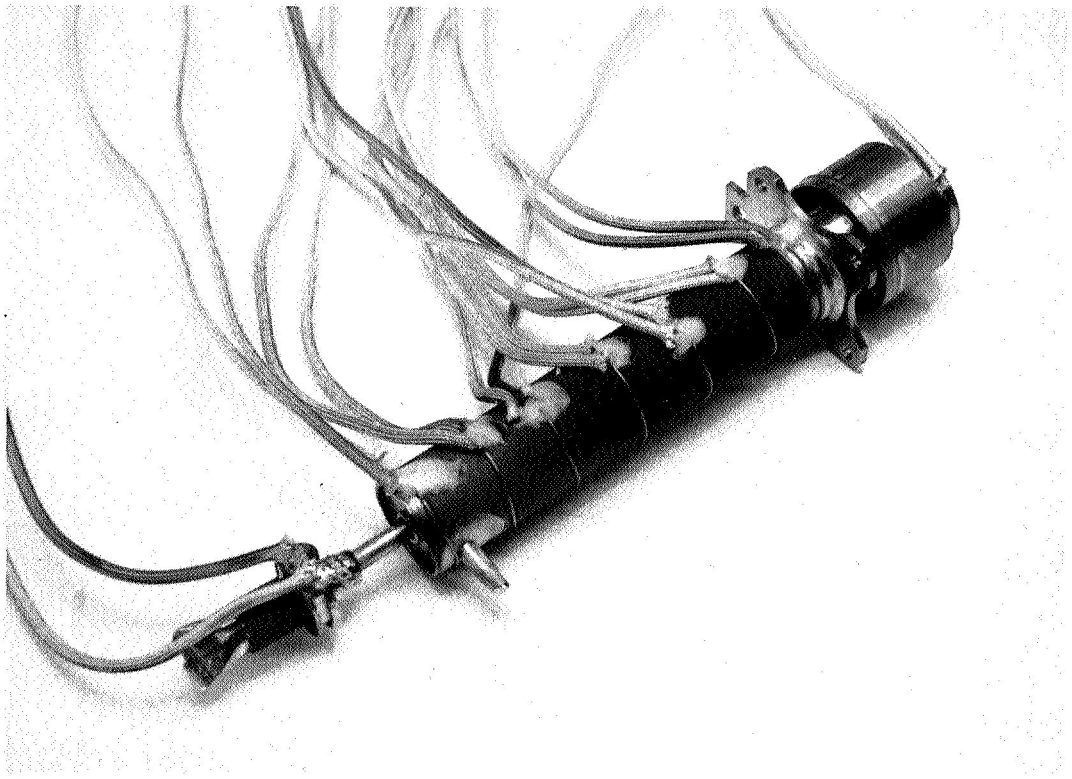

Figure 27

Further examination of the tubulation from which sodium had been distilled into the heat pipe revealed that a large quantity of glass fragments had been produced upon breaking the capsule, and that many of the smaller pieces of glass had collected in the fill tube, to the extent that this tube was almost completely plugged.

5.3 Fabrication of T/E-2-B

After T/E-2-A was vacuum-heated to remove its residue of sodium the niobium fill tube was cut, and a new tube was connected by means of an adapting piece made of niobium and brazed in place with palladium. The model was then outgassed and charged with sodium in the same manner as T/E-2-A except that care was taken to avoid breaking the sodium capsule at several places.

This model also failed to operate. It was opened by cutting the sodium fill tube, and it was placed in a vacuum furnace, where its temperature was raised to 1000°C. After 45 minutes of heating, no traces of sodium had been released, and it was concluded that the model did not contain any sodium. Inspection of the copper manifold used for sodium charging showed that the tube leading to the model had again become clogged by glass particles entrained by the sodium. This had occurred in spite of the effort made to avoid excessive crushing of the glass capsule, and it was concluded that, even when the glass capsules are cracked with the greatest care, they will still shatter into a large quantity of small fragments. Consequently, it was decided to incorporate a screen in the sodium fill manifold to retain the glass fragments.

5.4 Fabrication of T/E-2-C

When the next outgassing had been completed, a new sodium charging attempt was made, but this time it appeared that all of the sodium clung by capillary force to the sodium capsule, and again, none flowed into the heat pipe. The heat pipe model was reconnected to a new manifold, re-outgassed, and the sodium charge procedure was modified to drive the 2-gram sodium charge out of its glass capsule and through the filter screen by centrifugal force. Later examination of the manifold showed that practically all of the sodium had been driven into the heat pipe.

The weight of the completed heat pipe model T/E-2-C was 77.8 grams exclusive of electrical leads and mounting hardware.

6. TEST OF MODEL T/E-2

6.1 Test Data for Model T/E-2-C

Model T/E-2-C was instrumented in the same manner as T/E-2-A and tested at a range of power inputs to determine its ability to meet the design heat transfer conditions. Table 2 gives the observed temperature values. It is obvious that the collector face of this prototype, in contrast to that of model T/E-1-D, operated at a much higher temperature than the remainder of the heat pipe structure.

After measuring the response of the heat pipe to heat input, it was set for running continuously with the highest value of heat input at about 335 watts (including filament heating). At that time it was noted that, at the glowing edge of the collector, the temperature of the niobium tube welded to the collector would flicker in the region of the weld. This was certainly the result of intermittent capillary flow of liquid metal to the boundary between the cool wall and the hot collector, and the magnitude of the temperature excursions was approximately 50°C at a frequency of about 1 cycle per second. At the end of 23 hours of running in this condition, a sodium deposit was noticed on the bell jar, indicating a leak, and the test was terminated.

6.2 Analysis of the Failure of T/E-2-C

The model was first x-rayed to determine whether the installation of the capillary structure near the collector had been defective. This area cannot be inspected visually during assembly because then it lies at the bottom of a long cavity, and the visibility is further impaired by the presence of the collector insert, part No. 16. In order to explain the operation of the collector at temperatures much higher than heat

TABLE 2 SHEET 1

HEAT PIPE TEST DATA

DATE: March 23, 1967

OBSERVER: P. Broseur

MODEL: T/E-2-C

	1	2	3	4	5	6	7	8	9	10	11	12
Date									3-23	3-24	3-24	3-24
Time	10:16	11:19	11:48	13:23	14:00	14:39	15:05	SAME CONDITION TEMPERATURES READ WITH PYRO.	18:05	10:35	14:31	16:35
Elapsed Time, hrs									3.0	19.4	23.4	25.5
V_{eb}, volts	0	1023	1009	995	982	974	966		0 HRS	966	967	
I_{eb}, mA	0	43.9	76.9	123.1	191.9	251.1	321.0		ELAPSED TIMER AT	321.3	321.7	
V_{Fil}, volts	4.9	4.2	4.5	4.7	4.9	5.0	5.2		HEAT PIPE CONTINUE AT	5.1	5.0	
I_{Fil}, amps	21.0	18.8	19.9	20.3	21.1	21.8	22.1		321 mA INPUT	21.7	21.6	
T.C.'s: Reservoir (14)	6.29	8.65	9.97	11.23	12.61	13.60	14.56	—	SET LETTING	14.55	14.53	
°C	154	213	245	277	309	333	356			356	355	
HP #1 (top) (7)	12.96	18.50	21.88	25.08	28.83	31.42	33.68	822		33.46	33.43	
°C	318	450	529	604	693	754	810			804	803	
HP #2 (8)	12.18	18.62	21.99	25.18	28.87	31.40	33.64	822		33.39	33.33	
°C	299	452	532	607	693	754	808			802	801	
HP #3 (9)	11.42	18.69	22.13	25.36	29.17	31.72	34.02	822		33.84	33.82	
°C	280	454	535	611	701	762	817			813	812	
HP #4 (10)	10.76	18.76	22.12	25.36	29.19	31.73	34.03	922		33.89	33.86	
°C	265	456	535	611	702	762	8.8			815	814	
HP #5 (11)	10.20	18.63	22.03	25.27	29.08	31.61	33.88	822		33.67	33.64	
°C	251	453	533	608	699	759	814			809	808	
HP #6 (~~bottom~~) (12)	9.77	18.16	21.56	24.75	28.42	30.75	33.08	822		32.86	32.82	
°C	240	442	521	596	683	738	795			789	788	
HP #7 (bottom) (13)	9.58	17.77	21.35	24.75	28.32	30.68	32.82	818		32.78	32.73	
°C	235	432	517	596	680	737	788			788	787	
Collector (6)	17.14	24.34	29.57	34.34	38.85	41.6	48.5	—		45.4	45.2	
Pyrometer brightness, °C	418	587	710	825 / 937	1036	1007 / 1074	1139 / 1163	—		980	979	

SODIUM DEPOSIT SEEN ON BELL JAR LEADING FROM COLLECTOR FACE TEST TERMINATED.

H.V. shut off at data pt #4 did not reveal stray emf on TC #6.

Pyrometer

pipe temperature, it would be necessary to have either a loose assembly in which the capillary mesh screen was not in good contact with the collector, or the complete absence of the capillary mesh screen, as could occur if the screen slipped during insertion into the heat pipe. The x-ray obtained revealed a faint gap between the collector and the collector insert piece, which could be due to either one of the possibilities just mentioned: loose assembly or absence of capillary screen in that area.

The converter was then leak-checked, and the point at which the leak had occurred was found at the weld between the collector and the outer pipe.

After it was leak-checked, the converter was opened, and the collector end was potted and sectioned for metallographic examination. The heat pipe section collapsed during potting, but still it was evident that there was no capillary mesh screen between the collector and the collector insert piece. The elements of the other half of the potted structure were separated at the capillary screen boundary. There, the face of the collector insert piece was completely bare of capillary screen.

No unusual hardness was discovered over any part of the internal walls of the heat pipe, and therefore failure due to fracture at an embrittled area, such as occurred in T/E-1, was ruled out.

From the above analyses it was concluded that the collector overheating was caused by imperfect assembly of the capillary mesh screen and the resulting absence of capillary connection of the collector. Furthermore, the leak was attributed to thermal fatigue of the collector weld, which was produced by the rapid temperature fluctuations in that area during heat pipe operation.

To investigate the difficulty of assembly of the capillary structure near the collector, a back-up assembly for T/E-2 was also x-rayed. It was seen that, in the collector area, the capillary structure did not reach the end of the heat pipe, and as a result, the collector insert piece was completely loose and had fallen off to one side.

6.3 Analysis of T/E-1 and T/E-2 Performance

The heat pipe temperatures for T/E-1 and T/E-2 were very nearly the same at corresponding values of power input. An exact comparison was not made because it was known that the thermocouples attached to the wall of the heat pipe had not remained well bonded and read low. In order to ascertain the extent of this error, data point #7 for T/E-2 was read using the thermocouples, and data point #8 was taken under the same conditions, using the pyrometer to read heat pipe temperatures. The thermocouples showed a heat pipe temperature of 810°C near the top, which decreased to 788°C near the bottom, while the observed pyrometer temperature was 822°C all along the wall except at the very bottom, where it was 818°C. Thus the temperature along the wall was much more uniform than the thermocouple readings would indicate. Assuming a bell jar correction of 10°C and a pyrometer correction of 2°C, it was estimated that the true heat pipe temperature at a pyrometer reading of 822°C was 834°C, and therefore the thermocouple with the highest reading was low by 24°C.

Figure 28 is a plot of the true collector temperature achieved in Model T/E-2-C, as measured by a spot-welded thermocouple, versus the pyrometer brightness temperature readings. With this curve, it was possible to estimate that the brightness temperature reading of 970°C performed on T/E-1-D corresponded to a true collector temperature of 841°C.

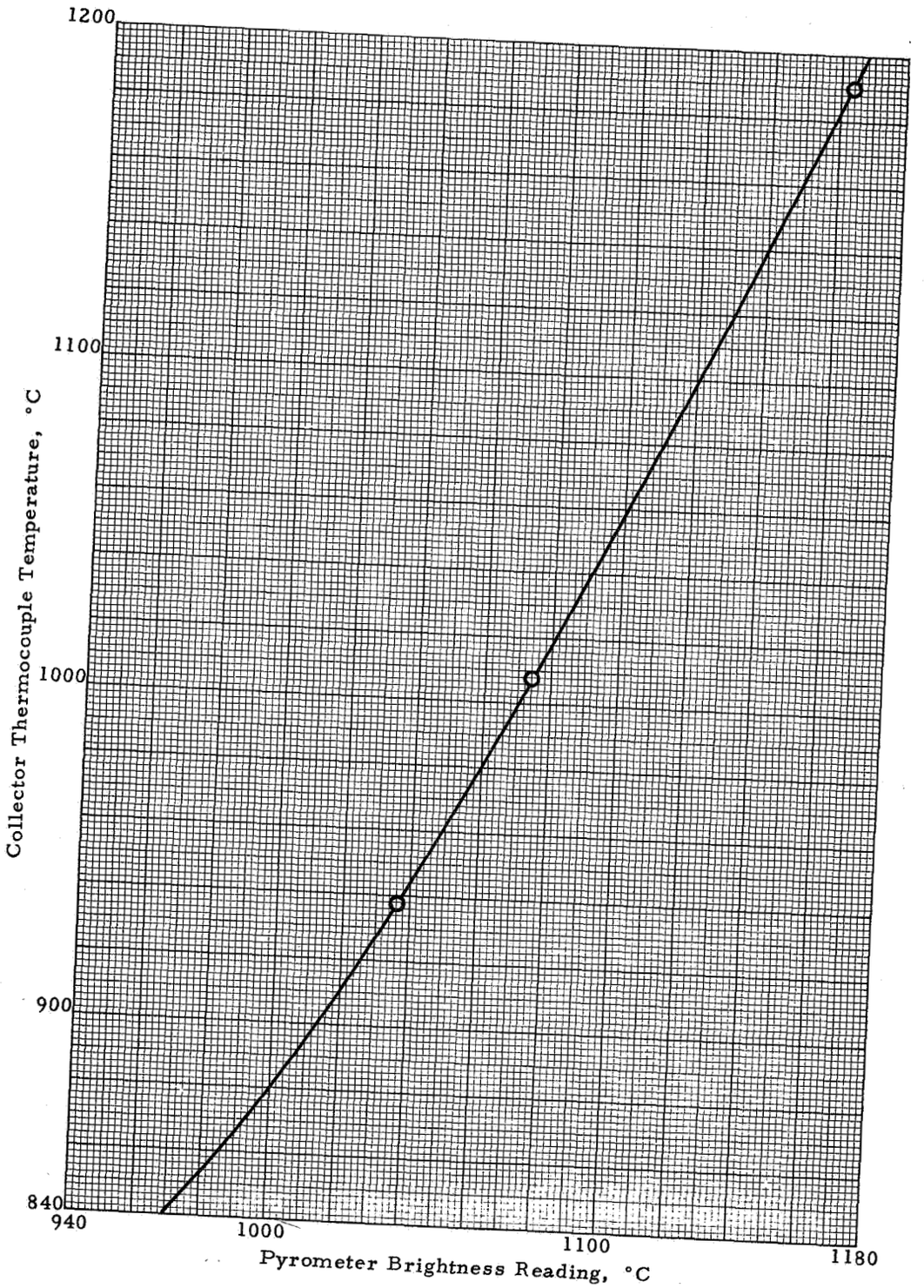
1200
1100
1000
900
840
Collector Thermocouple Temperature, °C
940
1000
1100
1180
Pyrometer Brightness Reading, °C

Figure 28

It is certain that T/E-1 achieved a slightly higher heat pipe temperature than T/E-2 at corresponding values of heat input because, with lower collector re-radiation, the heat load on the heat pipe was higher. Thus, at the conditions obtained with a bombardment current of 321 mA, it is reasonable to assume that the heat pipe temperature of T/E-1 was higher than 834°C, and therefore the temperature drop between the collector, which was estimated to be at 841°C, and the heat pipe must have been less than 10°C.

The most important result of the heat pipe tests was the relationship between collector heat transfer and collector temperature. To obtain this relationship, the T/E-1 data was used in spite of the fact that this model was not so well instrumented as T/E-2. The choice was made because T/E-1 achieved correct heat pipe operation, and the collector overheating of T/E-2 disturbed the heat-transfer conditions to an extent that could not be calculated accurately.

The collector temperatures of T/E-1 were obtained assuming the 841°C estimated value for data point #8, which was 27°C higher than the highest thermocouple reading, and arbitrarily scaling down the 27°C temperature correction for the data points at lower heat-transfer values.

The heat-transfer values were obtained by adding the filament heating to the electron-bombardment power input, and the filament heating was calculated by an analysis of the heat pipe temperature achieved with filament heating alone. Specifically, data points 2 and 3 of Table 1, where the filament power was the same but where the temperature distributions were different on account of the additional electron-bombardment power of data point 3, were compared in terms

of a simple heat-transfer balance to determine the magnitude of the filament heating effect. The result of this calculation was that the filament heat input for data points 2 and 3 was 17.1 watts. Assuming that the filament power input to the heat pipe was proportional to the power actually delivered to the filament, as measured by filament voltage and filament current, the filament power input for the other data points could be calculated.

Table 3 gives a summary of the calculations, and the resulting values of collector temperature and collector heat transfer are plotted in Figure 29.

From data generated with a T-200 collector-radiator model and compared with the performance of a T-200 converter, the collector heat transfer could be related to converter output current at 1700°C by the relation:

$$Q_{collector}\ (watts) = 105.7 + 1.92\ I_o\ (amperes) \qquad (1)$$

Figure 29 was then used to predict the collector temperatures that would be achieved in a heat-pipe converter as a function of output current at 1700°C. The predicted curve is given in Figure 30, which also shows the pertinent data for the "no-heat-pipe" converter T-206, developed under JPL Contract 951263, to show that the heat pipe improves considerably the collector heat transfer of the T-200 converter.

Finally, Table 2 shows that, in spite of the overheating of the collector and the consequent greater transfer of heat to the cesium reservoir, the reservoir temperatures were well within the range of control required by the design. For instance, at the design value of output current of 51 amperes, the optimum reservoir temperature is about 621°K (data point 5, sheet 4, T-206 data). According to equation 1,

TABLE 3

SUMMARY OF HEAT PIPE CALCULATIONS

Data Point	Highest Thermocouple Reading, °C	Estimated Temperature Difference, °C	Collector Temperature, °K	Calculated Filament Power, W	Electron-Bomb. Power, watts	Total Power Input, watts
3	463	17	753	17.1	44.7	61.8
4	542	19	834	18.6	76.8	95.4
5	622	21	916	20.2	121.1	141.3
6	712	23	1008	22.4	188.3	210.7
7	766	25	1064	23.2	244.4	267.6
8	814	27	1114	24.8	310.6	335.4

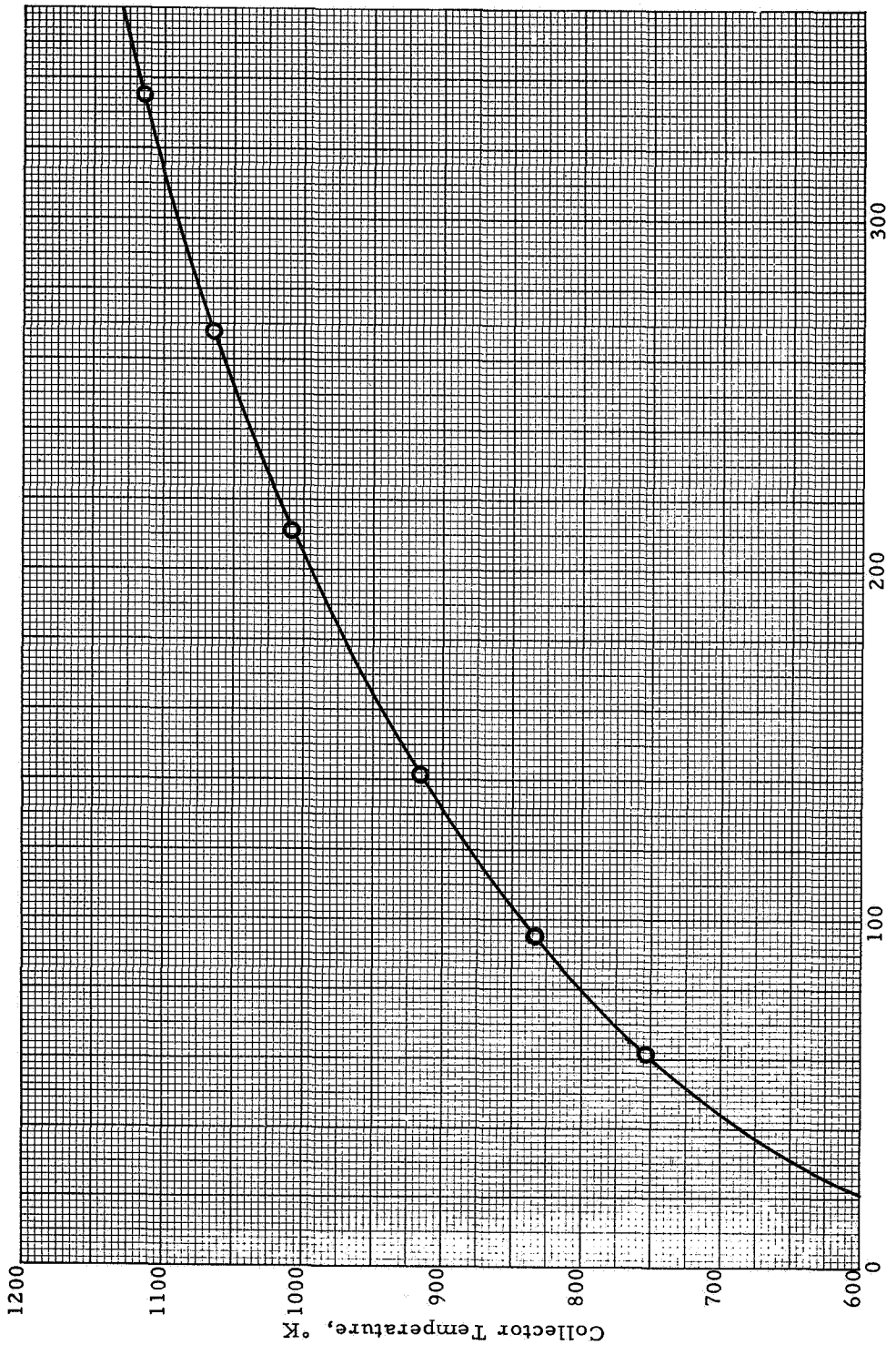
Collector Temperature, °K
1200
1100
1000
900
800
700
600
Collector Power Input, Watts
0
100
200
300

Figure 29

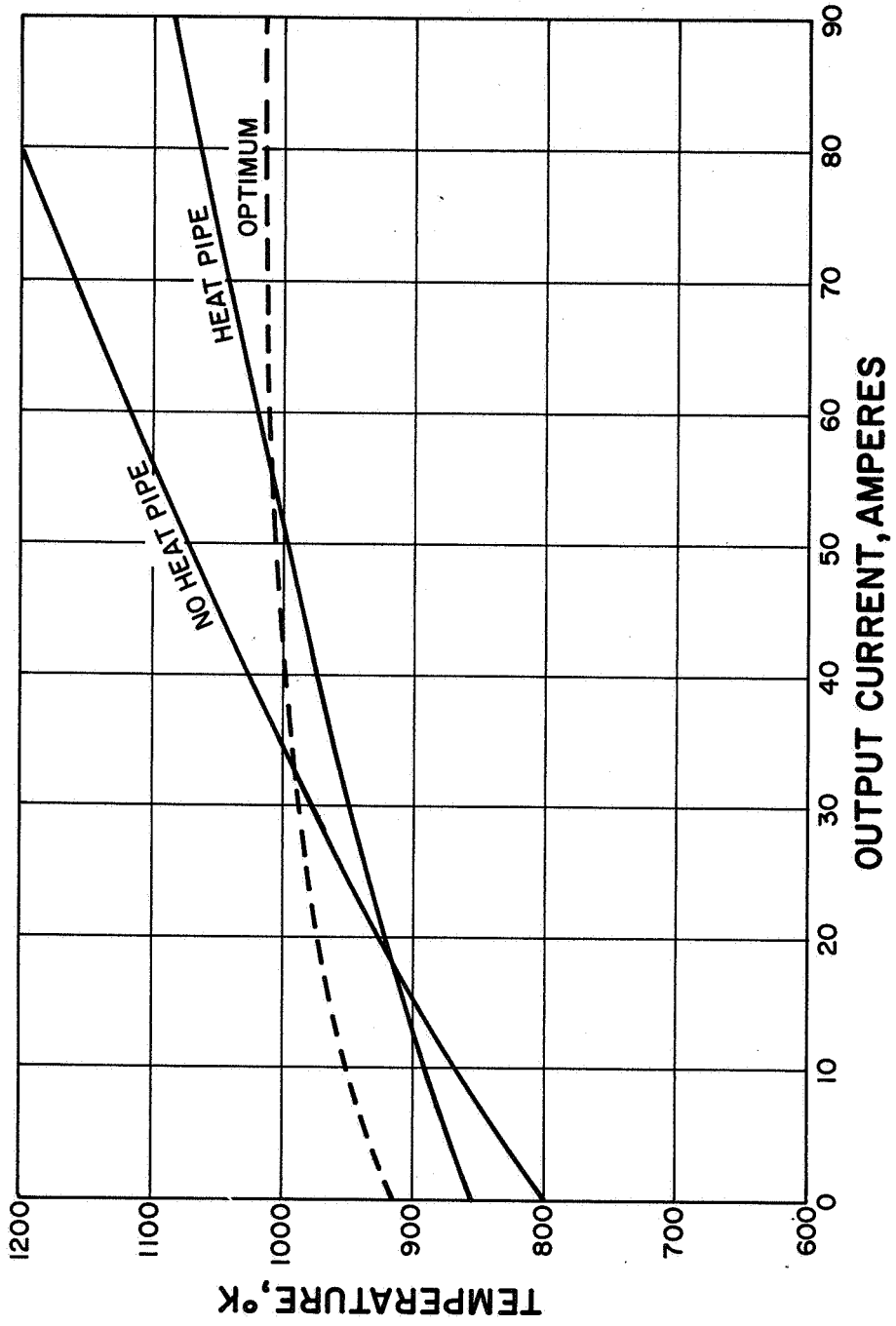
NO HEAT PIPE
HEAT PIPE
OPTIMUM
TEMPERATURE, °K
1200
1100
1000
900
800
700
600
OUTPUT CURRENT, AMPERES
0
10
20
30
40
50
60
70
80
90

Figure 30

the heat transfer corresponding to an output of 51 amperes is 203.7 watts. It can be seen in Table 2 that, at near this value of heat input, the reservoir temperature obtained in T/E-2 was of the order of 309°C, or 582°K, which is almost 40°C below the desired value, and therefore reservoir overheating was easily avoided by the T/E-2 design.

7. FABRICATION OF MODEL T/E-3

The fabrication of model T/E-3 was undertaken using the radiator and collector heat pipe structure (used as a back-up for T/E-2) which is mentioned in section 6.2. To use this structure it was necessary to disassemble it in order to correct a faulty positioning of the capillary structure. The disassembly was carried out by grinding off the end cap of the heat pipe and pulling out the tight-fitting capillary structure. A new capillary was inserted, and a new end cap was welded in place. The capillary was made using a mandrel of slightly reduced diameter to ensure a looser fitting of the capillary into the heat pipe. After the end cap was welded in place, it was noticed that the heat of welding had caused a very minor reaction of the casting with the niobium in the vicinity of the weld. This reaction is known to embrittle the niobium, and it was therefore decided to carefully check the worthiness of the welded assembly. It was placed in a vacuum furnace and cycled abruptly four times to 900°C for a total of 18 hours, and the structure was leak-tight after test. It was then accepted for assembly of T/E-3.

The assembly proceeded normally, and it included mounting a rhenium emitter structure in order to make possible the fabrication of a complete converter heat pipe.

After complete fabrication, the heat pipe was outgassed overnight with a resistance heater at 500°C while maintaining the sodium reservoir at 350°C for 36 hours. The sodium was then transferred to the heat pipe, and the heat pipe fill tube was pinched off by electron bombardment.

To proceed with the cesium charge, a cesium tubulation was fuse-brazed to the cesium tube, and a leak was discovered in the wall of the tantalum tube. To correct this difficulty, a niobium tube was welded over the tantalum tube so as to cover the leak, and this approach was successful. The converter was then outgassed with a molybdenum foil around the radiator to maintain a high collector outgassing temperature. The outgassing time was 15 hours at an emitter temperature of 1550°C and at a collector heat-pipe temperature of 700°C. Cesium distillation was then carried out by heating the capsule to 200°C for four hours. The completed assembly is shown in Figure 31. The final design of model T/E-3 is given in Figure 32. Of course, the drawing does not show the dimensional adjustments that were required in order to replace the capillary assembly and seal the tantalum tube leak in the model actually fabricated.

The completed model weighed 90.3 grams, exclusive of electrical leads and mounting hardware. The increase of 12.5 grams over the weight of model T/E-2-C is due mostly to the emitter structure added for the fabrication of model T/E-3. According to the weight breakdown presented in section 2.4, the weight of the emitter and the first emitter sleeve is 10.2 grams. The weight of the model is greater than that estimated in section 2.4 primarily because the heat pipe radiator tube used, part No. 9, was thicker than the tube assumed in that section.

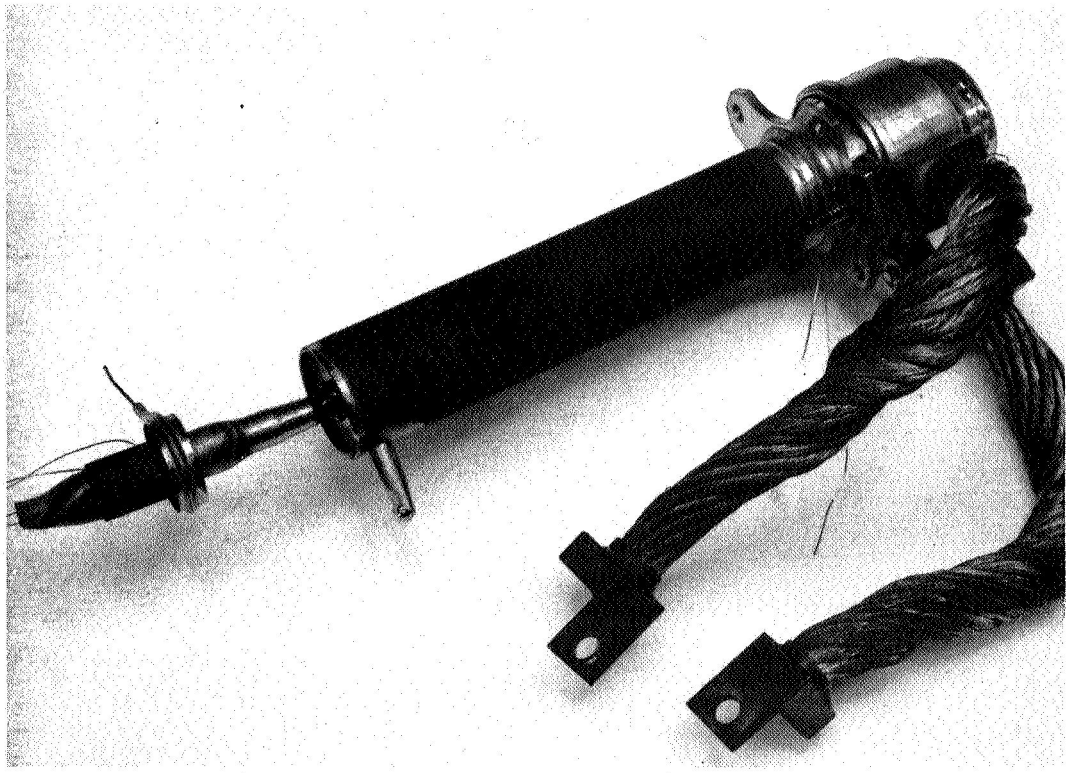

Figure 31

7751

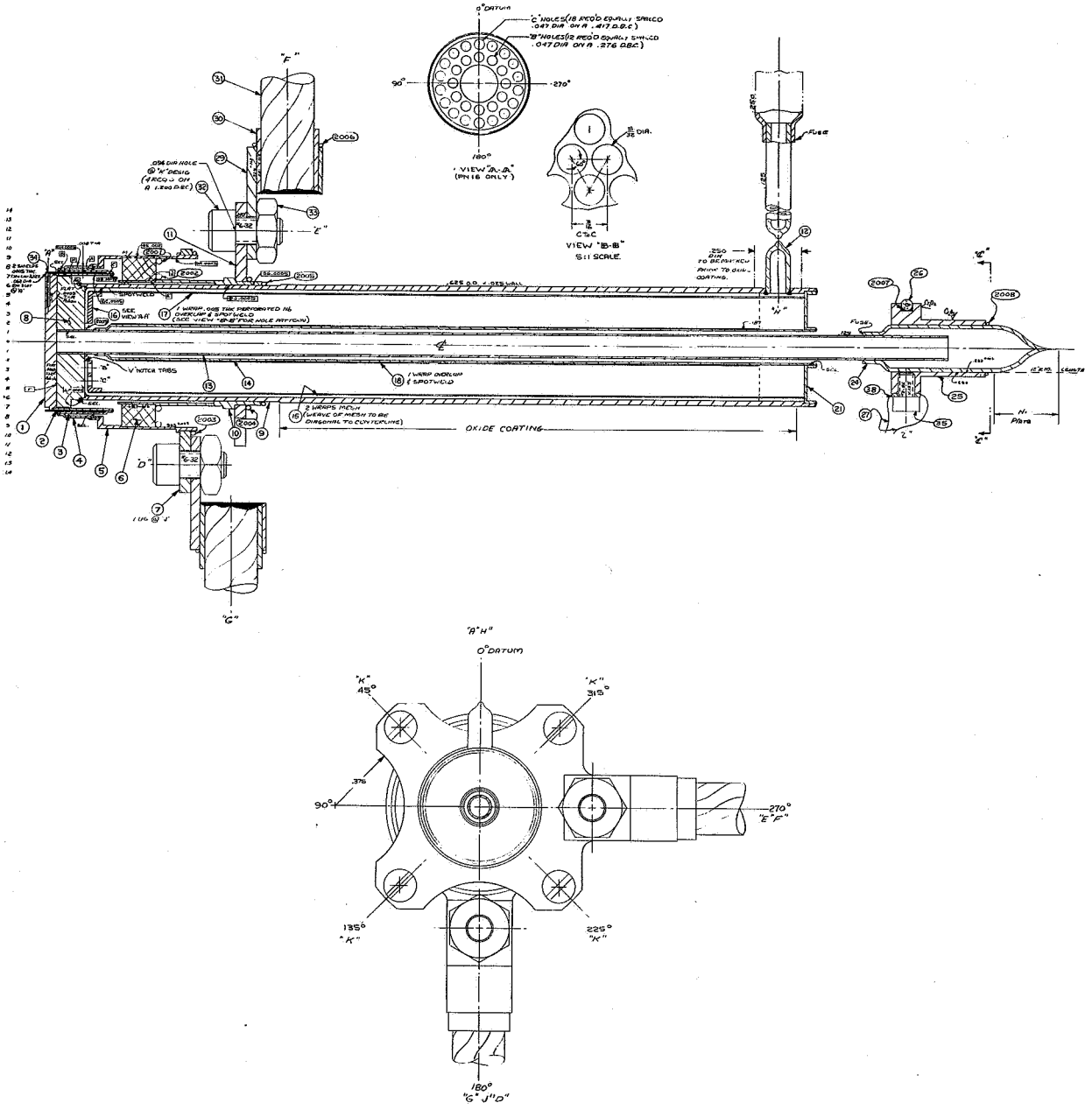

Figure 32

8. TEST OF MODEL T/E-3

Converter T/E-3 was instrumented with voltage taps on the output leads at the point of attachment to the converter, two thermocouples on the cesium reservoir, and two spot-welded thermocouples on the support flange close to the heat pipe, so as to afford a measurement of heat-pipe temperature.

Testing of T/E-3 consisted of five runs. The data obtained is presented in Appendix A, Sheets 1 to 7. In the first run the steady-state output chracteristics were measured at output voltages of 1.2, 1.0, 0.8 and 0.6 volts at emitter hohlraum temperatures of 1600, 1700 and 1800°C. The outputs observed were lower than those observed in the T-200 converter series. Typically, the output voltage of converter T/E-3 was 0.2 volt lower than that of T-206 at any selected output current and emitter temperature.

In the second run, the output characteristics at an emitter surface temperature of 2000°K were obtained under dynamic testing, and these are presented in Figure 33. These characteristics, when compared with those obtained with converter T-206, also show a voltage shift of 0.2 volt in the optimum curve. It is believed that this shift is principally due to emitter temperature measurement errors caused by overheating of the thin hohlraum wall separating the hohlraum from the heated face of the converter, and also to the higher collector work function obtained with niobium collectors.*

*These hypotheses are discussed in detail in the paper, "Advanced Converter Development," by P. Brosens, presented at the Thermionic Conversion Specialist Conference in Palo Alto, October-November 1967.

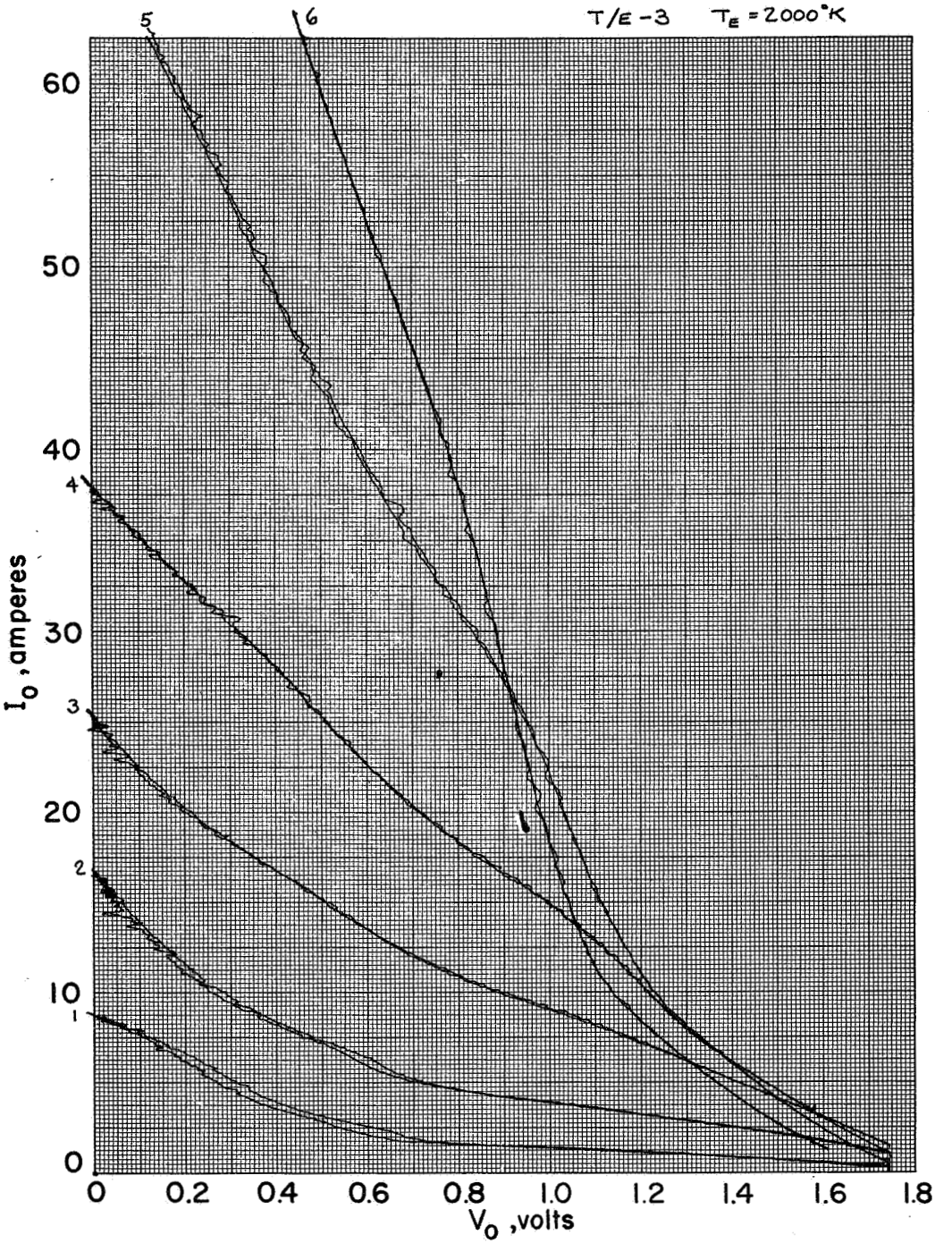
T/E-3 T_E = 2000°K
5
6
4
3
2
1
60
50
40
30
20
10
0
I_o, amperes
0
0.2
0.4
0.6
0.8
1.0
1.2
1.4
1.6
1.8
V_o, volts

Figure 33

In the third run, the converter was operated continuously at a hohlraum temperature of 1700°C with a load adjusted for an output of 0.6 volt at 52 amperes. The steady-state heat-pipe temperature was 720°C. The converter operated at this setting for 200 hours.

In the fourth run the converter was thermally cycled abruptly between near room temperature and operating temperature. The power input for an output of 52 amperes at 1700°C was turned on and off instanteously for 12 thermal cycles. Figure 34 shows a typical temperature recording which was obtained during the eighth cycle. Also, in the interval between the fifth and sixth cycles the converter was run for an additional 200 hours at steady-state and high current output.

The fifth run was conducted to determine the effect of the voltage tap location on the performance measured. The voltage tap on the emitter terminal was shifted to a more advantageous location, as illustrated in data sheet No. 7, but no effect was observed.

Figure 35 gives a simultaneous plot of the static and dynamic performance characteristics observed. As can be seen, the static data gives every indication that model T/E-3 performance does not become limited at high output currents. This symptom of collector overheating, consistently observed in the T-200 converters 201 to 207, was therefore eliminated with the use of the collector-radiator heat pipe.

7810

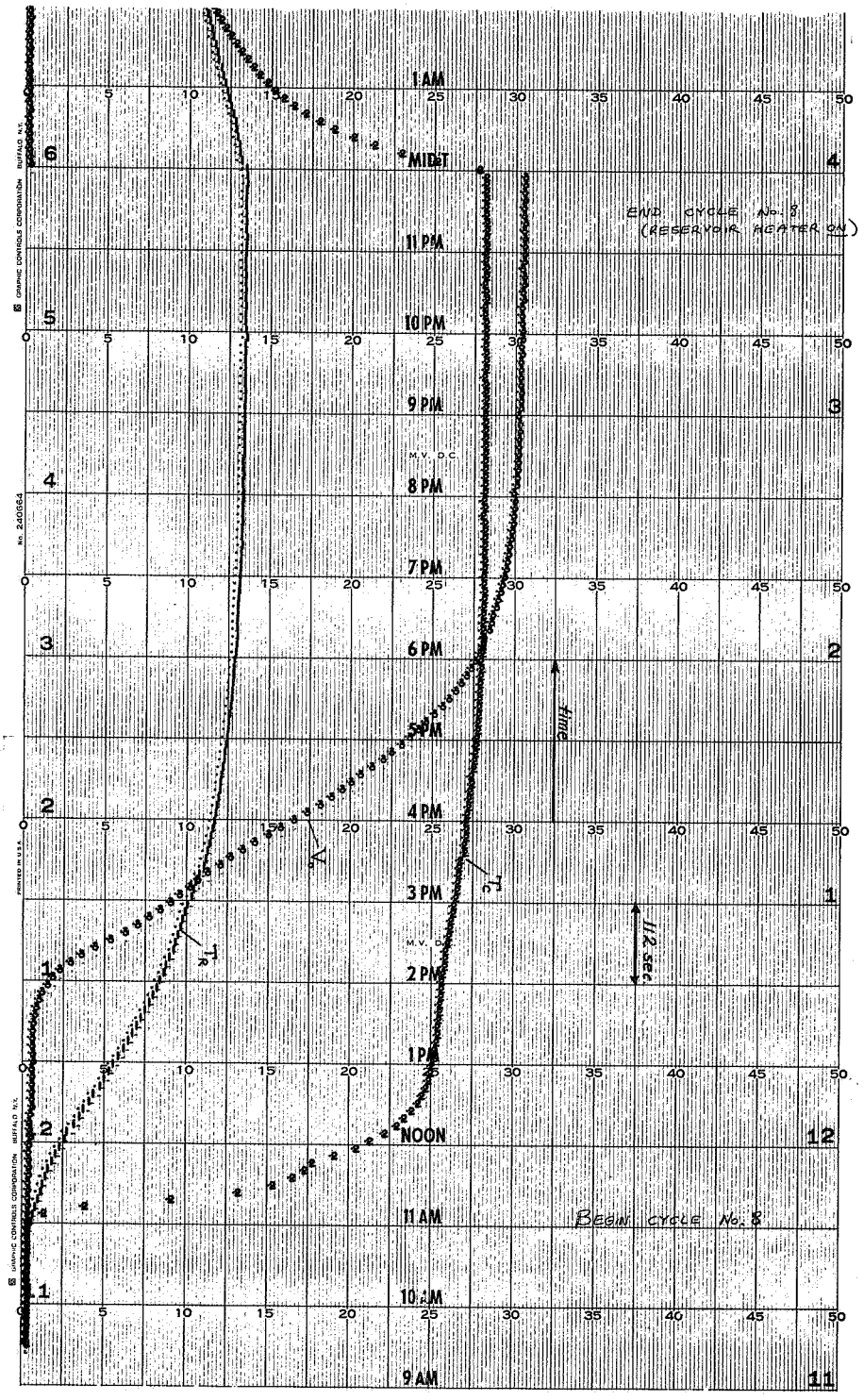

Figure 34

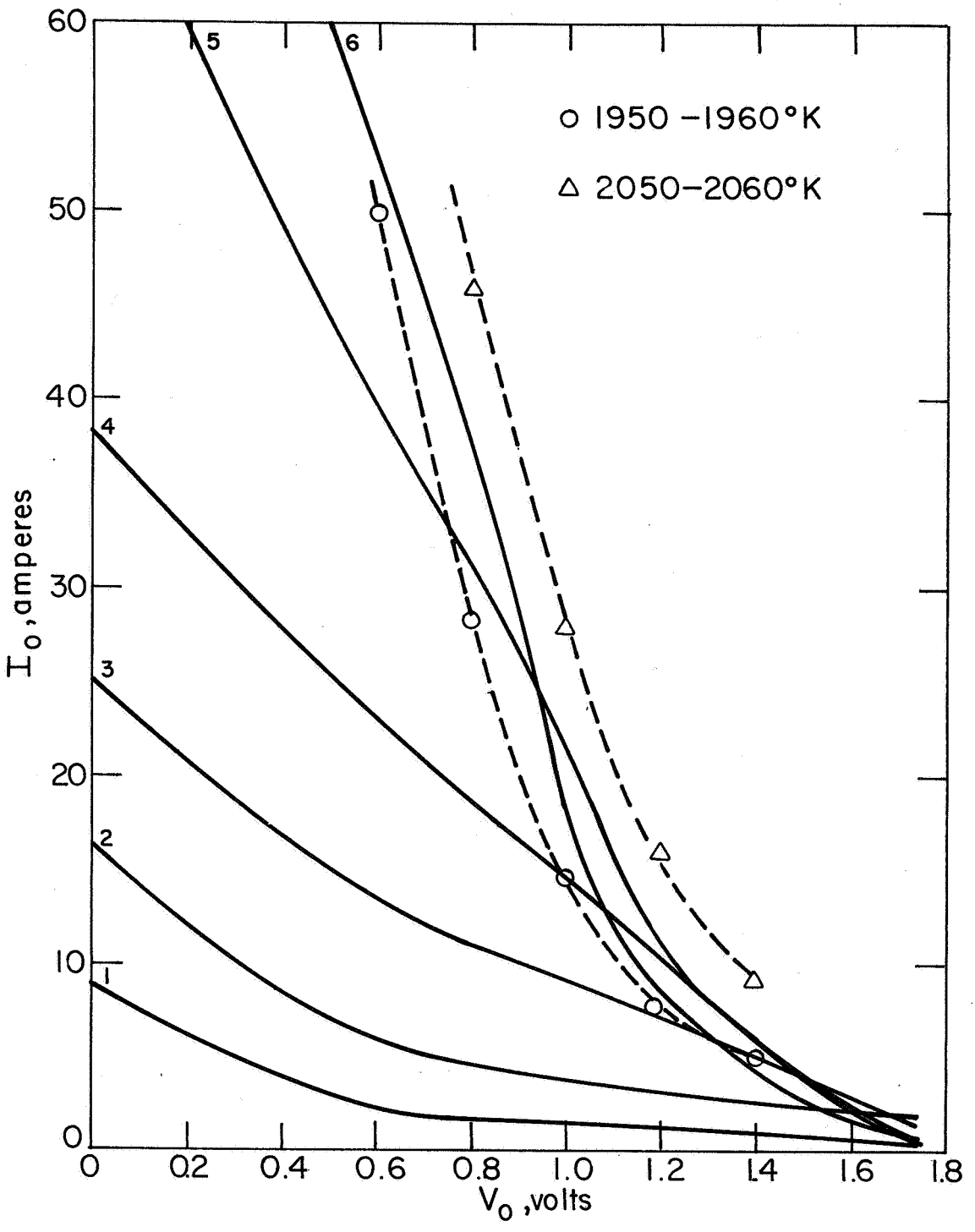
60
50
40
30
20
10
0
0
0.2
0.4
0.6
0.8
1.0
1.2
1.4
1.6
1.8
I_0, amperes
V_0, volts
5
6
4
3
2
1
○ 1950 –1960°K
△ 2050–2060°K

Figure 35

9. DESIGN OF MODEL T/E-4

Model T/E-4 was specifically designed for use in the converter models developed under the concurrent JPL Contract No. 951263. It is similar to the previous models T/E-1 to T/E-3, with the principal difference that the heat pipe diameter is larger. The previous models were fabricated using readily available niobium tubing. The diameter of that tubing was not large enough to match the size of the ceramic seal, so that an intermediate adapting piece was necessary. Also, the small diameter of the T/E-3 heat pipe hindered the development of the radiator area required for large output currents.

The design of T/E-4, shown in Figure 36, uses a niobium tube custom-made to match the size of the ceramic seal. The radiator area developed is 38.3 cm^2, which is 13% greater than the 33.8 cm^2 of T/E-3 actually measured. The test data of T/E-1 and T/E-2, summarized in Figure 30, had predicted that, for an output of 55 amperes, the heat-pipe temperature would be optimum and equal to 1020°K. This value was confirmed by the test of T/E-3, which showed a heat-pipe temperature of 994°K at an output current of 51.9 amperes (Sheet 3, data point No. 7, Appendix A). This heat-pipe temperature is higher than that originally predicted in the design calculations of 951°K at 51.0 amperes because, as explained in section 6.3, the collector heat transfer at 51.0 amperes is higher than that predicted by the calculations presented in section 2.2. The theoretical value calculated in section 2.2 was 207.0 - 40.8 = 166.2 watts, while Equation (1) of section 6.3 predicts a heat transfer of 203.7 watts. Figure 29 shows that the heat pipe temperatures corresponding to these values of heat transfer would be 951°K and 997°K.

The equilibrium temperature of the heat-pipe collector-radiator structure for model T/E-4 was predicted with a simple radiator model,

THERMO ELECTRON CORPORATION

7871

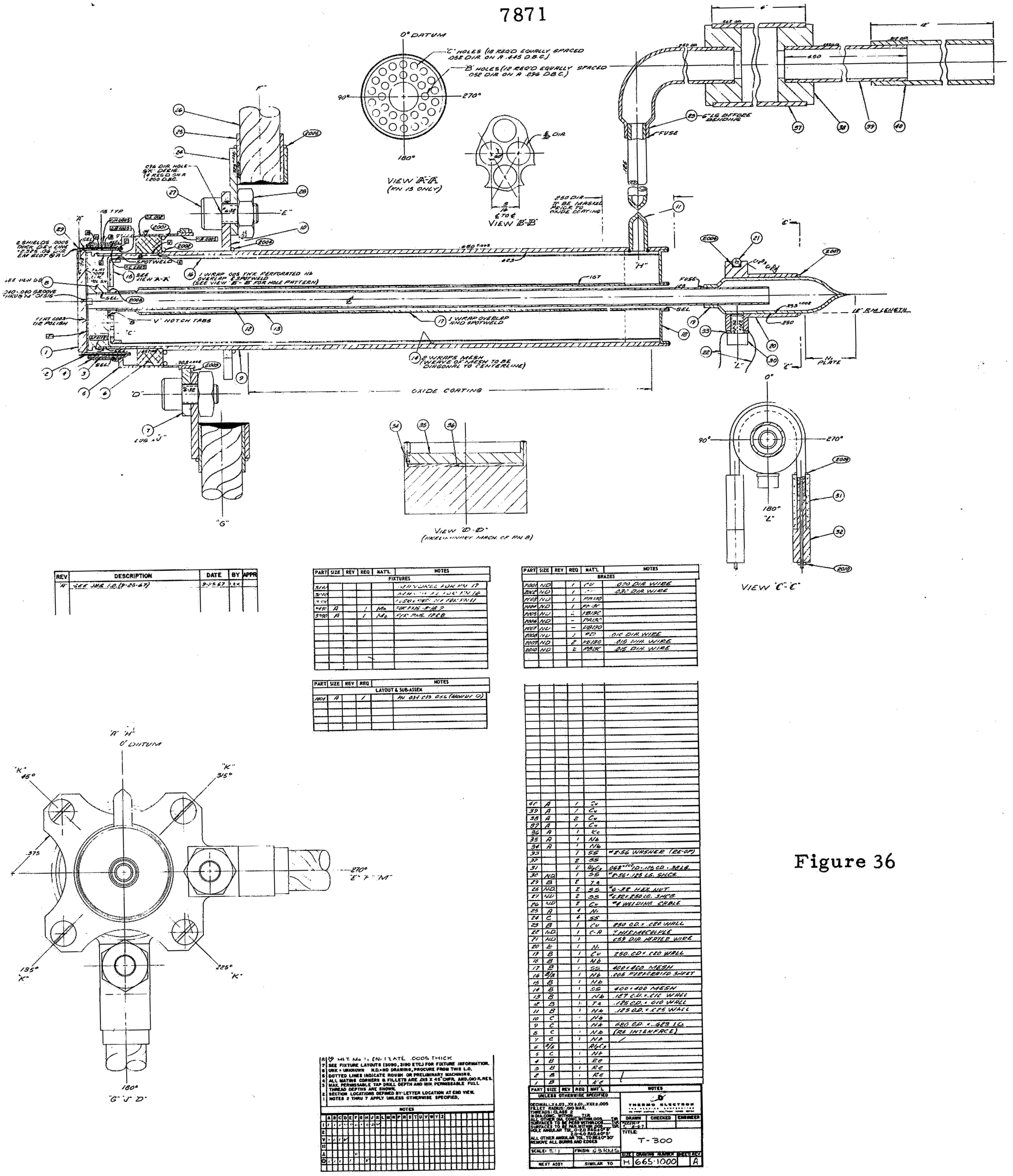

Figure 36

where it was assumed that the effective radiator emissivity is 0.85 and that the heat load at an emitter temperature of 1700°C is given as a function of output current by equation (1) of section 6.3.

With the assumed emissivity value, the stray losses of the collector structure could be calculated. The stray losses were assumed to be due to radiation from surfaces having a value of the product of area times emissivity of $A\epsilon$ and operating at the collector-radiator temperature. The heat balance for the collector-radiator structure was then:

$$(A\epsilon + 0.85\, A_R)\, \sigma\, T_R^4 = Q_{collector}$$

where A_R is the radiator area. For model T/E-1, the actual radiator area was 33.8 cm^2, and at a bombardment power of 310.6 watts the radiator temperature achieved was estimated to be 841°C (section 6.3). At this temperature, the emissive power of a black body is 8.73 watts/cm^2. Substitution of the values in the above equation yielded $A\epsilon$ = 6.80 cm^2.

Thus, for models which are of identical geometry except for the size of the radiator area it was concluded that the relationship between heat input and radiator temperature is:

$$(6.80 + 0.85\, A_R)\, \sigma\, T_R^4 = Q_{collector}$$

For the model T/E-4 design, which has a radiator area of 38.3 cm^2 (coated length of 2.75 in., diameter of 0.685 in.), the radiator temperature predicted for any value of output current is then obtained from:

$$\sigma T_R^4 = (105.7 + 1.92 I_o)/6.80 + 32.55)$$

$$= 2.69 + 0.0488 I_o \quad \text{watts/cm}^2$$

If the model T/E-4 design is used in converters which deliver a power of 50 watts at an emitter temperature of 1700°C, and at voltages ranging from 0.6 to 0.8 volt, the corresponding collector-radiator temperatures will be as follows:

V_o, volts	I_o, amperes at 50 watts	Q_R, watts	σT_R^4, watts/cm^2	T_R, °K
0.6	83.3	265.6	6.75	1044
0.7	71.5	243.0	6.18	1022
0.8	62.5	225.7	5.74	1003

These collector-radiator temperatures are practically exactly the optimum collector temperatures at the output current values tabulated.

10. FABRICATION OF MODEL T/E-4

The fabrication sequence used for model T/E-4 was similar to that used for the previous models. Figure 37 shows the initial subassemblies and parts. In the sequence the first step was welding of the sodium fill tube to the collector radiator tube, and then brazing of the double-walled cesium tubulation to the collector face. These two subassemblies were then welded together along the periphery of the collector. The resulting assembly, shown at the top left of Figure 37, was then ready for insertion of the capillary structure, which is shown disassembled in the same figure. The capillary assembly consisted of wrapping and spot-welding the perforated capillary support sheet around a mandrel and the end disc, as shown in Figure 38. This assembly was then covered with 2 turns of 400-mesh screen, which was folded over at the end and secured by a spot-welded end disc of mesh screen, as shown in Figure 39. The assembly was slipped into the heat-pipe radiator, and the end of the perforated niobium support sheet was folded over, as shown in Figure 40. The end cap was placed in position, and welded with a heat sink in inert gas. Figure 41 shows the heat sink around the completed weld.

The model was then ready for outgassing. It was connected to the sodium fill manifold, and the same outgassing procedure used for T/E-3 was followed: The heat pipe was heated to 500°C for 33 hours while the ends of the chamber holding the sodium capsule were maintained at 400 and 350°C. At the end of this period of time, the assembly was allowed to cool for 13 hours, the sodium capsule was broken, and the gases that it released were pumped out. The heat-pipe-and-sodium-reservoir assembly was then pinched off from the vacuum pumping

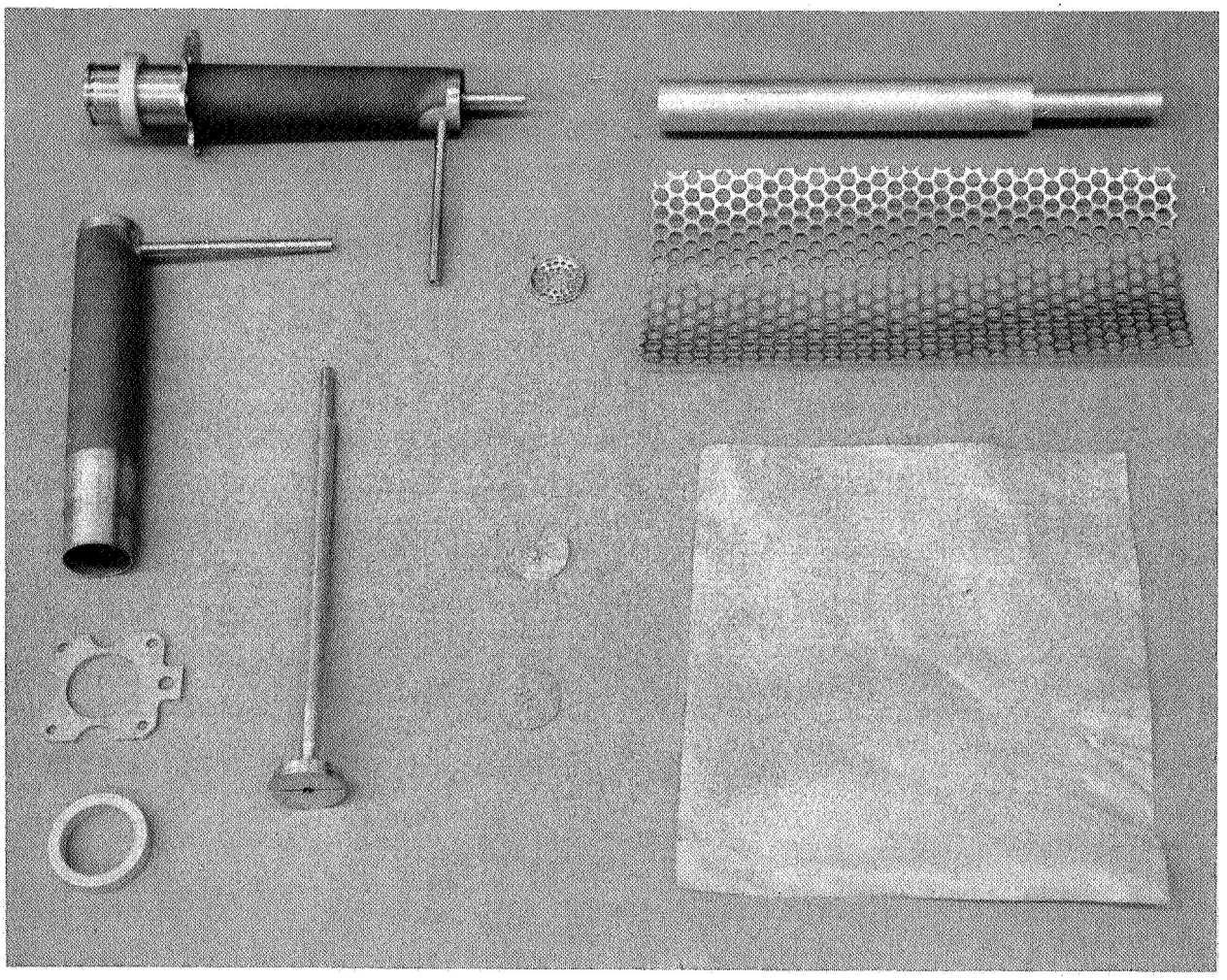

Figure 37

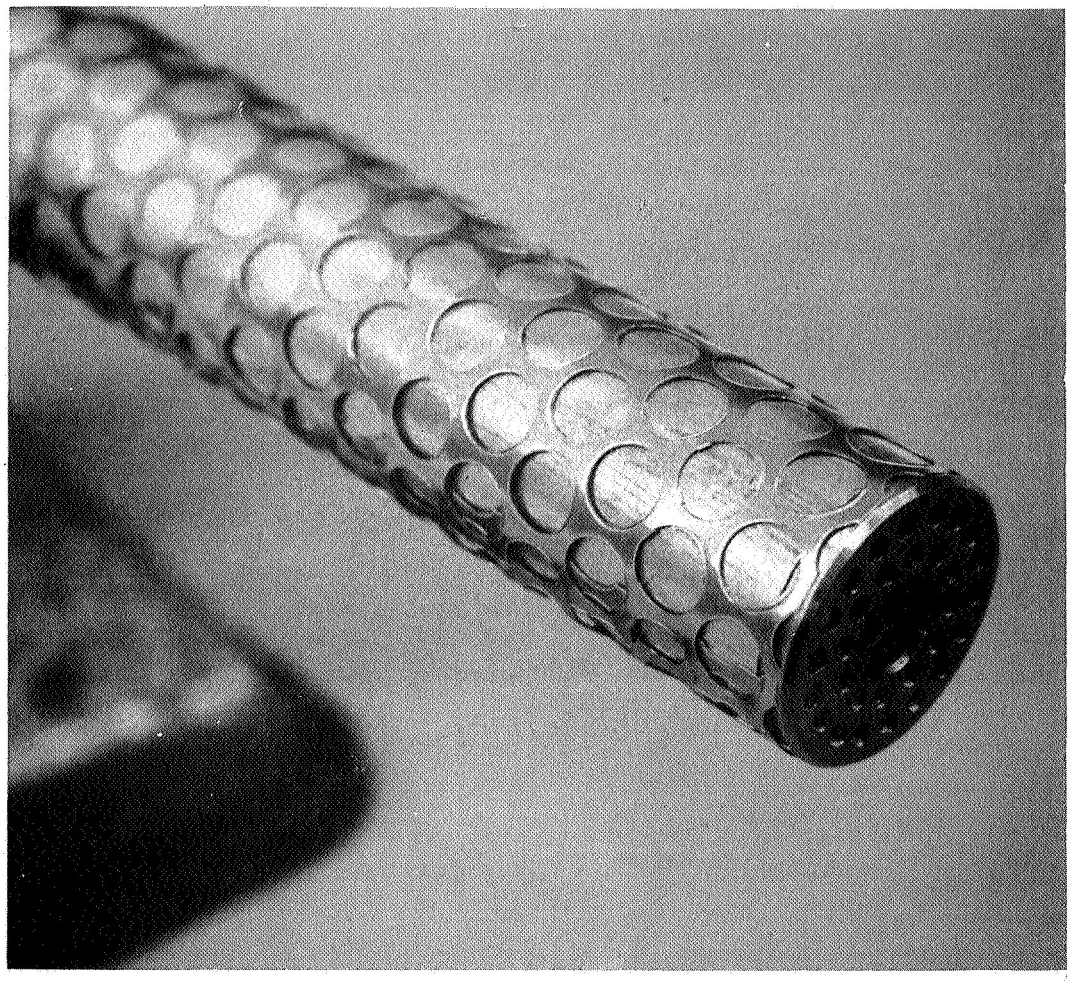

Figure 38

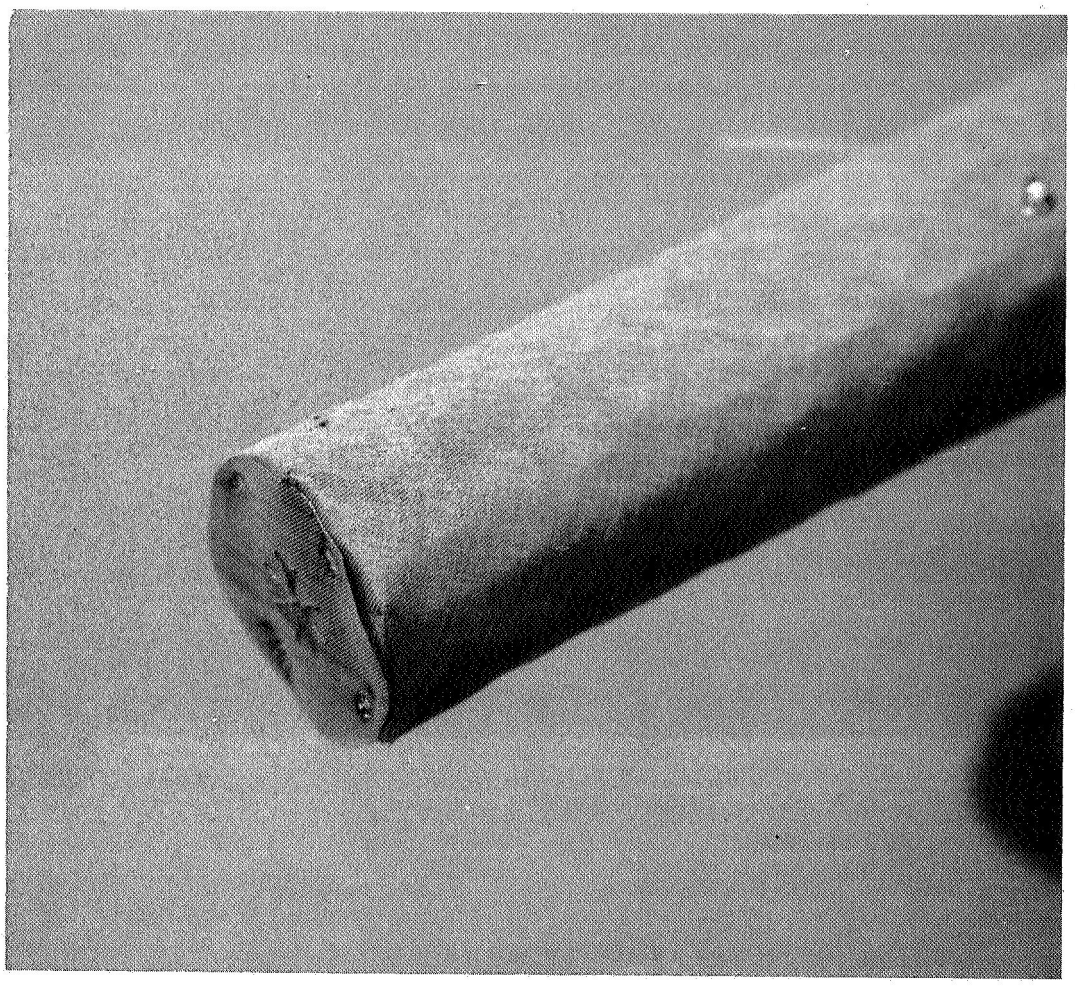

Figure 39

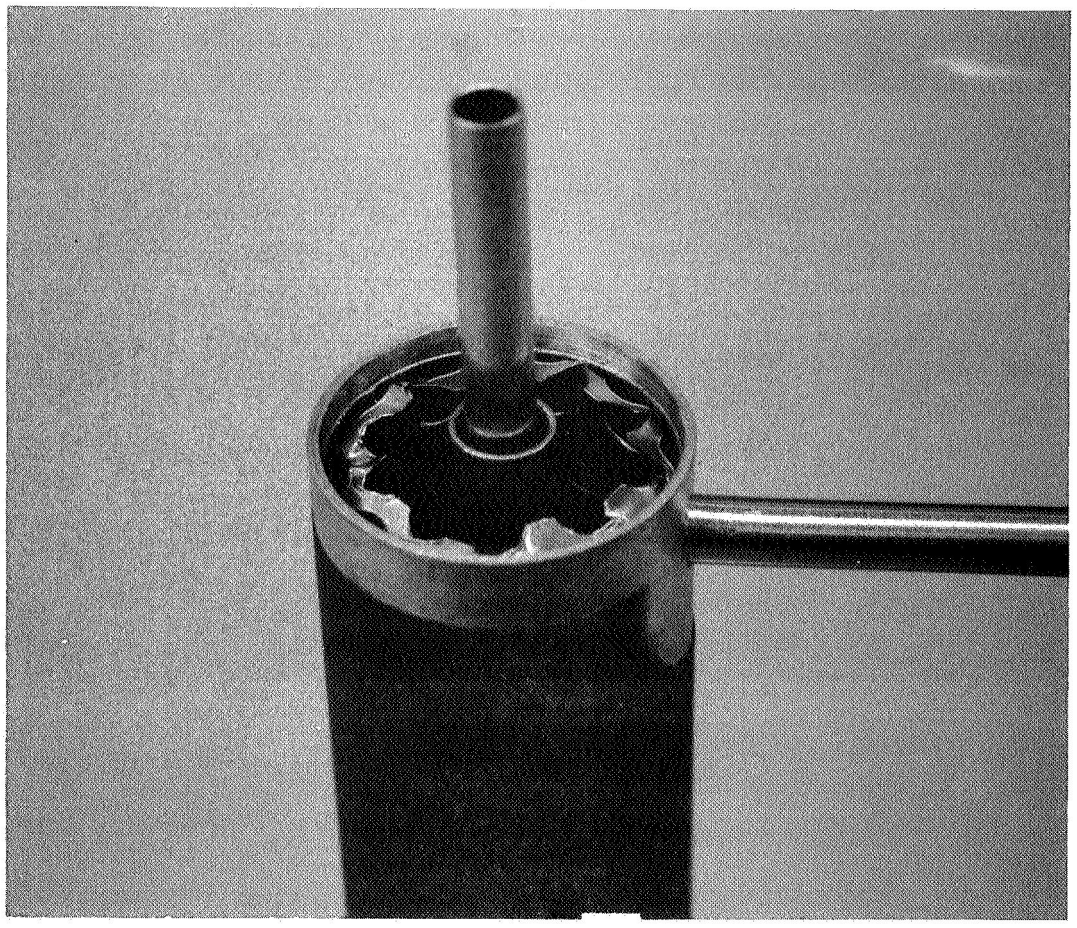

Figure 40

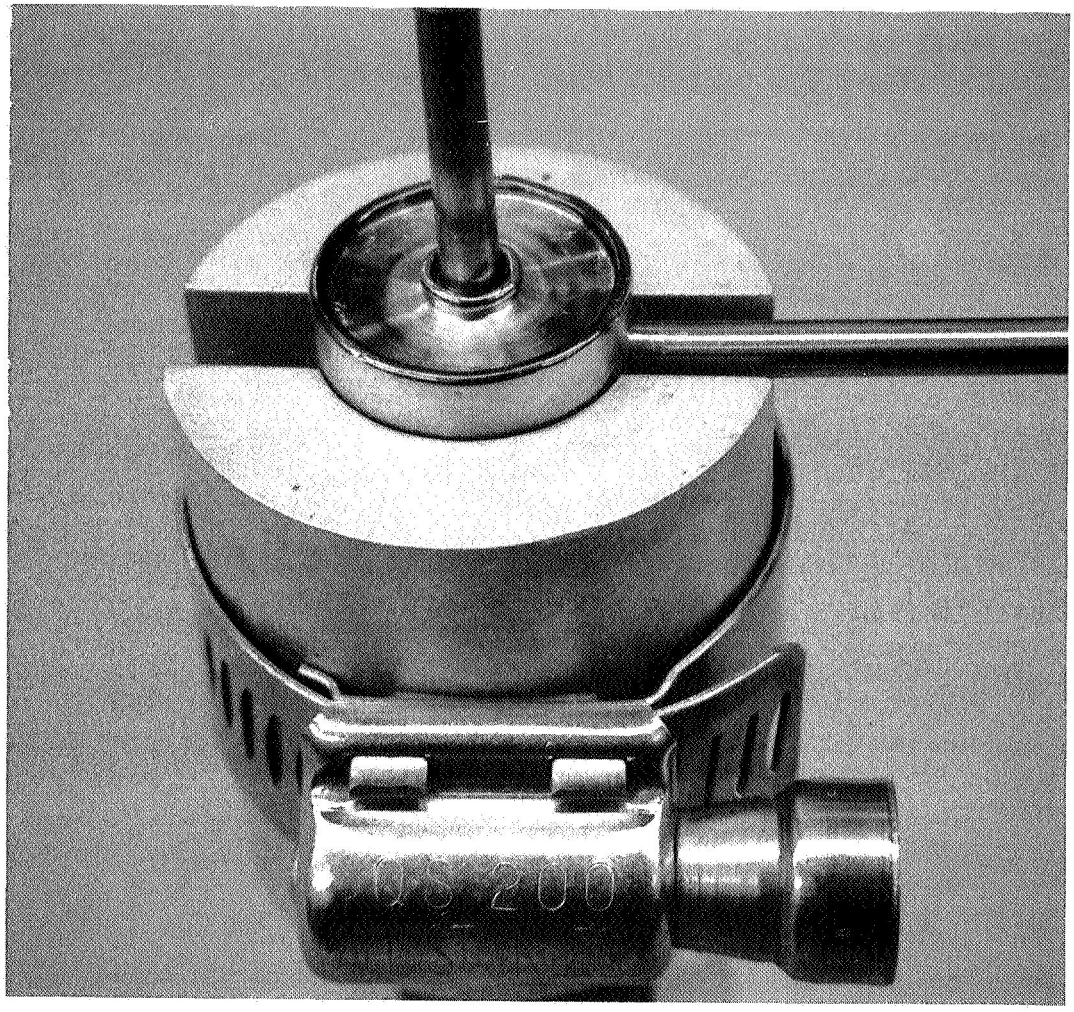

Figure 41

system, and it was transferred to an oven at 150°C for two hours. This caused melting of the sodium, which was then transferred by gravity flow to the heat pipe. The sodium reservoir was pinched off along its copper discharge tube, and a second pinch-off along the niobium fill tube was performed by electron bombardment. This completed the fabrication of model T/E-4, which was then set up for test.

11. TEST OF MODEL T/E-4

Tests on model T/E-4 consisted of a heat-transfer run, designated as Run No. 1 on Table 4, a thermal-cycling run, designated as Run No. 2 on Table 5, and a steady-state run, designated as Run No. 3 on Table 6.

The heat-transfer run was intended to determine the heat-pipe and collector temperatures achieved for various values of heat input, and the procedures used paralleled closely those followed in the test of models T/E-1 and T/E-2.

The heat pipe was instrumented with four thermocouples: one just below the collector face, one on the heat pipe support flange very close to the heat pipe, one at the bottom end of the heat pipe on the end cap weld, and one on the cesium reservoir.

As noted on Table 4, the thermocouple below the collector face intercepted some of the electron-bombardment power and overheated; as a result, its indications were in error. During the second thermal cycle, the collector overheated, and the thermocouple leads melted; this thermocouple was then removed.

The heat pipe operation in the first two runs was satisfactory. In the second thermal cycle it was noted that if a large amount of power (335 watts) is applied suddenly to the heat pipe, it is possible to overheat the collector, probably as a consequence of drying up the capillary wick in a film-boiling mode of sodium evaporation. In subsequent thermal cycles, the power input was applied in two steps: 200 watts for 1 minute, and then the full power. No further evidence of collector overheating was then observed.

TABLE 4

HEAT PIPE TEST DATA

DATE: 10-26-67 Sheet 1

MODEL: T/E-4 RUN No. 1 OBSERVER: R. Brosens

	1	2	3	4	5	6	7	8	9	10	11	12
Time	12:53	13:39	14:43	15:05	15:27	15:54	16:09	16:18				
V_{eb}, volts	0	976.3	0	1014	994.6	981.2	971.9	962.6				
I_{eb}, mA	0	224.2	0	60.5	120.7	185.0	253.6	334.0				
EB Power	0	218.9	0	62.2	120.0	181.5	246.5	321.5				
V_{Fil}, volts	0	5.1	5.1	4.4	4.8	5.02	5.25	5.5				
Filament Power	0	104.5	106.0	81.0	91.2	102.9	111.3	120.4				
I_{Fil}, amps	0	20.5	20.8	18.4	19.8	20.5	21.2	21.9				
T.C.'s: Reservoir (14)	1.1	12.6	5.9	8.5	10.5	11.9	12.9	13.9				
°C	28	309	144	209	258	292	317	341				
HP #1 (top) (12)	1.0	30.9	13.1	21.4	25.6	29.0	31.9	34.4				
°C	25	742	321	518	616	697	766	827				
HP #2 ( )	—	—	—	—	—	—	—	—				
HP #3 ( )	—	—	—	—	—	—	—	—				
HP #4 ( )	—	—	—	—	—	—	—	—				
HP #5 ( )	—	—	—	—	—	—	—	—				
HP #6 (bottom) (13)	1.1	30.4	9.1	17.0	23.5	28.1	31.2	33.6				
°C	28	730	224	414	567	675	749	807				
Collector (11)	1.2	34.3	16.1	23.3	28.6	32.9	37.0	40.9 *				

* NOTE: Thermocouple on collector visibly hotter than collector, indicating direct bombardment. Heat pipe completely uniform in color.

THERMO ELECTRON CORPORATION

TABLE 5

HEAT PIPE TEST DATA — DATE: 10-26-67 — Sheet 2

MODEL: T/E-4 — RUN NO. 2 (Thermal Cycling) — OBSERVER: P. Brosens & E. Peredetto.

THERMAL CYCLE No.*	1	2	3	4	5	6	7	8	9	10	11	12
	10-26-67	10-27-67	—	—	—	—	—	—	—	—	—	10-27-67
Time	16:27	9:06	9:45	10:13	10:42	11:10	11:37	12:04	13:17	13:45	14:12	14:39
V_{eb}, volts	962.3	967.9	965.5	965.0	964.4	963.2	963.5	963.5	962.8	962.6	962.5	963.2
I_{eb}, mA	335.5	331.0	328.3	328.2	329.9	334.7	326.2	326.0	327.1	326.9	326.9	326.9
V_{Fil}, volts	5.5	5.2	5.3	5.3	5.3	5.3	5.3	5.3	5.3	5.3	5.3	5.3
I_{Fil}, amps	21.9	21.0	21.2	21.2	21.4	21.3	21.2	21.2	21.2	21.3	21.2	21.2
T.C.'s: Reservoir (14)	14.0	13.4	13.2	13.2	13.5	13.2	13.2	13.1	13.1	13.2	13.1	13.2
°C	343	329	324	324	331	324	324	321	321	324	321	324
HP #1 (top) (12)	34.3	34.2†	34.1	34.1	34.0	34.2	33.9	34.0	33.9	33.9	33.9	33.9
°C	824	822	819	819	817	822	815	817	815	815	815	815
HP #2 ( )	—	—	—	—	—	—	—	—	—	—	—	—
HP #3 ( )	—	—	—	—	—	—	—	—	—	—	—	—
HP #4 ( )	—	—	—	—	—	—	—	—	—	—	—	—
HP #5 ( )	—	—	—	—	—	—	—	—	—	—	—	—
HP #6 (bottom) (13)	33.9	33.2	33.2	33.2	33.5	33.2	33.2	33.4	33.0	33.3	33.0	33.4
°C	815	798	798	798	805	798	798	802	793	800	793	802

* NOTE: Heat Pipe at end of applied too Cooling cooling fast. time 6.6 mV = 162°C 15 MINUTES/CYCLE - †Collector Heat Pipe temperature overheats if power is

TABLE 6

HEAT PIPE TEST DATA — Sheet 3

DATE: 10-27-67

OBSERVER: P. Brosens, E Pendutto

MODEL: T/E-4 — RUN No. 3 (Life Test)

	1	2	3	4	5	6	7	8	9	10	11	12
	10-27-67	10-28	10-29	10-30	10-31	11-1	11-2	11-2				
Time	15:00	15:00		15:00	14:20	14:30	14:30	15:35				
Elapsed hours	0.0	24		72.9	96.3	120.3	144.6	145.6				
V_{eb}, volts	963	962		960.2	959.9	959.8	959.5	959.4				
I_{eb}, mA	326.9	329.9		329.9	327.9	325.9	324.4	328.0†				
V_{Fil}, volts	5.3	5.2		5.2	5.3	5.2	5.1	5.1				
I_{Fil}, amps	21.5	21.1		21.0	21.0	20.8	20.0	20.0				
T.C.'s: Reservoir (14)	9.9*	13.9		13.9	13.9	13.9	14.3	14.9				
HP #1 (top) (12)	33.9	33.9		33.9	33.9	33.9	33.9	34.0				
HP #2 ( )	—	—		—	—	—	—	—				
HP #3 ( )	—	—		—	—	—	—	—				
HP #4 ( )	—	—		—	—	—	—	—				
HP #5 ( )	—	—		—	—	—	—	—				
HP #6 (bottom) (13)	33.1	33.9		33.9	32.9	33.9	33.9	33.9				

* Reservoir still warming up

† Shut down at 145.6 hrs due to evident sodium leak.

THERMO ELECTRON CORPORATION

In the steady-state run, the heat pipe operated 145 hours at maximum heat input, corresponding to an output of 124 amperes, and then it developed a leak. The bell jar of the test system was opened, and the heat pipe was removed for visual observation. It was found that a strong reaction had occurred in the region of the electron-beam weld, just below the collector face, where the heat-pipe tube is joined to the collector face. Although no further examinations were made, it was obvious that the capillary structure at the collector face had melted and reacted with the adjacent niobium wall at the same time that the collector face had overheated during the second thermal cycle, and the collector thermocouple had melted. A failure of this type can be avoided by protecting the heat pipe from massive and sudden heat loads, and also by the use of a refractory-metal wick structure instead of a stainless steel one.

12. INTERPRETATION OF MODEL T/E-4 HEAT TRANSFER DATA

The contribution to power input due to electron-bombardment filament radiation was determined in the same manner that was used for model T/E-2. As can be seen from the data on Table 4, data points 2 and 3 were obtained with almost identical filament power, and they differed by the fact that the power input for data point 2 included 218.9 watts of electron-bombardment power, while no electron-bombardment power was applied in obtaining data point 3. The average heat-pipe temperatures achieved for these two data points were 736°C and 272°C, respectively. Assuming that these temperatures were the effective temperatures at which the model was radiating heat, the following two thermal balance equations were written:

$$218.9 + Q_F = \epsilon A \sigma (736 + 273)^4$$

$$0 + Q_F = \epsilon A \sigma (272 + 273)^4$$

where Q_F stands for the heat input due to filament radiation, and ϵA for the effective black-body area of the heat-pipe structure. Solving for Q_F, the value for filament heating obtained was 20.4 watts. Assuming that filament heating was proportional to the applied filament power, the values of collector heating achieved at the other operating conditions recorded on Table 4 were calculated, and they are tabulated further below.

The heat pipe temperatures achieved at the support flange and at the end cap weld differed substantially at the lower temperatures, and this was not observed in models T/E-1 and T/E-2. It is an indication that, in model T/E-4, some residual gases interfered with the proper

condensation of sodium vapor. At the higher heat fluxes, the discrepancy had a tendency to vanish, but it still measured approximately 15°C. This penalized the performance of the heat pipe because it could not utilize efficiently the radiator area at the colder end, and consequently the collector temperature was higher than normal.

Assuming that the temperatures recorded at the support flange were close to the collector temperatures achieved, and using equation (1) of section 6.3, the observed thermal performance of T/E-4 was tabulated as follows:

Data Point Number	4	5	6	7	8
Bombardment Power, watts	62.2	120.0	181.5	246.5	321.5
Filament Contribution, watts	15.6	17.5	19.8	21.4	23.2
Total Input, watts	77.8	137.5	201.3	267.9	344.7
Collector Temperature, °K	791	889	970	1039	1100
Corresponding Current, amperes	—	16.6	49.8	84.5	124.5

The values of collector temperature were than plotted as a function of output current, and Figure 42 gives the optimum collector temperature characteristic, and compares it with the predicted and observed characteristics for model T/E-4. As can be seen, the observed characteristics agreed very well with the predicted curve. Also, the collector temperatures achieved by model T/E-4 were optimum over a broad, useful output current range which extends from 40 amperes, where the collector is 50°C below optimum to 85 amperes, where the collector is 30°C above optimum. Figure 42 from the JPL 950671 - Task II Final Report shows that for these excursions of collector temperature away from optimum, the output will be less than 1% different from the fully optimized condition.

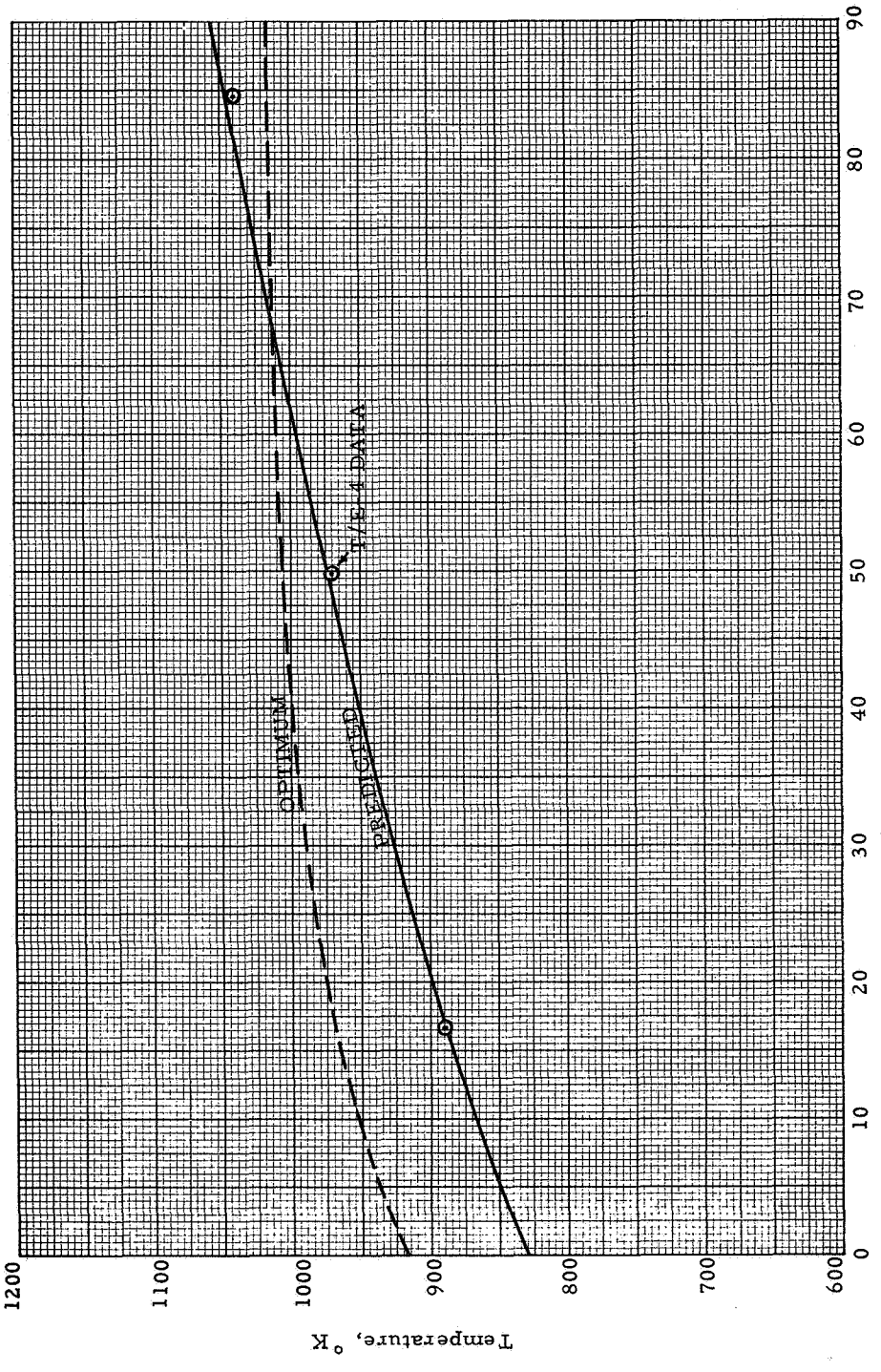
Temperature, °K
1200
1100
1000
900
800
700
600
0
10
20
30
40
50
60
70
80
90
Output Current, amperes
OPTIMUM
PREDICTED
TYPE-4 DATA

Figure 42

13. CONCLUSIONS

The effort conducted under this program encountered greater technical difficulties than were originally anticipated. More devices had to be assembled than scheduled, primarily due to an unexpected embrittling reaction of niobium with chromium oxide coatings, and also because of difficulty in controlling the flow of sodium into the heat-pipe structure during charging. The detrimental effects of these difficulties on the rate of progress of the work were countered by redirection of the effort by JPL to allow concentration on the more important aspects of heat pipe development.

Under the redirected effort it has been possible to meet all the original goals. A compatible heat-pipe collector-radiator structure has been developed which is of the proper size to handle the heat load of a T-200 converter, it has a known thermal response, and it has been shown to withstand both thermal cycling and a nominal duration of operation at heavy thermal inputs.

The heat pipe model T/E-3 demonstrated for the first time the operation of a SET-type converter with a collector-radiator heat pipe. All JPL requirements were met without failure of the model.

One of the most interesting results was presented in Figure 35, which compares the dynamic and static performance obtained with T/E-3. With the previous T-200 converters, this comparison had always shown agreement at low output currents, but at higher currents the static data had been far below the dynamic data because the collector-radiator structure had been unable to handle the larger heat transfer, and the collector overheated. The heat pipe of T/E-3 was designed to

avoid this limitation, and Figure 35 shows that the design was successful. The static data has remained in agreement with the dynamic data at all measured values of output current.

With the model T/4 effort, a different-sized heat pipe has been developed which fits ideally the dimensional and thermal constraints of the T-200 converter with a simple structure. This model has also met all JPL requirements. It has permitted overcoming a basic deficiency in the thermal characteristics of the T-200 converter developed under the concurrent JPL Contract 951263, and also reducing very significantly the weight of the T-200 converter.

Further refinements in heat-pipe collector-radiator technology will be found in the development of converters T-208, T-209 and T-210 of JPL Contract 951263.

APPENDIX A

MODEL T/E-3 DATA

THERMO ELECTRON
ENGINEERING CORPORATION

Sheet 1 of 7

Converter No. T/E-3 Run No. 1 Observer P. Brosens

VARIABLE		1	2	3	4	5	6	7	8	9	10
Date		6-22-67	6-22	6-22	6-22	6-23	6-23	6-23	6-23	6-23	
Time		15:43	16:10	16:37	17:15	16:10	16:28	16:49	17:15	17:38	
Elapsed Time, Hours		1.3	1.7	2.2	2.8	4.0	4.3	4.7	5.3	5.5	
T_O, °C		1585	1585	1585	1585	1682	1682	1682	1682	1682	
T_O Corrected, °C	(3)	1590	1590	1590	1590	1688	1688	1688	1688	1688	
$\Delta T_{Bell\ Jar}$, °C	(1)	10	10	10	10	12	12	12	12	12	
T_H, °C		1600	1600	1600	1600	1700	1700	1700	1700	1700	
ΔT_E, °C		11	11	12	18	11	12	14	17	22	
T_E, °K		1862	1862	1861	1853	1962	1961	1959	1956	1951	
V_o, volts	(2)	1.195	1.008	.800	.601	1.400	1.190	0.997	0.800	0.598	
I_o, amps		3.9	5.3	10.9	30.7	4.9	7.6	14.6	28.4	49.9	
P_o, watts											
I-V Trace No.					(5)						
T_R	mv	12.6	12.9	13.2	14.3	13.2	13.3	13.7	14.5	15.4	
	°C	309	317	324	350	324	326	336	355	376	
	°K	582	590	597	623	597	599	609	628	649	
T_C Heat Pipe	mv	16.3	22.9	23.9	26.9	24.4	24.9	26.0	27.9	30.1	
	°C	398	553	576	647	588	600	626	671	723	
	°K	671	826	849	920	861	873	899	944	996	
T_C base inner	mv										
	°C										
T_C base outer	mv										
	°C										
$T_{Radiator}$	mv										
	°C										
V_{eb}, volts		986	985	983	975	983	981	978	972	964	
I_{eb}, mA		197.5	201.0	214.9	277.7	240.1	248.1	271.5	312.9	381.4	
$E_{Filament}$, volts		4.8	4.8	4.8	4.9	4.6	4.7	4.8	5.0	5.2	
$I_{Filament}$, amps		22	22	22	23	21	22	22	23	24	
$I_{Coll.Heater}$, amps		—	—	—	—	—	—	—	—	—	
$I_{Res.Heater}$, amps		2.11	2.19	2.19	2.29	2.14	2.11	2.20	2.24	2.17	
Vacuum, 10^{-6} mm Hg		5.2	4.4	4.1	4.5	3.0	3.1	3.2	4.0	5.8	
Measured Efficiency, %											

NOTES:
(1) $\Delta T = 10 + 0.25\,I$
(2) VOLTAGE TAPS AT LEAD ATTACHMENT POINTS
(3) PYROMETER CORRECTIONS (CALIB. 5-17) +5°C @ 1600°C, +6°C @ 1700°C
(4) BELL JAR CORRECTIONS +10°C @ 1600°C, +12°C @ 1700°C.
(5) SHUT DOWN OVERNIGHT

THERMO ELECTRON
ENGINEERING CORPORATION

Converter No. T/E-3 Run No. 1 & 2 Observer P. Broseus

VARIABLE		1	2	3	4	5	6	7	8	9	10
Date		6-26	6-26	6-26	6-26	6-26	6-26	6-26	6-26	6-26	6-26
Time (1)		15:20	15:30	15:40	16:01	16:25	17:22	17:32	17:38	17:44	17:52
Elapsed Time, Hours		11.6	11.8	12.0	12.3	12.7	13.6	13.8	13.9	14.0	14.2
T_O, °C		1779	→	→	→	1682	1720	1721	1722	1723	1725
T_O Corrected, °C		1786	→	→	→	1688	1726	1727	1728	1729	1731
$\Delta T_{Bell\ Jar}$, °C		14	→	→	→	12	12	12	12	12	12
T_H, °C		1800	→	→	→	1700	1738	1739	1740	1741	1743
ΔT_E, °C		12	14	17	22	22	11	12	13	14	16
T_E, °K		2061	2059	2056	2051	1951	2000	2000	2000	2000	2000
V_O, volts		1.400	1.200	1.000	0.800	0.600	—	—	—	—	—
I_O, amps		9.2	15.9	28.0	46.1	50.4	4	8	11	18	25
P_O, watts						(2)					
I-V Trace No.							1	2	3	4	5
T_R	mv	13.8	14.4	14.9	15.5	15.3	11.0	11.8	12.6	13.4	14.3
	°C	338	353	364	379	374	271	290	309	329	350
	°K	611	626	637	652	647	544	563	582	602	623
T_C	mv	26.6	27.5	28.9	30.9	30.2	24.2	24.9	25.9	26.9	28.6
	°C	640	661	694	742	725	583	600	623	647	687
	°K	913	934	967	1015	998	856	873	896	920	960
T_C base inner	mv										
	°C										
T_C base outer	mv										
	°C										
$T_{Radiator}$	mv										
	°C										
V_{eb}, volts		971	968	964	957	962	979	978	975	972	968
I_{eb}, mA		306.9	330.8	370.5	433.0	380.0	235.4	244.0	270.8	290.2	331.7
$E_{Filament}$, volts		5.0	5.0	5.1	5.3	5.2	4.7	4.7	4.8	4.8	5.0
$I_{Filament}$, amps		23	23	23	24	24	22	22	22	22	23
$I_{Coll.\ Heater}$, amps		—	—	—	—	—	—	—	—	—	—
$I_{Res.\ Heater}$, amps		2.21	2.22	2.22	2.26	2.23	0.5	—	1.71	1.85	2.86
Vacuum, 10^{-6} mm Hg		2.8	2.8	3.0	4.8	4.0	2.6	2.6	2.6	2.6	2.6
Measured Efficiency, %											

NOTES: (1) TURNED ON AT 9:30 AM
(2) FILAMENT POWER VERY HIGH. CHOSE NOT TO GO TO 0.6V. @ 1800°C COMPARE WITH DATA POINT SHEET 1 #9.

THERMO ELECTRON
ENGINEERING CORPORATION

Converter No. T/E -3 Run No. 2 & 3 Observer P. Brosens

VARIABLE		1	2	3	4	5	6	7	8	9	10
Date		6-26	6-26	6-27	6-27	6-27	6-28	6-28	6-28	6-29	6-30
Time		17:58	18:10	11:43	13:34	17:30	10:02	12:50	14.46	9:34	9:44
Elapsed Time, Hours		14.3	14.4	32.0	33.9	37.8	54.3	57.1	59.1	77.9	102.0
T_O, °C		1726	1683	1673	1683	1680	1683	1684	1680	1683	1692
T_O Corrected, °C		1732	1688	1678	1688	1685	1688	1689	1685	1688	1698
$\Delta T_{Bell\ Jar}$, °C		12	11	11	11	11	11	11	11	11	11
T_H, °C		1744	1699	1689	1699	1696	1699	1700	1696	1699	1709
ΔT_E, °C		17	23	23	23	23	23	23	23	23	23
T_E, °K		2000	1949	1939	1949	1946	1949	1950	1946	1949	1959
V_O, volts		—	0.600	0.588	0.600	0.599	0.598	0.598	0.599	0.601	0.603
I_O, amps		30	50.9	51.9	51.2	51.6	51.6	51.9	51.3	51.9	52.5
P_O, watts											
I-V Trace No.		6									
T_R	mv	15.2	15.0	15.3	15.1.	15.1	15.3	15.2	15.1	15.0	15.2
	°C	372	367	374	369	369	374	372	369	367	372
	°K	645	640	647	642	642	647	645	642	640	645
T_C	mv	28.7	30.1	29.9	30.0	30.2	30.0	30.0	29.9	29.9	29.9
	°C	690	723	718	721	725	721	721	718	718	718
	°K	963	996	981	994	998	994	994	981	981	981
T_C base inner	mv				760						
	°C										
T_C base outer	mv			(2)							
	°C										
$T_{Radiator}$	mv										
	°C										
V_{eb}, volts		967	962	961	961	962	959	960	960	961	961
I_{eb}, mA		345.0	382.9	379.9	381.2	380.3	380.4	381.2	380.0	381.4	382.3
$E_{Filament}$, volts		5.0	5.1	5.2	5.2	5.2	5.2	5.2	5.2	5.2	5.2
$I_{Filament}$, amps		23	23	23	23	23	23	23	23	23	23
$I_{Coll.Heater}$, amps		—	—	—	—	—	—	—	—	—	—
$I_{Res.Heater}$, amps		2.42	2.17	2.17	2.17	2.16	2.17	2.17	2.18	2.18	2.19
Vacuum, 10^{-6} mm Hg		2.8	2.9	2.6	2.5	2.5	2.4	2.4	2.3	2.3	2.3
Measured Efficiency, %											

NOTES: (1) LEFT TO RUN OVERNIGHT
(2) PYROMETER READINGS ON HEAT PIPE, TOP TO BOTTOM. READINGS AFFECTED BY BACKGROUND LIGHTING IN LAB.

Converter No. T/E-3 Run No. 3 & 4 Observer P. Brosens

VARIABLE		1	2	3	4	5	6	7	8	9	10
Date		7-2	7-5	7-5	7-5	7-5	7-5	7-5	7-5	7-5	
Time		10:59	9:57	10:12	12:13	12:30	12:40	13:56	14:12	14:22	
Elapsed Time, Hours		151.3	222.2	222.5	224.5	224.8	225.0	226.2	226.5	226.7	
T_O, °C		1693	1679	—	—	1679	—	—	1678	—	
T_O Corrected, °C		1699	1685	—	—	1685	—	—	1684	—	
$\Delta T_{Bell\ Jar}$, °C		11	11	—	—	11	—	—	11	—	
T_H, °C		1710	1696	—	—	1696	—	—	1695	—	
ΔT_E, °C		23	23	—	—	23	—	—	23	—	
T_E, °K		1960	1946	—	—	1946	—	—	1945	—	
V_o, volts		0.607	0.601	—	—	0.601	—	—	0.594	—	
I_o, amps		52.3	52.2	—	—	52.4	—	—	51.9	—	
P_o, watts											
I-V Trace No.			(1)	(2)	(3)		(4)	(5)		(6)	
T_R	mv	14.9	15.0		8.9	14.8		8.9	14.9		
	°C	364	367		219	362		219	364		
	°K	637	640		482	635		482	637		
T_C	mv	29.4	30.0		1.9	29.9		2.1	29.9		
	°C	706	721		49	718		52	718		
	°K	979	994		320	991		325	991		
T_C base inner	mv				CYCLE #1			CYCLE #2			
	°C										
T_C base outer	mv										
	°C										
$T_{Radiator}$	mv										
	°C										
V_{eb}, volts		970	970		1040	969		1040	969		
I_{eb}, mA		384.0	378.0		0	378.9		0	380.0		
$E_{Filament}$, volts		5.1	5.1		0	5.0		0	5.0		
$I_{Filament}$, amps		23	22		0	22		0	22		
$I_{Coll.Heater}$, amps		—	—		—	—		—	—		
$I_{Res.Heater}$, amps		2.19	2.17	2.17	2.17	2.17	2.17	2.17	2.17	2.17	
Vacuum, 10^{-6} mm Hg		2.2	2.0		2.1	2.0		1.9	1.8		
Measured Efficiency, %											

NOTES: (1) END OF 200 HOURS STEADY STATE.
(2) SHUT OFF EB BOMBARDMENT, CYCLE #1. RESERVOIR HEATER LEFT ON.
(3) TURNED POWER ON TO FULL BOMBARDMENT $T_o \rightarrow 1940°C$
(4) SHUT OFF, CYCLE #2.
(5) SAME AS NOTE (3).
(6) SHUT OFF, CYCLE #3.

THERMO ELECTRON
ENGINEERING CORPORATION

Converter No. T/E -3 Run No. 4 Observer P. Brosens

VARIABLE		1	2	3	4	5	6	7	8	9	10
Date		7-5	7-5	7-5	7-6	7-6	7-6	7-6	7-6	7-6	7-14
Time		15:31	15:44	15:54	10:10	10:28	10:33	11:20	11:35	11:43	10:55
Elapsed Time, Hours		227.8	228.0	228.2	246.4	246.8	246.9	247.6	247.9	248.0	439.2
T_O, °C		—	1691	1688	—	1683	1681	—	1688	1690	1688
T_O Corrected, °C		—	1697	1694	—	1689	1687	—	1694	1696	1694
$\Delta T_{Bell\ Jar}$, °C		—	11	11	—	11	11	—	11	11	11
T_H, °C		—	1708	1705	—	1700	1698	—	1705	1707	1705
ΔT_E, °C		—	23	23	—	23	23	—	23	23	23
T_E, °K		—	1958	1955	—	1950	1948	—	1955	1957	1955
V_O, volts		—	0.597	0.600	0	0.607	0.609	0	0.596	0.595	0.593
I_O, amps		—	50.4	50.9	0	51.9	51.9	0	51.0	51.1	50.5
P_O, watts											
I-V Trace No.		(1)		(2)	(3)		(4)	(5)		(6)	
T_R	mv	8.9	14.9	14.9	9.0	14.9	14.9	2.5	14.9	14.9	14.9
	°C	219	364	364	222	364	364	62	364	364	364
	°K	482	637	637	495	637	637	335	637	637	637
T_C	mv	2.3	29.9	29.9	1.9	29.9	29.9	2.9	29.9	29.9	29.5
	°C	57	718	718	47	718	718	71	718	718	709
	°K	330	991	991	320	991	991	344	991	991	982
T_C base inner	mv	CYCLE #3			CYCLE #4			CYCLE #5			
	°C										
T_C base outer	mv										
	°C										
$T_{Radiator}$	mv										
	°C										
V_{eb}, volts		1040	969	969	1035	965	965	1035	965	965	964
I_{eb}, mA		0	381.4	381.1	0	378.9	378.7	0	380.2	380.9	381.6
$E_{Filament}$, volts		0	5.0	5.0	0	5.0	5.0	0	5.0	5.0	5.1
$I_{Filament}$, amps		0	22	22	0	22	22	0	22	22	22
$I_{Coll.\ Heater}$, amps		—	—	—	—	—	—	—	—	—	—
$I_{Res.\ Heater}$, amps		2.17	2.16	2.17	2.19	2.20	2.17	0	2.17	2.17	2.17
Vacuum, 10^{-6} mm Hg			1.8	1.8	2.2	2.0	2.0	2.1	2.1	2.1	1.9
Measured Efficiency, %											

NOTES: (1) TURNED FULL POWER ON OUTPUT AT END OF 10 MIN: 0.58V 48.9A.
(2) POWER OFF
(3) FULL POWER TURNED ON
(4) POWER OFF RESERVOIR HEATER OFF
(5) POWER ON, RESERVOIR ON
(6) LEFT UNIT TO RUN IN STEADY STATE AT THIS SETTING

THERMO ELECTRON
ENGINEERING CORPORATION

Sheet 6 of 7

Converter No. T/E -3 Run No. 4 Observer P. Brosens

VARIABLE		1	2	3	4	5	6	7	8	9	10
Date		7-14	7-14	7-14	7-14	7-14	7-14		7-16	7-16	
Time		13:19	14:32	14:52	15:15	16:50	17:13		16:18	16:42	
Elapsed Time, Hours		441.6	442.8	443.1	443.5	445.1	445.5		492.6	493.0	
T_O, °C		1683	—	1683	1682	—	1680		—	1678	
T_O Corrected, °C		1689	—	1689	1688	—	1686		—	1684	
$\Delta T_{Bell\ Jar}$, °C		11	—	11	11	—	11		—	11	
T_H, °C		1700	—	1700	1699	—	1697		—	1695	
ΔT_E, °C		23	—	23	23	—	23		—	23	
T_E, °K		1950	—	1950	1949	—	1947		—	1945	
V_O, volts		0.597	0	0.595	0.601	0	0.600		0	0.602	
I_O, amps		51.2	0	51.9	52.0	0	51.6		0	52.2	
P_O, watts											
I-V Trace No.		(1)—	(2)		(3)	(4)		(5)	(6)	(7)	
T_R	mv	14.4	8.2	14.3	14.4	7.8	14.3		R.T.	14.4	
	°C	353	202	350	353	192	350			353	
	°K	626	475	623	626	465	623			626	
T_C	mv	29.5	2.3	29.5	29.6	2.3	29.5		R.T.	29.5	
	°C	709	57	709	711	57	709			709	
	°K	982	330	982	984	330	982			982	
T_C base inner	mv		CYCLE #6			CYCLE #7			CYCLE #8		
	°C										
T_C base outer	mv										
	°C										
$T_{Radiator}$	mv										
	°C										
V_{eb}, volts		965	1040	965	965	1040	965		1042	964	
I_{eb}, mA		383.0	0	381.3	382.3	0	381.8		0	382.3	
$E_{Filament}$, volts		5.1	0	5.1	5.1	0	5.1		0	5.1	
$I_{Filament}$, amps		21	0	21	21	0	21		0	21	
$I_{Coll.\ Heater}$, amps		—	—	—	—	—	—		—	—	
$I_{Res.\ Heater}$, amps		2.00	2.00	2.01	2.02	2.01	2.02		0	2.02	
Vacuum, 10^{-6} mm Hg		1.8	1.9	1.9	1.9	1.9	1.9		2.0	2.1	
Measured Efficiency, %											

NOTES: (1) OPTIMUM RESERVOIR PRESSURE APPEARS TO HAVE DECREASED. POWER OFF FOR NEXT CYCLE
(2) POWER ON
(3) POWER OFF
(4) POWER ON T_R & T_C READ ON RECORDER 32 in/hr chart speed
(5) POWER OFF RES. & CONV.
(6) ALL POWER ON
(7) POWER OFF FOR 35 MIN (DARK PERIOD OF EARTH ORBIT) RESERVOIR ON.

THERMO ELECTRON
ENGINEERING CORPORATION

Sheet 7 of 7

Converter No. T/E -3 Run No. 4 & 5 Observer P. Brosens

VARIABLE		1	2	3	4	5	6	7	8	9	10
Date		7-16	7-16	7-17	7-17	7-17	7-17	7-17	7-17	7-18	
Time		17:20	17:40	10:44	11:10	11:55	13:07	14:00	14:32	13:02	
Elapsed Time, Hours		493.6	494.0	511.0	511.3	512.2	513.4	514.3	514.8	516.6	
T_O, °C		—	1676	—	1678	—	1674	—	1674	1684	
T_O Corrected, °C		—	1682	—	1684	—	1680	—	1680	1690	
$\Delta T_{Bell\ Jar}$, °C		—	11	—	11	—	11	—	11	11	
T_H, °C		—	1693	—	1695	—	1691	—	1691	1701	
ΔT_E, °C		—	23	—	23	—	23	—	23	23	
T_E, °K		—	1943	—	1945	—	1941	—	1941	1951	
V_O, volts		0	0.600	0	0.611	0	0.608	0	0.604	0.600	
I_O, amps		0	51.9	0	51.9	0	51.9	0	51.8	51.9	
P_O, watts											
I-V Trace No.		(1)	(2)	(3)	(4)	(5)	(6)	(7)	(8)		
T_R	mv	8.5	14.3	1.6	14.3	2.5	14.5	2.4	14.5	14.9	
	°C	209	350	40	350	62	355	59	355	364	
	°K	482	623	313	623	335	628	632	628	637	
T_C	mv	3.4	28.5	1.2	29.5	3.0	29.9	2.9	29.5	29.9	
	°C	83	685	30	709	73	718	71	709	718	
	°K	356	958	303	982	346	991	344	982	991	
T_C base inner	mv	CYCLE #9		CYCLE #10		CYCLE #11		CYCLE #12			
	°C										
T_C base outer	mv										
	°C										
$T_{Radiator}$	mv										
	°C										
V_{eb}, volts		1041	965	1035	963	1035	963	1035	963	964	
I_{eb}, mA		0	380.4	0	380.1	0	377.9	0	377.3	381.0	
$E_{Filament}$, volts		0	5.0	0	5.0	0	5.0	0	5.0	5.2	
$I_{Filament}$, amps		0	21.0	0	20.5	0	20.5	0	20.5	21.0	
$I_{Coll.\ Heater}$, amps		—	—	—	—	—	—	—	—	—	
$I_{Res.\ Heater}$, amps		2.02	2.02	0	2.01	0	2.01	0	2.01	2.05	
Vacuum, 10^{-6} mm Hg		2.0	2.1	2.1	2.2	2.0	2.0	2.0	2.0	4.0	
Measured Efficiency, %											

NOTES: (1) POWER ON. RESERVOIR VOLTAGE AT POWER SUPPLY = 0.95 VOLT
(2) ALL POWER OFF.
(3) " " ON.
(4) " " OFF
(5) " " ON.
(6) " " OFF
(7) " " ON.
(8) " " OFF BELL JAR OPENED TO CORRECT VOLTAGE TAP CONNECTION FROM A TO B. END OF TEST.